Dissertation
submitted to the
Combined Faculties for the Natural Sciences and for Mathematics of the
Ruperto-Carola University of Heidelberg, Germany for the degree of
Doctor of Natural Sciences

presented by

M.Sc. Francesca Caroti
born in: Livorno
Oral-examination: 16.12.2016

Evolution of the extraembryonic tissue in flies: from *Megaselia abdita* to *Drosophila melanogaster*

Referees: Prof. Dr. Joachim Wittbrodt
Dr. Steffen Lemke

Acknowledgements

It is real! I arrived at the end! I couldn't have gone so far without the help of all the people that were with me in this adventure. First of all I would like to thank Steffen (Dr. Steffen Lemke). Not only you gave me the opportunity to work on this challenging project but you also let me grow scientifically and... you manage to deal with my not easy mood! Thank you!!! Many Thanks also to the Prof. Dr. Jochen Wittbrodt. You destroy me during my first TAC meeting but I learn a lot from you! You are a great example of scientist and I will try to follow it in my future career! I would like to thank the Prof. Dr. Ingrid Lohmann that follow and helped me during the development of my PhD project. Thanks to my colleagues! I know it has been hard work with me. Thanks Maike to take care of my smelly flies! Thanks "Robocoppo" (Lucas) for you help any time I needed even thought we cannot understand each other very well. Thanks Ever!!! Without you probably this project would be in a drawer... the genius of the unrolling! How not thank his sister. Paula, thank you!!! You are always there for all of us, even when you are sick! Thanks also for the last minute corrections of the thesis and... Latex!!! For this I have to thank also Colin that kindly helped me in between his experiments and courses! I thank all the Lemke's! The new ones brought freshness to the environment and the one that started the lab with me... well we walked together all the way! A special thank goes to Silvi. We have been together from the very first to the very last day of this trip in the happy moments and in the dark ones. From a colleague you became a friend and now you are Dr. Awesome Shit!!! We enjoyed many moments and many "merenda time" with the post it! I still have it on my desk! On the way I got to know also Tina and Arturo and I very glad I had the opportunity to enjoy your company and have fun together! Actually also merenda! I have to say, if you didn't notice I love merenda!!! Another special person that I got to know how colleague and ended up as an awesome person and friend is a Portuguese guy that loves Monica Bellucci!!! Thank you Pedrito!!!! Without your help I am not sure I would have been able to reach this point. Not only you gave suggestions and helped me in the scientific part but you always been there any time I needed to talk. Thanks to have shared your passion for books and photos! And thanks for the awesome port wine!!!

I love it!!! These five years (maybe a bit more) have been great thanks to the COS people! I would like to thank the “mensa group” for the laughs and the gossip time! Awesome! And awesome parties!!! Papaya, Anne-Laure, Andrea, Zaida, Rainer, Mouli, Paola... all crazy and great prople!!! Thank you all!!! We had a great time together in between my troubles!!! Thank you Katrin and Julie for your support especially in this last period!!! You are funny!!! I hope I didn't forget anyone! And now... it's time to switch language... for my family! Un grazie veramente grande va a tutta la mia famiglia che mi ha sostenuto durante tutto questo lungo e tortuoso percorso. Un grazie speciale a babbo, mamma e Veronica! Senza di voi non so se sarei arrivata a questo traguardo. Avete sempre creduto in me! Grazie!!! Grazie anche a marco, Elettra e Fanny (my hairy daughter!), siete speciali!!! Un abbraccio grande!!!

Thank you!!! I love you all!!!

Abstract

Embryonic development establishes the body plan, organs, and the shape of the adult animal organism. This process involves cells and tissues that eventually will not be part of the growing embryo, so-called extraembryonic tissues. In insects, extraembryonic tissues contribute to embryonic development by fulfilling important roles during specific morphogenetic movements, such as blastokinesis, germband retraction and dorsal closure, but also in the protection of the embryo against egg desiccation and pathogens. Within insects, extraembryonic tissues differ in number and topology, they may display diverse morphologies even between closely related species, and it is currently not yet clear which specific function each extraembryonic tissue fulfills and how its development is genetically regulated. Most of our current understanding of extraembryonic development and function in insects stems from studies in *Tribolium castaneum* and *Drosophila melanogaster*. The two species show several morphological differences, not only at the extraembryonic level but also in the morphology of the embryo. Specifically, *T. castaneum* has two extraembryonic tissues called amnion and serosa: the serosa separates from the embryo, grows over it, and eventually encloses the embryo, the amnion stays attached to the embryo and covers its ventral side. *D. melanogaster*, by contrast, develops only one single extraembryonic tissue called amnioserosa that remains in constant contact with the embryo and stays on its dorsal side. The diversity in form, development, and function of extraembryonic tissues in insect species provides an outstanding model to address how form and function of specific epithelia evolved, and how these changes were genetically encoded. In my thesis, I have taken advantage of intermediate characters in extraembryonic development of *Megaselia abdita* (Diptera, Phoridae), which features a similar embryonic development as *D. melanogaster* but maintained two extraembryonic tissues and thus part of the ancestral extraembryonic development described in *T. castaneum*. I have focused my attention on a detailed *in vivo* analysis of extraembryonic development at a morphogenetic and cellular level by establishing and using light-sheet microscopy. I acquired evidence that links extraembryonic tissues behavior in *M. abdita* to orthologues of the T-box transcription factor Dorsocross and the tumor necrosis factor Eiger, which in *D. melanogaster* are key genes that contribute to specification and morphogenesis of the amnioserosa. *In vivo* observations and functional studies suggest an important interaction of the extraembryonic tissues of *M. abdita* with the extracellular matrix that seems to be

finely regulated. In conclusion, the results of this study increase our knowledge on morphology and development of extraembryonic tissues in *M. abdita* and provided an *in vivo* technique for non-model organisms to study *in toto* dynamics of early development.

Zusammenfassung

Während der Embryonalentwicklung wird der Bauplan des Körpers, der Organe und der äusserlichen Erscheinung des ausgewachsenen Tieres festgelegt. Dieser Prozess bezieht Zellen und Gewebe mit ein, die letztendlich nicht Teil des wachsenden Tieres darstellen, dassogenannte extraembryonale Gewebe. In Insekten erfüllt das extraembryonale Gewebe wichtige Rollen während spezifischen morphogenetischen Bewegungen, wie der Blastokinese, dem Zurückziehen des Keimbandes und des dorsalen Verschlusses. Weiterhin schützt es den Embryo gegen Austrocknung und Pathogene im Laufe der Embryonalentwicklung. Zwischen den Insekten unterscheidet sich das extraembryonale Gewebe in Zahl und räumlicher Struktur und kann sogar diverse Morphologien zwischen eng verwandten Arten darstellen. Bisher ist noch nicht bekannt, welche spezifischen Funktionen das extraembryonale Gewebe erfüllt und wie seine Entwicklung genetisch reguliert ist. Der Großteil unseres Verständnisses der Entwicklung des extraembryonalen Gewebes stammt aus Studien mit *Tribolium castaneum* und *Drosophila melanogaster*. Beide Arten zeigen mehrere morphologische Unterschiede, nicht nur auf dem extraembryonalen Level, sondern auch in der Morphologie des Embryos. Im speziellen besitzt *T. castaneum* zwei extraembryonale Gewebe, das Amnion und die Serosa. Die Serosa separiert sich vom Embryo und wächst um den Embryo, bis sie ihn umschließt. Das Amnion hingegen bleibt mit dem Embryo verbunden und bedeckt seine ventrale Seite. Im Gegensatz dazu findet man in *D. melanogaster* nur ein extrembryonales Gewebe, genannt Amnioserosa, welches in konstantem Kontakt mit dem Embryo steht und die dorsale Seite bedeckt. Die Diversität des extraembryonalen Gewebes in Form, Entwicklung und Funktion in Insekten bietet sich als herausragendes Model an um Fragen zu adressieren, die sich mit der Evolution von Form und Funktion spezifischer Epithelien beschäftigen und erklären wie diese Veränderungen genetisch festgelegt werden. In meiner Dissertation hab ich mir die Eigenschaften der extraembryonalen Entwicklung von *Megaselia abdita* zum Vorteil gemacht. Diese stellt eine Zwischenstufe dar, die Ähnlichkeiten zur Embryonalentwicklung von *D. melanogaster* aufweist, aber durch die Entwicklung zwei extraembryonaler Gewebe charakterisiert ist und somit Teil des ancestralen Embryonalentwicklungsprogrammes ist, welches für *T.castaneum* beschrieben wurde. Ich habe ein besonderes Augenmerk auf eine detaillierte *in vivo* Analyse der extraembryonalen Entwicklung gelegt, mit gesondertem Fokus auf morphogenetische und zelluläre Entwicklungen, und hierfür Light-sheet Mikroskopie etabliert und

angewendet. Ich konnte einen Zusammenhang zwischen dem Verhalten des extraembryonalen Gewebes und dem Ortholog des T-Box Transkriptionsfaktors Dorsocross und dem Tumor necrosis Faktor Eiger in *M.abdita* zeigen. In *D. melanogaster* stellen diese die entscheidenden Gene dar, welche die Amnioserosa spezifizieren und ausbilden. Beobachtungen des lebenden Organismus und funktionale Untersuchungen legen einen wichtigen Zusammenhang zwischen dem extraembryonalen Gewebe von *M. abdita* und der extrazellulären Matrix nahe, welches selbst sehr genau reguliert zu sein scheint. Schlussfolgernd vergrößern die Ergebnisse dieser Studie unser Wissen über die Morphologie und Entwicklung des extraembryonalen Gewebes in *M. abdita* und bieten eine Technik zur Untersuchung von Nicht-Modelorganismen im lebenden Embryo, um Dynamiken während der frühen Entwicklung *in toto* zu analysieren.

Abbreviations

D. melanogaster	*Drosophila melanogaster*
E. balteatus	*Episyrphus balteatus*
E. coli	*Escherichia coli*
M. abdita	*Megaselia abdita*
Mab	*Megaselia abdita*
O. fasciatus	*Oncopeltus fasciatus*
T. castaneum	*Tribolium castaneum*
A	amnion
A-P	anterior-posterior
Amp	ampicillin
AS	amnioserosa
bp	base pairs
BMP	Bone morphogenetic protein
BSA	bovine serum albumin
CF	Cephalic furrow
Co.	Company
cv-2	*crossveinless-2*
D,Da	Dalton
DMSO	Dimethylsulfoxid
DNA	deoxyribonucleic acid
dNTP	deoxynucleotide triphosphate
doc	*dorsocross*
dpp	*decapentaplegic*
D-V	dorsal-ventral
EDTA	ethylendiamine tetraacetic acid
egr	*eiger*
en	*engrailed*
et al.	and others

EtOH	Ethanol
Fig.	Figure
GBE	germband extension
GET	Glucose-EDTA-Tris
GFP	green fluorescence protein
GPI	glycosylphosphatidylinositol
h	hour
hsp70	heat shock protein 70
IPTG	Isopropyl-β-D-thiogalactopyranosid
JNK	Jun N-terminal kinase
k	kilo (103)
kb	kilo base pairs
l	liter
LB	lysogeny broth
M	molar (mol/l), Mega (10 textsuperscript6)
mCherry	monomeric Cherry
mcs	multiple cloning site
MetOH	Methanol
min	minute
ml	millilitre
mmp	*matrix metalloprotease*
mol	6,023 x 1023
Mr	relative molecular weight
n	nano (10-9)
nt	nucleotide
O	oxygen
ORF	open reading frame
ori	origin of replication
PCR	polymerase chain reaction
pH	negative common logarithm of proton concentration

RNA	ribonucleic acid
RNAP	RNA polymerase
RNase	ribonuclease
rpm	rounds per minute
RT	room temperature
S	serosa
sec	second
spp.	Species
stg	*string*
Tab.	Table
TAE	Tris-acetate-EDTA-buffer
TGF-β	Transforming growth factor beta
TIMP	tissue inhibitor of metalloproteases
TNF-α	tumor necrosis factor alpha
Tris	Tris-(hydroxymethyl-) amino methane
U	units
UTR	untranslated region
UV	ultraviolet radiation
V	volt
v/v	volume per volume
w/v	weight per volume
X-Gal	5-Brom-4-chlor-3-indol-β-D-galactopyranosid
zen	*zerknüllt*
℃	degree Celsius
λ	bacteriophage lambda, radiation
µ	micro (10-6)

Contents

1 Introduction

The development of an organism is highly organized by critical steps including blastoderm development, cleavage, gastrulation, neurogenesis and organogenesis. One of the first events of high morphogenetic activity during embryonic development is gastrulation. During this process, a hollow sphere of cells is determined and rearranged to internalize mesoderm and endoderm, the ectoderm is defined and extraembryonic tissues are formed, which will not contribute to the embryo but aid embryonic development, e.g. as a protective envelope or by contributing to morphogenetic movements. During gastrulation, the single layered blastula is transformed into a three-layered structure consisting of ectoderm, mesoderm, and endoderm [Wolpert, 1992]. This morphogenetic process, is one of the most important steps during early development of multicellular organisms and, within a given group of animals (e.g. flies), it is readily comparable. Although there are strong similarities, gastrulation in flies has diverged from species to species to display morphological differences [Goltsev et al., 2007, Rafiqi et al., 2008], which can be used as an entry point to study the genetic basis of morphogenesis. During embryonic development of flies, two main morphogenetic differences have been previously observed and described, i.e. a different mode of mesoderm internalization [Goltsev et al., 2007, Urbansky et al., 2016] and a different mode of extraembryonic tissue development [Rafiqi et al., 2008, Rafiqi et al., 2010, Rafiqi et al., 2012]. A detailed functional analysis based on quantitative cell and tissue behavior has recently revealed a comprehensive genetic model to explain the evolutionary transition in mesoderm internalization [Urbansky et al., 2016]. Further on, the differences in extraembryonic tissue development have been accounted by a genetic model [HallgrÍmsson et al., 2012, Schmidt-Ott et al., 2010, Schmidt-Ott and Kwan, 2016], and indicated that our understanding of extraembryonic tissue development in non-Drosophila flies lacks critical steps to understand the cell

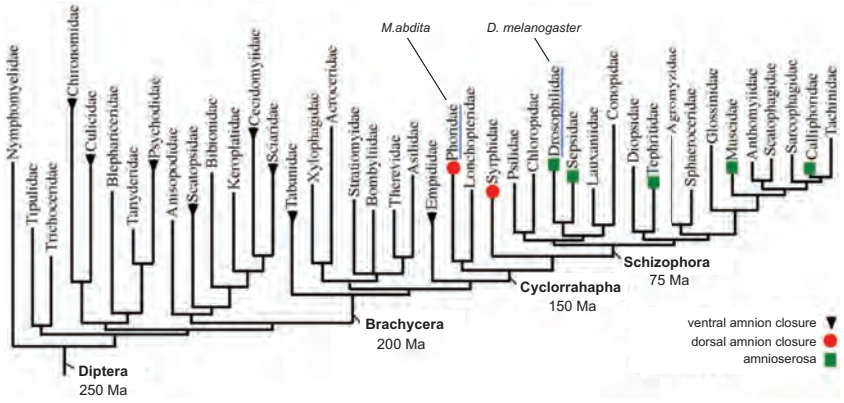

Figure 1.1: Phylogenetic tree of Diptera. The phylogenetic tree is based on substitutions per site. The families with a serosa and a ventral amnion are marked with a black triangle, families with a serosa and a dorsal amnion with a red circle, families with an amnioserosa with a green square. Are highlighted the Phoridae and the Drosophilidae of which *M. abdita* and *D. melanogaster* are part respectively. These are the two relevant species for this study. Ma, millions of years ago. Adapted from [Wiegmann et al., 2011].

behavior and tissue dynamics.

In this thesis, I revisit the extraembryonic tissue development in *Megaselia abdita* during gastrulation events focusing on previously unexplored aspects of cell and tissue dynamics. Specifically, I aim to address the transition from extraembryonic layer with two distinct tissues (amnion and serosa) in basal cyclorrhaphan flies like *M. abdita* to a single extraembryonic tissue (amnioserosa) typical for schizophoran flies like *Drosophila melanogaster* (Fig. 1.1). *M. abdita* was chosen as a satellite species, because it is the closest specie to *D. melanogaster* that is having two extraembryonic tissues, which is accessible and can be easily maintained under lab conditions.

1.1 Gastrulation and extraembryonic development in *D. melanogaster*

The embryos of *D. melanogaster* are about 500µm covered by two protective layers: the chorion, which is the external egg shell, and the vitelline membrane, the internal protective barrier. The embryo starts to develop as syncytium where nuclei divide rapidly and synchronously [Campos-Ortega and Hartenstein, 1997, Anderson, 1972]. During the first nine divisions, the nuclei migrate from the center to the periphery [Foe and Alberts, 1983]. Once

they reach the cortical position of the embryo, the nuclei divide synchronously for additional four times. At the end of the 13th division, the embryo begins to cellularize (Fig. 1.2A). During this process, the membrane first slowly invaginates around each nucleus. At the end of the process each nucleus is elongated and surrounded by the cell membrane but is still in contact with the yolk [Foe and Alberts, 1983, Turner and Mahowald, 1977]. Exceptions are the pole cells (germ cells), which are the first cells to be formed at the posterior pole of the embryo. When the membrane fuses at the basal side of each nucleus, it forms also a single large yolk cell, which contains some nuclei that are transcriptionally active during embryogenesis. Once cellularization is complete, cells on the ventral side of the embryo start to invaginate forming the ventral furrow [Leptin and Grunewald, 1990]. These cells internalize in a coordinated manner forming a tube, which will collapse at the end. The cells on the other hand will start to migrate along the lateral epithelium, to give rise to the mesoderm. At the same time the cephalic furrow is forming (Fig. 1.2B) [Turner and Mahowald, 1977]. This is a dorso-ventral furrow located at the end of the head region and separates the head from the rest of the embryo. After the mesoderm has invaginated, the posterior pole of the embryo flattens, the ventral side starts to elongate and the pole cells are pushed on the dorsal side of the embryo [Turner and Mahowald, 1977]. This process is known as germband extension and it last until the germband reaches almost the cephalic furrow [Anderson, 1966, Campos-Ortega and Hartenstein, 1997]. The first phase of the extension is a fast process (Fig. 1.2B) and it slows down when the pole cells are internalized and the posterior midgut starts to invaginate (Fig. 1.2C). During this process, two dorsal transversal folds, the dorsal folds, are formed (Fig. 1.2B,C) [Campos-Ortega and Hartenstein, 1997]. They are not simply a passive reaction of the germband movement. The formation of these folds is genetically regulated since they appear always in the same place at the same time, whereas their function is still unknown. During further development the anterior midgut ingresses at the anterior side of the embryo (Fig. 1.2D) and, while the germband extension proceeds, cells of the dorsal epithelium stretch and their columnar form becomes squamous (Fig. 1.2E,F) [Turner and Mahowald, 1977]. These cells form the unique extraembryonic tissue, the amnioserosa that remains in constant contact with the embryo. During its stretching, the embryo shows a rudimental amnioserosal fold along

the extrembryonic tissue. After the germband is completely elongated and the amnioserosa is at its maximum stretch, the germband moves toward the posterior pole (Fig. 1.2G) [Campos-Ortega and Hartenstein, 1997]. This movement is called germband retraction. At the same time the amnioserosa spreads out from its compression (Fig. 1.2G). Once the germband is completely retracted, the amnioserosa recedes to the dorsal part of the embryo (Fig. 1.2H). The amnioserosa contracts and reduces its area by bringing the two side of the dorsal opening closer to each other (Fig. 1.2I) [Turner and Mahowald, 1979]. In the end the amnioserosa is degraded and dorsal hole is completely sealed (Fig. 1.2J). The yolk sac of *D. melanogaster* embryos is a polynucleate cell attached to the amnioserosa through βPS integrin and this interaction is essential for normal amnioserosa contraction, contributing to the force [Narasimha and Brown, 2004]. Moreover, the yolk nuclei transcription is required for the expression of the integrins that are involved in several developmental processes as the midgut formation [Narasimha and Brown, 2004]. Therefore, the yolk cell has not only the function to provide a food source to the embryo but also has an active and essential role during the embryonic development. The expression of βPS integrin is necessary for the survival of the amnioserosa, because the loss of the connection via integrins between the extraembryonic tissue and the yolk sac will lead to cell death among the amnioserosal cells [Reed et al., 2004]. Furtheron, it has been shown that the attachment of the amnioserosa to the germband is required for a proper germband retraction and that βPS integrin is involved in this interaction [Schöck and Perrimon, 2003]. This observation points out that the amnioserosa and the yolk sac have an essential role during embryonic morphogenesis.

1.2 Gastrulation and extraembryonic tissue development in *Megaselia abdita* and other insects

The extraembryonic tissue is common to several animals, it protects and feed the embryo to which it will not directly contribute. Insects develop extraembryonic membranes that include the serosa, the amnion and the yolk sac. These

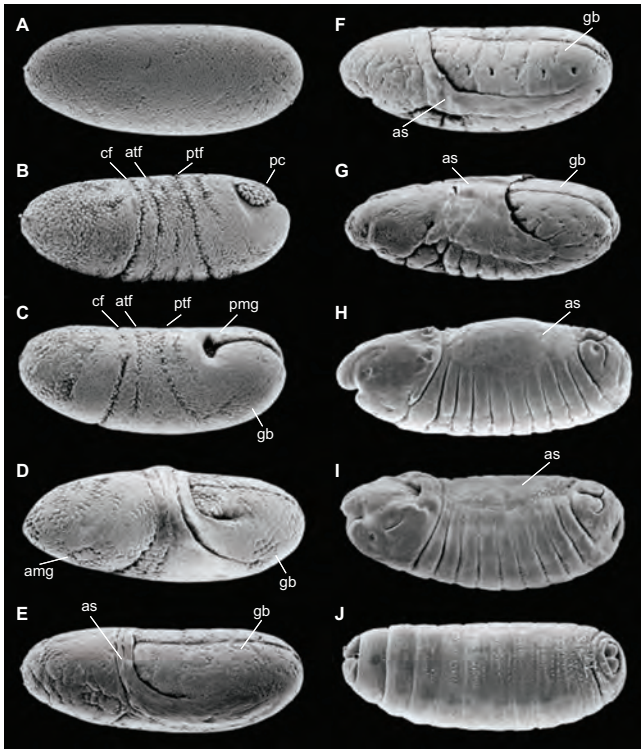

Figure 1.2: Embryonic development of *D. melanogaster*. Scanning electron microscope images of *D. melanogaster* embryonic development are shown here. (A) Cellularization: nuclei are at the periphery of the embryo and cell membranes are invaginating and the pole cells are at the posterior pole of the embryo. (B) Onset of germband extension: the germband begins to elongate and move the pole cells dorsally; cephalic furrow, anterior and posterior transvers folds are appearing. (C) Early-germband extension: the germband continues to extend and the posterior midgut invaginates. (D) Mid-germband extension: the anterior midgut invaginates and the dorso-lateral cells of the embryo are stretched. (E,F) Late-germband extension: the amnioserosa is stretched and its cells change shape. (G) Beginning germband retraction: the germband retracts at the posterior pole and the amnioserosa spreads out from its compressed state. (H) Complete germband retraction: the germband' s tip reaches the posterior pole of the embryo and the amnioserosa is now completely dorsal. (I) Dorsal closure: the amnioserosa reduces its area bringing closer the two sides of the epithelium to close the dorsal opening. (J) End of embryogenesis: the dorsal hole is completely closed and the amnioserosa has been degraded. Abbreviations: anterior midgut (amg); amnioserosa (as); anterior transverse furrow (atf); cephalic furrow (cf); germband (gb); pole cells (pc); posterior midgut (pmg); posterior transverse furrow (ptf). Anterior is left. Adapted from http://rsr.org/files/images/science/embryos-fly-series.jpg.

tissues are essential for a proper embryonic development, in embryo immunity and desiccation resistance (reviewed in [Horn et al., 2015, Panfilio, 2008]). The extraembryonic membranes show different morphologies between insect species. Many insects form the serosa, a tissue that develops from the blastoderm cells and does not contribute to the embryo neither to the amnion. The amnion forms from the margin of the germ rudiment and its topology is different between species. In fact, in some insects the amnion closes on the ventral side of the embryo, e.g. *Oncopeltus fasciatus* and *Tribolium castaneum*, while in others it remains dorsal, e.g. *M. abdita* and *Episyrphus balteatus*. Species of higher Diptera, e.g. *D. melanogaster*, develop only the amnioserosa on the dorsal side of the embryo. The yolk sac is common to all the species, while the developing embryo shows sever morphological differences among the insect species. For example, the true bugs as *O. fasciatus* have an opposite orientation of the embryo along the AP-axis in respect to the egg and only later the embryo reverts its orientation with the help of the extraembryonic tissues [Panfilio et al., 2006]. Other differences are observed in the length of the germband. Instead in Diptera the embryonic development is comparable between the different flies facilitating the study of the extraembryonic tissue evolution. Therefore, I used *M. abdita* as model organism to study the evolution of the extraembryonic tissue in its last step to understand the transition from the two tissues to one single tissue layer. The embryos of *M. abdita* are slightly longer than the *D. melanogaster* embryos. They are about 530µm, they have the chorion and the vitelline membrane, from which the posterior pole is the first to detach. The synchronized mitotic division, the cellularization process and the morphological movements as ventral furrow and cephalic furrow formation, germband extension and retraction, are comparable to *D. melanogaster* [Wotton et al., 2014]. The entire embryogenesis in *M. abdita* is only a couple of hours slower than in *D. melanogaster*. The main phenotypic difference between the embryos of these two species is the extraembryonic tissue development. As mentioned above, *M. abdita* has two extraembryonic tissues, the amnion and the serosa. They start to develop as a unique tissue but during the slow phase of germband extension, the serosa detaches, crawls over the embryo and eventually encloses it while the amnion remains on the dorsal side of the embryo and in contact with it. After germband retraction, the serosa breaks on the posterior-ventral side of the embryo and recedes to the dorsal side where it is contracted into

the dorsal hole [Wotton et al., 2014].

1.3 The extraembryonic tissue and its morphological differences between *M. abdita* and *D. melanogaster*

In *M. abdita*, as well as in *D. melanogaster*, the dorsal cells of the embryo will form the extraembryonic tissue and are specified during cellularizarion (Fig. 1.3.1). These cells change shape when they start to be stretched during germband extension (Fig. 1.3.2). At the same time, the amnioserosal fold is formed in both species. In *D. melanogaster* this fold remains quite stable and is formed exclusively by the amnioserosa while in *M. abdita* it progresses and it is formed by the amnion and the serosa. In Megaselia these two tissues split, the amnion remains in contact with the embryo as the amnioserosa in Drosophila, instead the serosa crawls over the embryo from dorsal to ventral and eventually encloses it (Fig. 1.3.3,4). The cells of the amnioserosa and serosa are stretched, even though the serosal cells undergo to higher stretching compare the amnioserosal cells. The dorsal opening of *D. melanogaster* is covered by the amnioserosa while in *M. abdita* it is covered by the amnion [Wotton et al., 2014]. After germband retraction, the embryo of Drosophila closes dorsally and the amnioserosa is internalized. In Megaselia, the dorsal opening of the embryo begins to close, the serosa ruptures at a ventral-posterior position, it retracts and in the end it is contracted into the embryo ([Wotton et al., 2014].

1.4 Genetics of extraembryonic tissue development in insects: similarities and differences

Even though the morphology of the extraembryonic tissue is different among flies, it is specified by the same homeobox transcription factor zerknüllt (zen). *zen* is derived from a duplication of the *hox3* gene during early radiation of

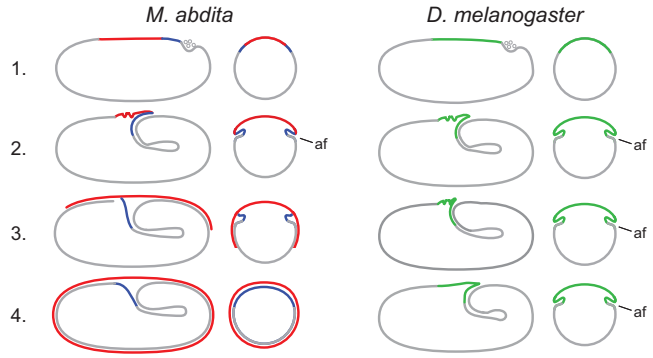

Figure 1.3: The extraembryonic tissues in *M. abdita* and *D. melanogaster*. Schema of *M. abdita* and *D. melanogaster* embryos during gastrulation represented in a lateral-middle section and in a cross section. (1) At the onset of germband extension in both species the extraembryonic tissue is in contact with the embryo. (2) During germband elongation the amniotic fold forms including amnion and serosa in *M. abdita* and exclusively the amnioserosa in *D. melanogaster*. (3) In *M. abdita* the serosa detaches from the amnion and crawls over the embryo, instead in *D. melanogaster* the amnioserosa remain in contact with it. (4) The serosa fuses and encloses the Megaselia embryo while the amnioserosa is still in constact with the epithelium. Red: serosa; blue: amnion; green: amnioserosa; grey: embryo. Amniotic fold, af. Anterior is left; dorsal is up.

insect, it lost its ancestral role in segment specification and acquired a new role during extraembryonic tissue specification [Schmidt-Ott et al., 2010]. Within the fly evolution, the extraembryonic tissue is still specified by zen but its expression is changed. For example, in *O. fasciatus Of-zen* is expressed first in the ventral and lateral side of the embryo and from the mid-germband stages it is expressed in the serosa [Panfilio et al., 2006]. *T. castaneum* has two zen genes, *Tc-zen1* and *Tc-zen2*. Both are similarly expressed in the presumptive serosa and at the anterior pole of blastoderm embryos [van der Zee et al., 2005]. During and after gastrulation they are expressed in the serosa and, while *Tc-zen1* remains confined to the serosa, *Tc-zen2* is expressed in the late amnion [van der Zee et al., 2005]. In lower flies as *M. abdita*, *Mab-zen* seems to specify exclusively the serosa and persists until the end of germband extension. Instead in higher flies like *D. melanogaster zen* specifies the entire amnioserosa and it is active only until mid-germband extension. Here, *zen* is among the first zygotically active genes and its expression is detectable during early blastoderm stage [Doyle et al., 1986]. At this time zen is activated by maternal genes, it is distributed in a broad domain (40% of the embryonic circumference) and is expressed in a dorsal-on/ventral-off pattern [Rushlow et al., 2001]. At mid-cellularization, *zen* activation becomes dependent on *decapentaplegic* (*dpp*), a

member of the TGF-β family as BMP, which is expressed in the same domain as *zen* [Padgett et al., 1987,St Johnston and Gelbart, 1987]. Genes of the TGF-β family can function as morphogens therefore they can induce different cell fates depending on their concentration. The highest concentration of *dpp* is in the dorsal midline of the embryo and decreases towards the lateral sides [Marqués et al., 1997, Rushlow et al., 2001]. For *zen* activation only a low level of *dpp* is necessary but for the refinement of its expression in the amnioserosa anlage (10% of the embryonic circumference), it requires high levels of *dpp* [Doyle et al., 1986, Rushlow and Levine, 1990]. In *D. melanogaster dpp* and *zen* regulate other genes, as *dorsocross* (*doc*) and *eiger* (*egr*), that are involved in the extraembryonic tissue development. *D. melanogaster* has three *doc* redundant paralogues: *dorsocross1* (*doc1*), *dorsocross2* (*doc2*) and *dorsocross3* (*doc3*), which are closely related members of a T-box family gene, and are present in a cluster. These genes originate from duplication events [Reim et al., 2003]. During cellularization these genes are expressed on the dorsal side of the embryo with the shape of a cross, giving origin to their name. The expression pattern of *doc1*, *doc2* and *doc3* is essentially identical within areas that receive high level of *dpp* but their expression in the dorsal midline depends on *dpp* and *zen* combined inputs (Reim et al., 2003). These three genes are necessary during embryogenesis for proper amnioserosa [Reim et al., 2003], heart [Reim and Frasch, 2005] and hindgut [Hamaguchi et al., 2012] development and have redundant functions. In *D. melanogaster* the *doc* genes are essential for full differentiation and maintenance of the amnioserosa, including the arrest of proliferation in this tissue since they inhibit *string*, a *cdc25* homolog [Reim et al., 2003]. The gene *eiger* is a homolog of the tumor necrosis factor alpha (TNF-α), which acts through the Jun N-terminal kinase (JNK) signaling pathway and it is involved in cellular and tissue processes as cell death, cell proliferation and tissue growth regulation. During gastrulation *egr* is expressed in the presumptive amnioserosa and it is activated by *dpp* and *zen* (Wang, 2006; PhD thesis). *egr*'s signaling is involved in a positive feedback process, promoting the interaction between *dpp* and its receptor. At the same time *crossveinless-2* (*cv-2*), another target gene of *zen*, inhibits *dpp* signaling. These feedback of *egr* and *cv-2*, refine *dpp* and *zen* patterns [Gavin-Smyth et al., 2013, Morisalo and Anderson, 1995, Schmidt-Ott et al., 2010]. It has been reported that in *D. melanogaster* the *doc* genes and *egr*, remodel the extracellular matrix (ECM)

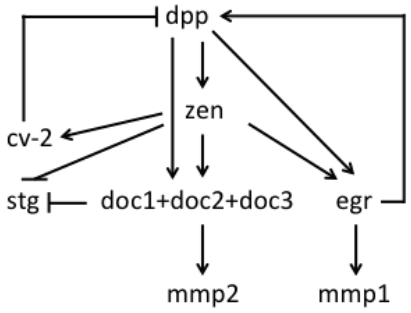

Figure 1.4: Genetic pathway related to *zen* in *D. melanogaster*. Schematic summary of the genetic pathway related to *zen* in *D. melanogaster*. This genetic network regulates the extraembryonic tissue specification and maintenance with the ecception of *mmp1* and *mmp2* that are responsible of the ECM modification in different tissues at later stages.

by activation of matrix metalloproteases (MMPs). Specifically, *egr* activates *mmp1*, but not *mmp2*, in disc eversion and tumor invasion [Pallavi et al., 2012, Srivastava et al., 2007], while the *doc* genes activate *mmp2* [Sui et al., 2012] to allow folds formation and progression in wing imaginal discs. The genes *doc* and *egr* regulate the activation of MMPs exclusively at late stages and it has been shown that in *D. melanogaster* the MMPs are not essential until the first instar larvae [Page-McCaw et al., 2003]. Therefore, there is no link between the amnioserosa and the MMPs.

1.5 MMPs - function and genetics

The MMPs are conserved proteins through multicellular organisms. Proteins belonging to this family have been described in plants [Maidment et al., 1999], in invertebrates like worms [Wada et al., 1998], sea urchin [T Lepage, 1990], hydra [Leontovich et al., 2000] and flies [Llano et al., 2000], and in vertebrates as fish [Wyatt et al., 2009], mouse [Page-McCaw et al., 2007] and human, where 24 *mmp* genes and four tissue inhibitor of metalloproteases (TIMPs) genes have been identified [Lohi et al., 2001, Marchenko et al., 2001, Uría and López-Otín, 2000, Brew et al., 2000]. The MMPs are translated as zymogen (inactive enzyme) and their signal peptide targets are the secretory vesicles. These proteins have a conserved pro domain, which contain a cysteine in the consensus sequence, and a catalytic domain that binds Zn^{2+} through the three

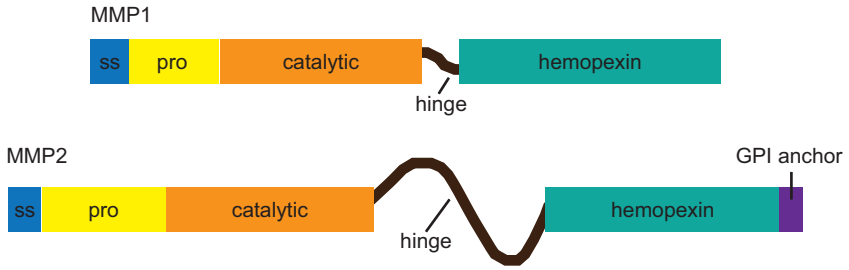

Figure 1.5: Schema of *D. melanogaster* MMPs. Each MMP of *D. melanogaster* has a signal sequence (ss), a pro domain (pro), a catalytic domain, a flexible hinge domain and a hemopexin domain. MMP2 has also a GPI anchor at the C-terminus. N-terminus is left.

conserved histidines. The cysteine-thiol and the zinc ion of the two domains interact to keep the proMMPs in an inactive state. After the catalytic domain the protein contains a flexible hinge region and the hemopexin-like domain for substrate binding and interaction with TIMPs. Some MMPs can have a transmembrane and a cytosolic domain, and a glycosylphosphatidylinositol (GPI) anchor signal. The proMMPs are activated by disruption of the thiol-Zn^{2+} interaction. *D. melanogaster* has only two MMPs (MMP1 and MMP2) and one common TIMP (Page-McCaw et al., 2003). MMP1 has a classical structure while MMP2 has an insertion between the catalytic and the hemopexin-like domain and a GPI-anchor at the C-terminal end (Fig. 1.5) [Llano et al., 2002]. Drosophila MMP1 is required for the growth of larval tracheae, it plays a role in the release of old cuticle in molding and with MMP2 in pupal head eversion [Page-McCaw et al., 2003]. The second MMP is also important for the fusion of the wing imaginal tissue. The double *mmp1-mmp2* mutant is able to complete embryogenesis and part of larval development, indicating that MMPs function is not required for *D. melanogaster* embryogenesis [Page-McCaw et al., 2003].

Aim

The aim of my thesis is to understand the cell- and tissue dynamics as well as the genetic basis of extraembryonic tissue development in *M. abdita*. My goal is to use this information in the context of available data on extraembryonic layer development in *M. abdita*, *D. melanogaster*, and other insects in order to develop a coherent model of how extraembryonic tissue behavior has changed during evolution. Specifically, how the single extraembryonic tissue in *D. melanogaster* (amnioserosa) evolved from its ancestor, which contained two distinct tissues, the dorsal amnion and the serosa. Due to this focus, the study is performed exclusively by functional and *in vivo* analyzes in *M. abdita* and by comparing its development with *D. melanogaster*.

2

Results

2.1 Extraembryonic development in *M. abdita* assessed by gene expression

Collective work in the fruit fly *D. melanogaster*, the scuttle fly *M. abdita*, the beetle *Tribolium castaneum*, and the bug *Oncopeltus fasciatus* suggests that extraembryonic tissue formation in insects is controlled by a genetic network downstream of the homeobox transcription factor Zerknüllt and the T-box transcription factor Dorsocross [Panfilio et al., 2006]; [Panfilio et al., 2013]; [Horn and Panfilio, 2016]; [Rafiqi et al., 2008]; [Rafiqi et al., 2010]. While *zen* has been shown to specify the amnioserosa and thus all dorsal extraembryonic tissues in *D. melanogaster*, in flies and insects with amnion and serosa the gene specifies the serosa only. Three copies of *dorsocross* in *D. melanogaster* collectively maintain amnioserosa development at late stages [Reim et al., 2003], while a single dorsocross copy is present in *T. castaneum* and it is required for extraembryonic morphogenesis but not maintenance of the serosa [Horn and Panfilio, 2016]. In Megaselia, only one single *dorsocross* gene has been reported and thought to function during extraembryonic tissue maintenance. To explore possible links between gene copy number, expression, and function of *dorsocross* in *M. abdita*, I have analyzed in detailed its expression. In addition I have also analyzed the expression of *egr*, which encodes a putative tumor necrosis factor in the JNK pathway and has been shown to be a target of *zen* in *D. melanogaster*. In *M. abdita*, *zen* is exclusively expressed in the

serosa until the end of the germband extension while in *D. melanogaster* it is active only until 50% germband elongation. It was shown [Rafiqi et al., 2008] that when *Mab-zen* is knocked down, Megaselia forms only one extraembryonic tissue that has the amniotic fate but that lost the expression of genes specific of the serosa. Based on this result, Rafiqi and colleagues proposed that the amnioserosa evolved by the loss of late *zen* expression. Since the amnioserosa of *D. melanogaster* shows the expression of serosa and amnion markers, we hypothesized that the transition from two tissues to one tissue could be due to a different regulation of genes downstream of *zen* and that subsequently *zen* regulation changed probably becoming shorter as it was no longer necessary in late stages. In particular, it has been shown in *D. melanogaster* that *dorsocross* has also a morphogenetic role late in development, as for example, in wing imaginal discs eversion [Sui et al., 2012], while in *T. castaneum* in the morphogenesis of the extraembryonic tissues. These morphogenetic roles could be a key passage to understand what happened during the evolution of the extraemrbyonic tissue.

2.1.1 Establishing a staging scheme by gene expression: *Mab-engrailed* in wild-type embryos

To be able to reliably stage embryos in fixed tissue, I cloned and used *engrailed* as developmental marker. This segment-polarity gene has been used previously to stage insect embryos ([Brown et al., 1994]; [Lemke and Schmidt-Ott, 2009]; [Schmidt-Ott et al., 1994]), and its expression allows to easily identify specific segments at different developmental times. Starting from the time when the serosa was fusing on the ventral side in wild-type embryos, *Mab-en* expression was analyzed by whole mount in situ hybridization or antibody staining in embryos developed at 25ºC. Similar to what was observed in other insects ([Brown et al., 1994]; [Lemke and Schmidt-Ott, 2009]; [Schmidt-Ott et al., 1994]), at the end of germband extension *Mab-en* was expressed in the ocular (Oc), antennal (Ant), intercalary (Ic), mandibular (Md), maxillar (Mx) and labial (La) segments of the head, in the three thoracic segments (T1-3) and the nine abdominal segments (A1-9) (Fig. 2.1). In particular, expression of *Mab-en* in the Oc segment could be used to stage development during critical windows of serosa development, i.e. split from the amnion and fusion on the

ventral side of the embryo. *Mab-en* was expressed in the Oc segment until 7h post deposition, corresponding to stages in which the wild-type serosa was not yet closed. By contrast, staining in Ic segment appeared from 6,5 to 10h post deposition, when the germband was retracting. These two segments co-expressed *Mab-en* only for 30 min (from 6,5 to 7h post deposition) and the serosa enclosed the embryo when *Mab-en* expression was no longer observed in the Oc segment but still in the Ic. This characteristic is important to relate the embryonic stage to the extraembryonic tissue development.

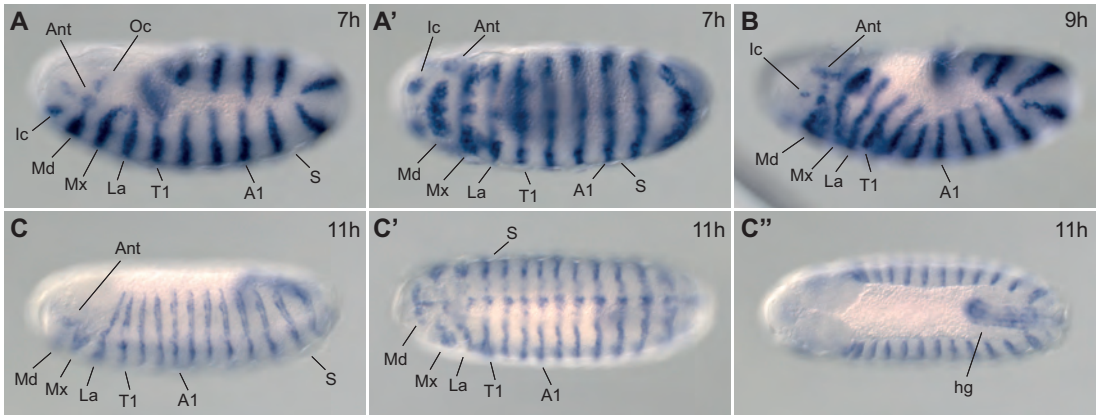

Figure 2.1: Embryonic development based on *Mab-en* expression. In situ hybridization of wild-type embryos at 6,5-7h (A-A'), 9,5h (B) and 11h post deposition (C-C"). The serosa is already fused (A-B) and not yet ruptured when the germband is completely retracted (C-C"). At 7h post deposition the embryo expressed en in both Oc and Ic segments (A-A') while at 9,5h *Mab-en* expression was visible only in the Ic but not in the Oc segment (B). At 11h (C) the morphology of the head changed and Mab-en is not any longer expressed in the Ic segment. The embryos are shown in a lateral (A, B, C), ventral (A', C') and dorsal (C") view. Abdominal segment 1 (A1); antennal segment (Ant); hindgut (hg); intercalary segment (Ic); labial segment (La); mandibular segment (Md); maxillary segment (Mx); ocular segment (Oc); serosa (S); thoracic segment 1 (T1).

2.1.2 Expression of *zen* in *M. abdita* coincides with the major steps of extraembryonic development

The expression of *zen* has been linked with major transitions in extraembryonic development of flies, beetles, and bugs [Schmidt-Ott and Kwan, 2016]. During early extraembryonic development, the continuous expression of this transcription factor in the serosa of *M. abdita*, *T. castaneum*, and *O. fasciatus* contrasts with the absence of zen expression in the amnioserosa of *D. melanogaster* during germband extension. Therefore, it has been suggested that this difference in *zen* expression might be critical for the serosa expansion and split from the adjacent amnion and/or ectoderm [Hilbrant et al., 2016]; [Rafiqi et al., 2008]. During late extraembryonic development, the onset of *zen* expression in the amnion has been associated with serosa rupture [Panfilio et al., 2006]; [Panfilio, 2009] [Panfilio and Roth, 2010]; [Schmidt-Ott and Kwan, 2016]; [van der Zee et al., 2005], suggesting that major morphogenetic events are triggered and controlled by the expression of this transcription factor. Here, I confirmed early expression of *Mab-zen* from cellularization onwards. During cellularization, *Mab-zen* mRNA was detected dorsally in a narrow stripe corresponding to the presumptive serosa (Fig. 2.2A). Unlike *D. melanogaster*, *zen* expression in *M. abdita* did not extend until the proctodeum since the amnion was located between this fold and the serosa. During germband extension, *Mab-zen* was expressed exclusively in the whole serosa (Fig. 2.2B), increasing in area as the serosa stretched and expanded (Fig. 2.2C,C'). This expression in the serosa, however, did not persist, and could not be detected between 6,5 and 8,5h post deposition, when the serosa was already detached from the embryo and ventrally fused (Fig. 2.2E). Interestingly, at 8,5-9h post deposition, *Mab-zen* was again expressed in the entire serosa (Fig. 2.2F) until its rupture and retraction. *Mab-zen* remained expressed in the serosa during dorsal closure, where the tissue covered the dorsal opening (Fig. 2.2G). This new expression data demonstrates that in *M. abdita* major steps of extraembryonic development coincide with the expression of *zen*.

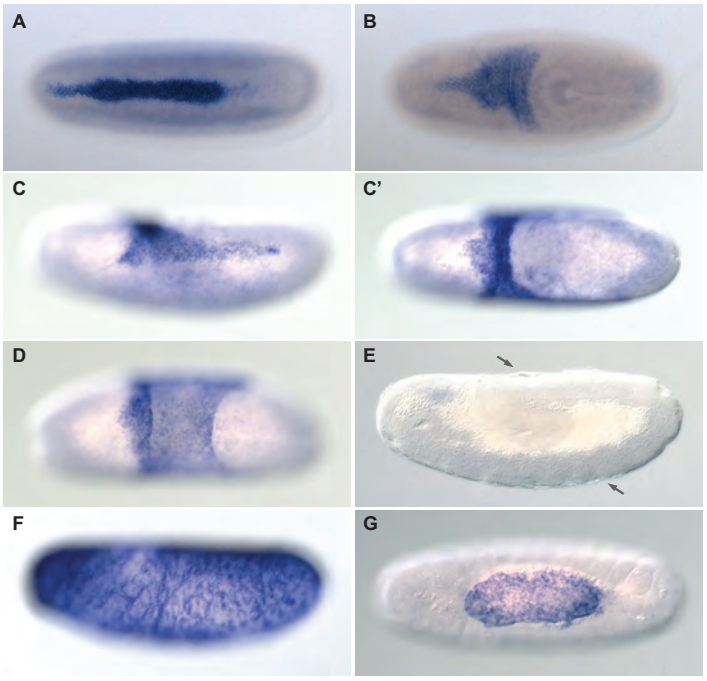

Figure 2.2: Expression of *zen* during serosa development in *M. abdita*. In situ hybridization of *Mab-zen* mRNA during cellularization (A), germband extension (B-F) and germband retraction (G). In (E) the arrows indicate the serosa that at 7 h post deposition was fused and showed no expression of *Mab-zen*. The embryos are shown in dorsal view in A-B,C'-D,G and in a lateral view in C,E-F. Anterior is left.

2.1.3 Two *dorsocross* paralogues pattern the extraembryonic tissue in *M. abdita*

The expression and function of three *doc* genes has been linked to extraembryonic differentiation and maintenance in *D. melanogaster* [Reim et al., 2003] (Reim et al., 2003), while expression and function of a single doc gene has been linked to extraembryonic morphogenesis in *T. castaneum* [Horn and Panfilio, 2016] (Horn et al., 2016). Previous reports suggested that the genome of *M. abdita* contains a single *doc* gene and thus the ancestral gene set. In contrast to the presumably ancestral function of *doc* in *T. castaneum*, the *Mab-doc* gene was reported to fulfill a more Drosophila-like function in the maintenance of the extraemrbyonic tissue [Rafiqi et al., 2010]. This raised the possibility of additional copies of doc present in the genome of *M. abdita*. Using extensive database searches, I was able to identify two copies of *doc*: *dorsocrossA* (*docA*), which has been previously reported [Rafiqi et al., 2010], and a newly identified heterologous that I designated *dorsocrossB* (*docB*). The homologue genes

Mab-docA and *Mab-docB* had an almost identical expression pattern during cellularization and early stages of gastrulation. The two genes were expressed along the dorsal midline of the embryo in the anlagen of the extraembryonic tissue, in the procephalic neuroectoderm (pne) and at the posterior end of the dorsal midline in a weak circumferential stripe at the posterior pole (Fig. 2.3A-B'). In the early stages of germband extension (20% extension, 0% posterior pole), the extraembryonic tissue anlage was shorter and wider than before (Fig. 2.3B-B'). When the germband elongation reached 50% of the embryos' length, the *Mab-doc* genes were expressed in the extraembryonic tissue, probably amnion and serosa, and *Mab-docA* was additionally expressed in the head region in a spot along the dorsal midline (Fig. 2.3C-C'). As the germband extension proceeded, *docA* and *docB* expression was maintained in the procephalic neuroectoderm and both of them were expressed in the clypeolabrum. Moreover, these genes are expressed in the nuclei of the amnion and in a metameric pattern, probably alternating with the tracheal placodes (Fig. 2.3D-E') as reported for *D. melanogaster* (Reim et al., 2003). When the germband reached its maximum extension, *docA* and *docB* also showed expression in the leading edge of the epithelium (Fig. 2.3F,F'). Prior to germband retraction, a new onset of gene expression of *docA* and *docB* was observed in the serosa (Fig. 2.3G,G'). When the germband retracted, *docA* and *–B* were still expressed in the epithelia at the border with the amnion, in some regions of the head, in the thoracic and abdominal segments, as well as in the posterior spiracles and in the peripheral nervous system (Fig. 2.3H-I'). The discovery of a second copy of *dorsocross* in *M. abdita* supports the hypothesis [Rafiqi et al., 2010] that these genes have a partial Drosophila-like role and that probably this function was acquired during evolution increasing the number of doc copies. Since *M. abdita* has an amnion and a serosa, it is possible that *Mab-docA* and *Mab-docB* may be involved in the regulation of the extraembryonic tissues morphogenesis as in *T. castaneum* [Horn et al., 2015] [Horn and Panfilio, 2016]. Therefore in *M. abdita* *dorsocross* could have a function in between *doc1-2-3* of *D. melanogaster* [Reim et al., 2003] and *Tc-doc* of *T. castaneum* [Horn et al., 2015] [Horn and Panfilio, 2016].

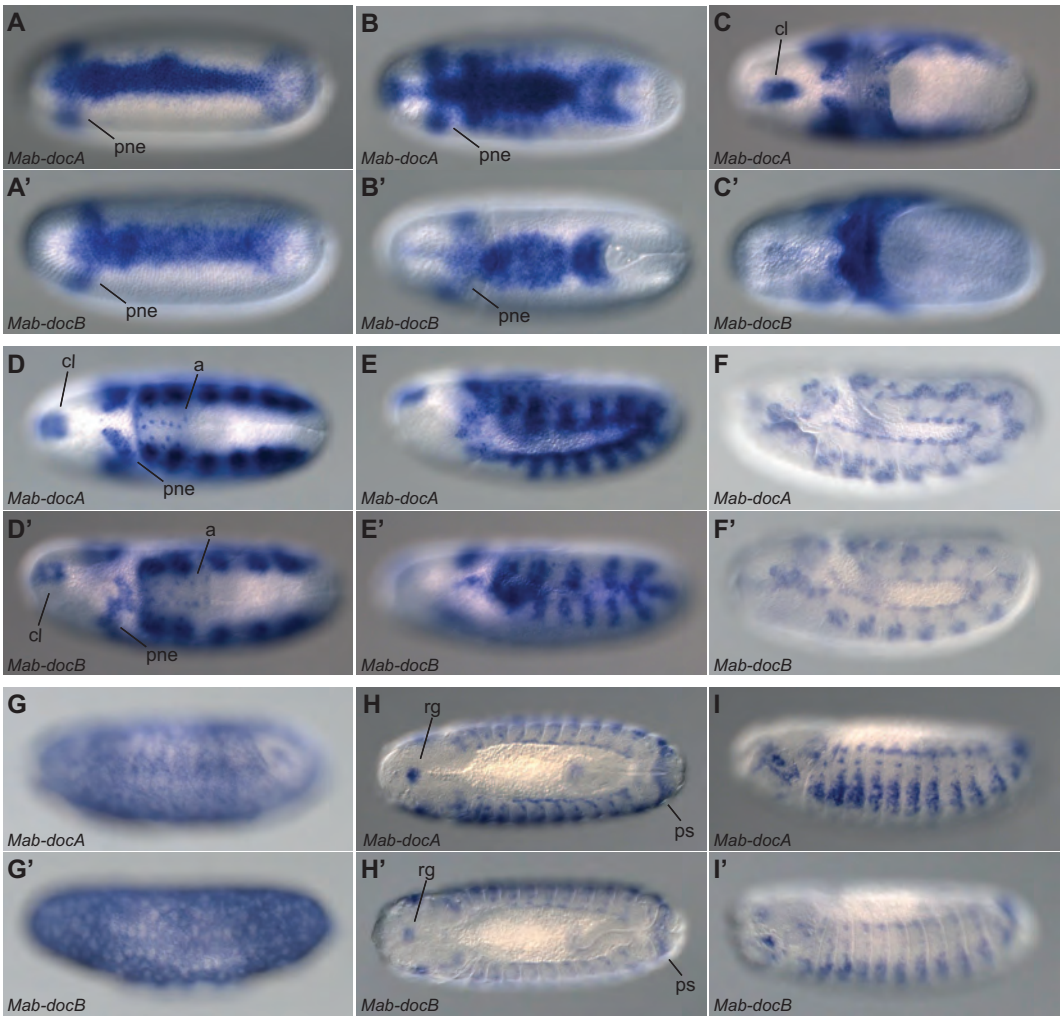

Figure 2.3: *Mab-docA* and *Mab-docB* share expression domains during early embryonic and extraembryonic development. The in situ hybridization shows the expression pattern during cellularization (A,A'), fast germband extension (B,B'), slow germband extension (C-E'), maximum germband extension (F-G') and germband retraction (H-I') of the genes docA and docB. In (G) the serosa is broken at the posterior pole for a technical issue. In (H,H') *Mab-docA* and *Mab-docB* are expressed in a head region that closely resembles the ring gland (Sánchez-Higueras et al., 2014). The embryos are in a dorsal view in (A-D') and (H,H'), in a lateral view in (E-G') and (I,I'). Anterior is left. Amnion (a); clypeolabrum (cl); procephalic neuroectoderm (pne); posterior spiracles (ps); ring gland (rg).

2.1.4 *Mab-egr* expression is consistent with the role in amnion development

During extraembryonic development of *M. abdita* and other insects with amnion and serosa formation, the two distinct tissues separate in a zen-dependent manner [Rafiqi et al., 2008] [van der Zee et al., 2005], suggesting that the initial origin of the amnioserosa as single extraembryonic tissue was associated with changes in the regulation of *zen* expression and/or changes in how *zen* activity affects cell behavior [Schmidt-Ott and Kwan, 2016]. Based on its function in *D. melanogaster*, a possible candidate gene that can combine downstream effector function of zen activity as well as upstream regulatory input, is the tumor necrosis factor homolog *eiger* (*egr*). In *D. melanogaster*, *egr* expression is regulated by *zen* and acts upstream of the JNK pathway, which in extraembryonic development has been shown to be regulating the amnioserosa cell shape and contraction, germband retraction and dorsal closure [Zhang et al., 2010]. In other contexts, expression of *egr* has been shown to induce apoptosis [Moreno et al., 2002]. At the same time *egr* is a downstream target of *zen* activity and in *D. melanogaster* also regulates *zen* activity in a feedback loop [Gavin-Smyth et al., 2013]. To test whether in *M. abdita egr* may contribute to extraembryonic development, the orthologue was cloned and is expression was studied during extraembryonic tissue development.

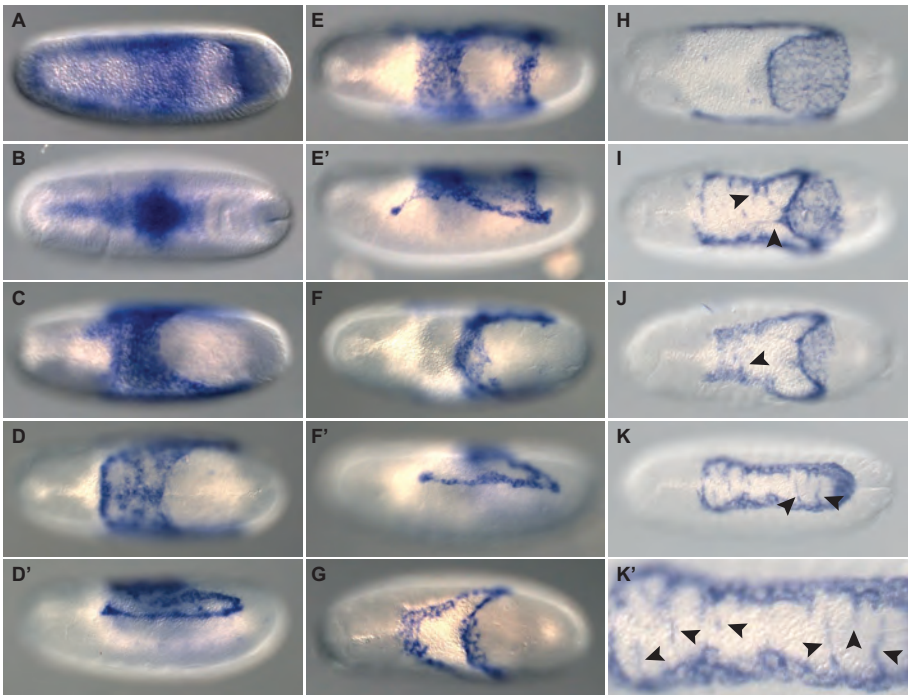

Figure 2.4: Expression of *egr* in *M. abdita* suggests that the tumor necrosis factor homolog is a marker of the developing amnion. In situ hybridization shows *egr* mRNA expression pattern at cellularization (A), onset of germband extension (B), mid- (C) and end (D-E') of germband extension, and prior (F-G), during (H-J) and end (K,K') of germband retraction. In early stages *Mab-egr* was expressed in the dorsal area where the extraemrbyonic tissue is specified (A-B) and at 50% germband elongation its expression seems to be in the serosa and the amnion (C). In later stages Mab-egr expression appeared restricted, possibly to the amnion (D-K). During germband retraction the cells expressing *Mab-egr* at the boundary of the dorsal opening, formed protrusion extending toward the dorsal midline (I-K'). Arrowheads indicate the filopodia. Anterior is left. The embryos in (A-D,E,F,G-K') are shown in the dorsal view while in (D',E',F') are in lateral view.

Mab-egr was expressed at the onset of gastrulation on the dorsal side of the embryo in a poorly defined transverse central domain (Fig. 2.4A). At the onset of germband extension, *egr* was detected on the dorsal midline of the embryo in a more defined domain overlapping in part with zen expression (compare Fig. 2.4B with Fig. 2.4A,B). Notably *egr* had a higher expression in the mid of the dorsal side of the embryo where, presumably, the amnion was specified. At 50% germband elongation, *egr* expression was wider and ranged from the posterior side of the head to the anterior tip of the germband (Fig. 2.4C). In progressive stages of germband extension, expression of *egr* was observed in successively broader domains. When the germband reached 60% of the embryo's length, egr expression seems to be restricted to the boundary with the ectoderm and on

the tip of the germband, either because the domain of activation was reduced or because the tissue in which it was expressed (presumably the amnion) changed shape. Its expression was still present on the dorsal side of the embryo and along the leading edge of the extraembryonic tissue, but not on the lateral side of the germband (Fig. 2.4D,D'). This suggests that at this stage of extraembryonic development the lateral flanks were no longer a homogeneous tissue but comprised a thin line of amnion cells adjacent to the ectoderm as well as a covering serosa. In embryos in which the anterior midgut was invaginated and the serosa was completely fused, the tissue, that presumably was the amnion, formed a rectangle on the dorsal side of the germband (Fig. 2.4E,E'). This tissue was not uniformly stained presenting a central-square like shape region with no expression. Moreover, *egr* continued to be expressed at the leading edge of the extraembryonic tissue (Fig. 2.4F,F'). Later, it became restricted to the boundary of the presumptive amnion in contact with the leading edge of the epithelial cells (Fig. 2.4G). During germband retraction, it was laterally attached at the leading edge and covered the anterior part of the germband (Fig. 2.4H). At this stage, protrusions from the lateral towards the dorsal side of the embryo appeared (Fig. 2.4I-J). When the germband retraction was completed, the tissue was attached to the embryo on each side, the protrusions began to touch each other from the opposite side and the dorsal opening was reduced (Fig. 2.4K,K'). The embryos were showing an open dorsal tissue with only two rows of cells wide at the lateral sides and wider at the posterior, which was the area covering the germband and that unfolded during the germband retraction. Our expression analysis of *Mab-egr* and personal communication with Chun Wai Kwan (Schmidt-Ott lab, University of Chicago) is consistent with the idea that *egr* marks the developing amnion. If this is the case, the amnion would not close immediately after the serosa detached, but rather only once the germband retracted completely. To test this possibility, further live imaging analysis is necessary.

2.2 Analyzing the contributions of *zen*, *doc*, and *egr* in extraembryonic development

To understand in which way *zen*, *doc*, and *egr* contribute to extraembryonic development in *M. abdita*, serosa formation was analyzed at various stages of development after knockdown of gene function by RNA interference (RNAi). To test whether a gene affected serosa development, the dsRNA was injected in *M. abdita* embryos at blastoderm stage, the embryos were left to develop at 25°C in a moist chamber and then fixed at different stages. After manual devitellinization, shape and fate of the extraembryonic tissue was detected by in situ hybridization, in which embryos were stained with a serosa marker (*Mab-zen* or *Mab-ddc*).

2.2.1 Function of *zen* in the extraembryonic tissue of *M. abdita*

To re-assess *Mab-zen* function in the context of tissue morphogenesis, the gene was knocked down and the serosa phenotype studied after 7h of embryonic development. In wild-type development, 7h-old embryos were characterized by complete germband extension, posterior and anterior hindgut invagination, and the serosa was complete and fused on the ventral side of the embryo (Fig. 2.5A). In *Mab-zen* RNAi embryos, careful analyses at the microscope revealed only a single dorsal extraembryonic tissue after 7h of development (117/118), which did not stain positive for the serosa marker *ddc* (Fig. 2.5B). These results confirm previous analyses suggesting that in the absence of *Mab-zen*, *M. abdita* does not develop a sersoa but only a single, amnioserosa-like extraembryonic epithelium [Rafiqi et al., 2008] [Rafiqi et al., 2010]. These embryos were stained also with DAPI, which confirmed the presence of big nuclei only in the area of the amnioserosa-like but not around the embryo as when the serosa is present (Fig. 2.5C,C'). The function of the genes downstream of *zen* was then studied.

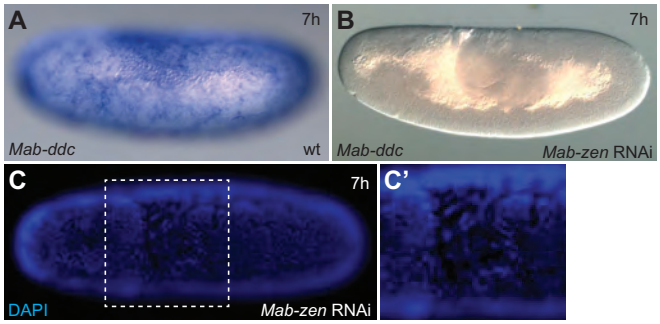

Figure 2.5: *Mab-zen* RNAi embryos have no serosa. (A) In situ hybridization of *M. abdita* wild-type embryo stained with *Mab-ddc* at 7h post deposition. The serosa is completely extended and fused. (B) In situ hybridization of *Mab-zen* RNAi embryo stained with *Mab-ddc*. This 7h old embryo is missing the serosa therefore it does not express the serosa marker. (C,C') Dorsal view of the embryo shown in (B) stained with DAPI. The close up (C') showed the nuclei of the extraembryonic tissue that are not as large as the one of the serosa at its maximum extension. (A,B) Embryos in a lateral view. (C,C') Embryo in the dorsal view. Anterior is left.

2.2.2 *Mab-docA* and *Mab-docB* function in the serosa: maintenance or morphogenesis?

Previous work analyzed the function of *Mab-docA* (the *Mab-dorsocross* gene already reported in the 2010). They identified a role during germband retraction and dorsal closure by the analysis of cuticles [Rafiqi et al., 2010]. Based on nuclear staining and tissue morphology, serosa formation and specification appeared to be not affected, and thus led to speculations that *Mab-docA* functions in amnion tissue maintenance [Rafiqi et al., 2010]. To test whether essential functions of *dorsocross* in *M. abdita* has been overlooked or were masked in previous analyses due to likely complementation by the second gene copy, both genes were knocked down by double RNAi experiments. After 7h post deposition it was observed that the serosa was not expanded but was on the dorsal side of the embryo (81/89, Fig. 2.6B,B'). Contrary to *Mab-zen* RNAi embryos, this dorsal extraembryonic tissue was expressing *Mab-zen* and *Mab-ddc*, suggesting that in *Mab-docA-B* double knockdown embryos, the serosa was specified and its fate maintained. In about a third of the embryo (23/89), the phenotype of double doc knockdown appeared most severe and resulted in an amnioserosa-shaped, dorsally limited, and non-expanding serosa (Fig. 2.6B), while in the remaining two thirds (52/89) the phenotype was milder (Fig. 2.6B') and produced a serosa that was covering the dorsal side until the

anterior and posterior poles. Using En staining, it was confirmed that the overall timing of the embryonic development was not affected (data not shown) and that the down regulation of *Mab-docA* and *Mab-docB* had a major effect on the extraembryonic tissue development. In addition to defects in extraembryonic tissue formation, *dorsocross* knock down in *M. abdita* embryos caused a change in the morphology of the head, which appeared reduced and more round than the wild type. This phenotype of the head was in line with the morphological defects reported in *D. melanogaster* mutants *Df(3L)DocA* and RNAi-treated embryos, where they have a reduction of the embryonic head structures and often the head involution fails at later stages [Reim et al., 2003]. These results suggest that in *M. abdita docA* and *docB* are not necessary for the initial specification of the serosa. Moreover, I noticed that when these two genes were knocked down, *Mab-zen* expression was prolonged beyond 7h post deposition, suggesting the existence of a feedback loop between *Mab-docA-B* and *Mab-zen* (Fig. 2.6C,C'). In *D. melanogaster*, *doc* function has been associated with extraembryonic tissue maintenance (Reim et al., 2003), instead in *T. castaneum* with extraembryonic tissue morphogenesis (Horn and Panfilio, 2016). To assess whether doc function in *M. abdita* fell into one of these two categories, extraembryonic development was analyzed following double knockdown of *Mab-docA* and *Mab-docB* also at later stages of development, i.e. nine and eleven hours after deposition. Following 9h of development, the serosa remained as a small, non-expanded tissue patch on the dorsal side in only one severely affected embryo (1/22, Fig. 2.6C), and showed an intermediate phenotype of a partially expanded serosa in mildly affected embryos (16/22, Fig. 2.6C'). Following 11h of development in *Mab-docA*/*Mab-docB* double knock down embryos, 64% of the embryos displayed a fully developed serosa (36/56, Fig. 2.6D). To test whether at late stage of development *Mab-docA* and *Mab-docB* were still efficiently knocked down, the expression of either gene was tested by in situ hybridization at 8-9h post deposition. Notably, both genes were expressed in a metameric pattern along the germband (12/14 embryos stained with *Mab-docA*; 27/48 embryos stained with *Mab-docB*) as in the wild type (Fig. 6E,F), suggesting that RNAi was no longer effective. Taken together, the functional analysis of dorsocross function in *M. abdita* suggested that the two genes are essential for serosa morphogenesis but not maintenance.

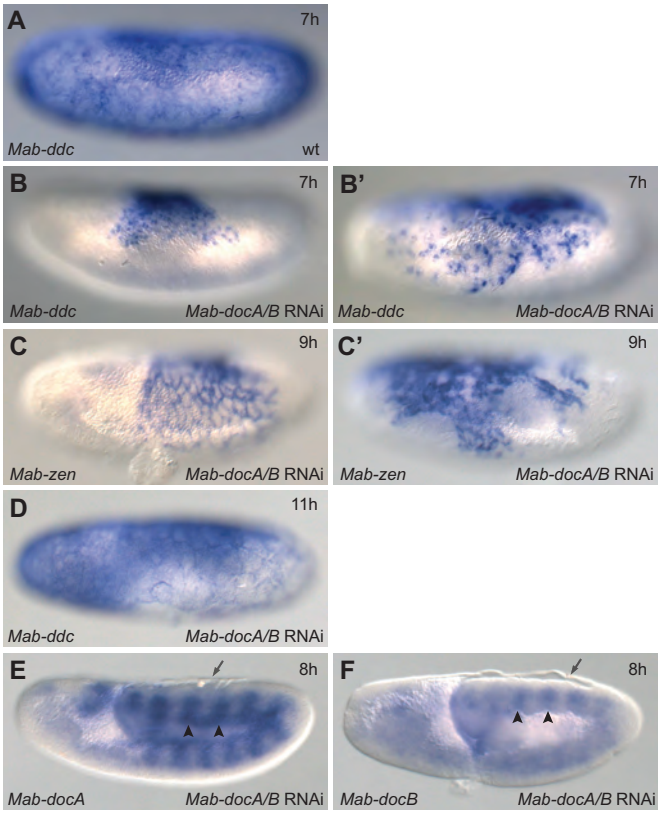

Figure 2.6: *Mab-docA* and *Mab-docB* are necessary for the serosa morphogenesis. In situ hybridization of *M. abdita* wild type and *Mab-docA/B* RNAi embryos at different developmental stages. (A) *M. abdita* wild-type embryo at 7h post deposition stained with *Mab-ddc*. (B,B') *Mab-docA/B RNAi* embryos at 7h post deposition stained with *Mab-ddc* showed strong (B) and mild (B') phenotype. (C,C') *Mab-docA/B* RNAi embryos at 9h post deposition stained with *Mab-zen* showed strong (C) and mild (C') phenotype. (D) *Mab-docA/B* RNAi embryos at 11h post deposition stained with *Mab-ddc* showed a completely extended serosa. (E,F) *Mab-docA/B* RNAi embryos at 8h post deposition tested for RNAi efficiency and stained with *Mab-docA* (E) and *Mab-docB* (F). (E,F) The arrowheads indicate the expression of *Mab-docA* and *Mab-docB* in the parasegments (only two are indicated). The arrow indicates the serosa that is still dorsal and not yet detached. Embryos are shown in a lateral view. Anterior is left.

2.2.3 *Mab-egr* is involved in the extraemrbyonic morphogenesis

Expression of *Mab-egr* in the putative amnion anlage (Fig. 2.4) suggested a role in amnion specification and/or morphogenesis. To test whether extraembryonic development was affected in *Mab-egr* RNAi embryos, the injected embryos were stained with *Mab-ddc* and/or *Mab-zen*. Following *Mab-egr* knockdown, a single dorsal extraembryonic tissue was observed in about 20% of embryos at 7h after

deposition, which was positive for *Mab-zen* and/or *Mab-ddc* staining and thus was likely to represent a non-expanded serosa (16/84, Fig. 2.7B). In about 30% of the embryos, serosa expansion was observed at a reduced rate, and the serosa covered the entire dorsal side of the embryo (24/84, not shown). In a bit more than 50% of the embryos, serosa development appeared unaffected (44/84, not shown). Notably, like for knockdown of *Mab-docA* and *Mab-docB*, serosa specification could be evaluated by staining for *Mab-ddc* as well as *Mab-zen*, which in wild-type embryos is typically lost at this stage (Fig. 2.2E). In addition of affecting serosa morphogenesis, *Mab-egr* may thus also play a role in serosa specification through regulating expression of *Mab-zen*.

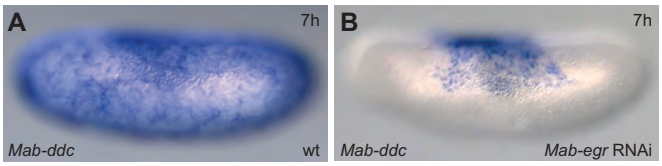

Figure 2.7: *Mab-egr* RNAi embryos had a reduced serosa. In situ hybridization of wild type (A) and *Mab-egr* RNAi (B) embryos at 7h post deposition. The embryos are stained with *Mab-ddc*. (B) *Mab-egr* RNAi embryo presented a strong phenotype. Anterior is left.

The common phenotype shown by *Mab-egr* RNAi and *Mab-docA/B* RNAi embryos, suggests that these genes may redundantly act on common target genes or developmental processes. To test this hypothesis, a triple-knock down of *Mab-docA*, *Mab-docB* and *Mab-egr* was performed. Also in this case, the embryos had a non-expanded serosa at 7h post deposition as in the double and single knock down respectively (compare Fig. 2.8B with Fig. 2.6B and Fig. 2.7B). This phenotype was observed in 96% (72/75) of the injected embryos, which was a higher rate than *Mab-docA/B* and *Mab-egr* individual knock down. This result supports the hypothesis that *Mab-egr* acts, at least partially, in redundancy with *Mab-docA* and *Mab-docB* on a common target gene. Notably, all three genes were involved in the serosa expansion and thus morphogenesis, but not in its specification since their knockdown did not prevent the formation of the serosa, contrary to the absence of *Mab-zen*.

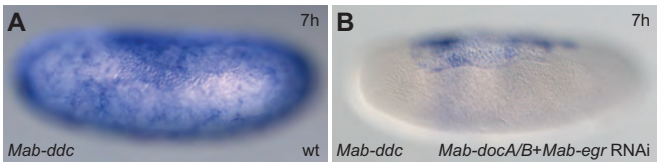

Figure 2.8: *Mab-docA*, *Mab-docB* and *Mab-egr* co-knock down. In situ hybridization of wild type (A) and *Mab-docA/B+MAb-egr* RNAi (B) embryos at 7h post deposition. The embryos are stained with *Mab-ddc*. (B) *Mab-docA/B+Mab-egr* RNAi embryo presented a strong phenotype. Anterior is left.

2.2.4 ECM remodeling during serosa expansion – a putative common cell biological target of *Mab-doc* and *Mab-egr* activity

Triple knockdown of *Mab-docA*, *Mab-docB*, and *Mab-egr* suggested that all three genes had a common developmental target in extraembryonic development that appears to be linked to expansion of the serosa. One such possible target could be the remodeling of the ECM, which in Drosophila has been shown be regulated, in part, by the two metalloproteases MMP1 and MMP2 [Llano et al., 2000] [Llano et al., 2002]. In *D. melanogaster*, *doc1*, *doc2* and *doc3* activate *mmp2* [Sui et al., 2012] while *egr* activates *mmp1* [Pallavi et al., 2012] [Srivastava et al., 2007]. The expression and knockdown functions of *Mab-docA-B* and *Mab-egr* in the extraembryonic tissue of *M. abdita* supported the hypothesis that the remodeling of the ECM could be necessary to initiate serosa expansion. To test this hypothesis, orthologues of *mmp1* and *mmp2* were identified in *M. abdita*, and their putative function in serosa expansion was investigated by functional knock down using RNAi at different stages of development. Following 7h post deposition, about half of the *Mab-mmp1* RNAi embryos were severely affected and characterized by a lack of serosa expansion (80/145, Fig. 2.9B) as judged by expression of *Mab-ddc*. In most of the remaining embryos, a milder phenotype was observed in which the serosa appeared to have expanded, albeit to a much lesser degree than in wild type (61/145, data not shown). Overall, the *Mab-mmp1* RNAi phenotypes resembled the triple RNAi knockdown phenotypes of *Mab-docA/docB/egr* RNAi embryos, although overall a significantly higher proportion of embryos displayed the severe phenotype with a complete lack of serosa expansion. Consistent with the role of MMPs in Drosophila, my results suggested that *Mab-mmp1* is involved in morphogenesis but not in specification or maintenance of extraembryonic tissues. Accordingly, *Mab-mmp1* RNAi embryos are likely to have specified both extraembryonic tissue types, a serosa and an amnion, and thus feature a single dorsal extraembryonic epithelium that is made up of two distinct domains: a central serosa and a peripheral amnion. This dorsal tissue is markedly different from the one that is formed in *Mab-zen* RNAi embryos, where lack of zen activity is thought to transform the remaining dorsal tis-

sue into an amnion [Rafiqi et al., 2008]. Previous results have indicated that a serosa in *M. abdita* may be not absolutely required for embryonic development, and that a dorsal, amnion-like extraembryonic epithelium in Mab-zen RNAi embryos may be sufficient for the development of viable larvae [Rafiqi et al., 2008]. To test whether, in the absence of wild-type serosa formation, development of viable larva was different depending on whether the remaining dorsal epithelium consisted of amnion-plus-serosa tissue or just an amnion-like extraembryonic epithelium, injected embryos were left develop until first instar larva and their cuticles were analyzed (data not shown).

In case of *Mab-zen* RNAi, about one third (17/54) of the cuticles had a wild-type phenotype. The others shown dorsal opening or the segments were not properly aligned and fused. In case of *Mab-mmp1* knocked-down embryos, 60% (21/35) developed wild-type cuticles, and only 40% were affected by showing a dorsal-open phenotype or defects in the region of the head. The defects reported in the head could be due to an improper head involution as reported for some *D. melanogaster mmp1* mutants (Page-McCaw et al., 2003). The possible difference of the phenotypes between *Mab-zen* and *Mab-mmp1* RNAi embryos could be explained by the presence of a single and uniform extraembryonic tissue in the absence of *Mab-zen* and of a single but composite tissue in the absence of *Mab-mmp1*. Alternatively, and possibly in analogy to late *Mab-doc* RNAi embryos, it may be possible that development of the full complement of extraembryonic tissue was delayed in *Mab-mmp1* RNAi embryos, but not stopped. Accordingly, serosa formation may have "caught up" at a later stage of development and thus enabled higher rates of wild-type larva formation. To distinguish between these possibilities, embryonic development was investigated at intermediate stages. At 9h post deposition, the serosa in *Mab-mmp1* RNAi embryos was not yet fused, mainly showing a mild phenotype (27/83) with the serosa expanded until mid lateral side, and only a few (3/83) had strong phenotype with a dorsal serosa (Fig. 2.9C). At 11h post deposition, the serosa was even more expanded. Precisely, none of the injected embryos showed a strong phenotype, 23% a mild phenotype (9/39) and 77% of the embryos (30/39) showed a fused serosa as the wild type. These differences in phenotypes depending on developmental age of the embryos either indicate that alternative genes and/or mechanisms compensate for the loss of mmp1 activity, or that gene knockdown becomes inefficient at later stages of

development. To test whether gene knock down by RNAi was efficient still at late stages of development, 11-hour-old *Mab-mmp1* RNAi embryos were tested for *mmp1* expression by in situ hybridization. Surprisingly, almost all (42/51) 11h old embryos expressed *Mab-mmp1* in the serosa of *M. abdita* embryos (Fig. 2.9D), suggesting that RNAi was no longer efficient at late embryonic stages in the serosa – possibly because this tissue is only in scarce contact with the rest of the embryo and shuts itself off the embryo-wide RNAi machinery. To test whether this lack of gene knock down could be overcome in a mutant background, *Mab-mmp1* was targeted by CRISPR/Cas9 in freshly deposited embryos. To this end, Cas9 mRNA and three different sgRNAs were co-injected to target *Mab-mmp1*. At 7h post deposition, *Mab-mmp1* CRISPR embryos showed a lack of serosa expansion in about 57% (77/136) of all embryos (Fig. 2.9E). Presumably, because the embryos presented mosaic mutants in which wild-type cells still contributed to Mab-MMP1 activity, the amount of embryos showing a reduced serosa at 7h post deposition was lower than the *Mab-mmp1* RNAi (57% versus 97%). At 11h post deposition, the serosa of the knocked out embryos was extended and fused as in the wild type in 84% (57/68) of the injected embryos (Fig. 2.9F).

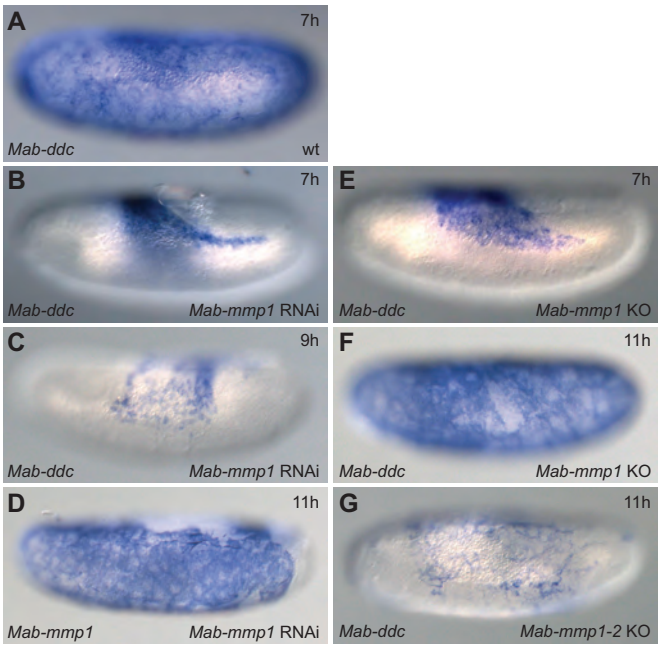

Figure 2.9: *Mab-mmp1* RNAi and knock out caused the same phenotype in the extraembryonic tissue. In situ hybridization of wild type, *Mab-mmp1* RNAi, *Mab-mmp1* and *Mab-mmp1-2* knock out by CRISPR/Cas9. (A) Wild-type embryo at 7h post deposition stained with *Mab-ddc*. (B,C) *Mab-mmp1* RNAi embryos at 7h (B) and 9h (C) post deposition stained with *Mab-ddc* showed a strong reduction of the serosa. (D) *Mab-mmp1* RNAi embryo at 11h post deposition stained with *Mab-mmp1*. The serosa is expanded and expressed *Mab-mmp1* mRNA, meaning a failure in the knock down of the gene. (E,F) *Mab-mmp1* knock out embryos at 7h (E) and 11h (F) post deposition stained with *Mab-ddc*. (G) *Mab-mmp1* and *Mab-mmp2* co-knock out embryo at 11h post deposition stained with *Mab-ddc*. The embryos in (D-G) showed a broken or reduced serosa due to a technical problem during manual devitellinization. The embryos are shown in a lateral view. Anterior is left.

In order to test whether *Mab-mmp2* had a redundant function with *Mab-mmp1*, double knock out of *mmp1* and *mmp2* was performed. Also in this case the CRISPR/Cas9 technique was used, co-injecting three sgRNAs per gene and the Cas9 mRNA at blastoderm stage. At 11h post deposition the embryos were showing a complete serosa in 94% (88/94) of the embryos (Fig. 2.9G). Taken together, both experiments confirmed the result obtained by RNAi, and may suggest that *mmp1* and/or *mmp2* in *M. abdita* facilitate the detachment and the initial expansion of the serosa but that they do not constitute the only molecular mechanism that contributes to the serosa detachment. However, because MMP1 and MMP2 have been reported to be a secreted and diffusible protein, I currently cannot exclude the possibility that non-mutant cells even-

tually secreted enough metalloprotease for the necessary activity to allowed the serosa detachment.

2.3 *M. abdita* wild-type extraembryonic development – an *in vivo* analysis

Work in established model systems has demonstrated the power of *in vivo* analyses of the dynamic processes in early development such as nervous system formation, gastrulation, and extraembryonic development [Keller, 2013]; [Hilbrant et al., 2016]; [Hara et al., 2016]; [Schöck and Perrimon, 2002]. The accurate description of wild type development at a high spatial and temporal resolution has repeatedly served as basis to understand core principles of developmental dynamics. In the context of insect extraembryonic development, time-lapse recordings of the process have provided, at the organismal level, a better understanding of dorsal closure [Jankovics and Brunner, 2006] [Solon et al., 2009], the role of extraembryonic epithelia during germband retraction, anatrepsis, and katatrepsis [Panfilio, 2009]; [van der Zee et al., 2005]. At the tissue and cellular level, time-lapse recordings were used to identify critical time windows and dynamics for extraembryonic tissue expansion, separation, fusion, and internalization. Time-lapse recordings have in particular allowed to follow developmental processes and thus generate a true map of the sequence of events. To follow up on the development of the cells which in fixed embryos showed expression of *Mab-egr*, and to better understand the dynamics of serosa separation, expansion, and ventral fusion, I decided to establish time-lapse recordings for *M. abdita*.

2.3.1 Technical considerations

Extraembryonic development in *M. abdita* is a dynamic process that lasts for 10 to 14 hours and takes place during almost the entire embryogenesis from gastrulation to dorsal closure. The serosa is specified at the blastoderm stage on the dorsal side of the embryo, expands and eventually fuses ventrally. Accordingly, the most important requirement for an *in vivo* analysis of this developmental process was to image the embryo in its entirety and as gentle as possible. A

microscope that allows long imaging, *in toto* and at high temporal resolution with low photo-toxicity is a Multiview Selective-Plane Illumination Microscope (MuVi-SPIM).

The use of a MuVi-SPIM for *in vivo* time-lapse recordings requires fluorescently labeled samples [Keller, 2013]. For model organisms, transgenic lines with ubiquitously expressed markers outlining cell membrane, nuclei, or other cellular components and structures are readily available [Edwards et al., 1997]; [Martin and Wood, 2002]; [Riedl et al., 2008]. However, such tools have not yet been established for *M. abdita*. During the course of my PhD, I therefore established a protocol for stable transgenesis in *M. abdita* and generated a transgenic line that expressed *Mab-His2Av-mCherry* as nuclear marker that could be used for MuVi-SPIM time-lapse recordings ([Caroti et al., 2015] and Appendix 2). Although the transgenic *M. abdita* retained the insertion, it was not possible to maintain the ubiquitous expression of *Mab-His2Av-mCherry* over more than ten generations ([Caroti et al., 2015] and Appendix 2), exposing one of several challenges in the usage of transgenic lines to introduce fluorescent markers. Aside from a loss or selective silencing of transgene expression, it has been difficult to identify *M. abdita* enhancer sequences that could be used for ubiquitous transgene expression. Until very recently [Vicoso and Bachtrog, 2015], available genome assemblies of *M. abdita* had been sufficient to identify genes, but not good enough to identify several kilobases of putative regulatory sequence upstream or downstream of the putative coding sequence. As possible alternative to ubiquitous transgenic expression, the injection of mRNA encoding, e.g., a His2Av-GFP fusion, have been successfully used for ubiquitous marking cell structures and outlines [Benton et al., 2013]; [Benton et al., 2016]. Unfortunately, such mRNA constructs did not seem to provide ubiquitous labeling in *D. melanogaster* and *M. abdita*, possibly because the protein did not diffuse ubiquitously and/or its expression was not high enough to allow *in vivo* analysis [Danai, 2012]. To analyze the shape and the morphology of the serosa at cellular and tissue level, I therefore decided to inject recombinantly expressed protein. To label cell membrane, actin is a possible candidate and has been used before, e.g. in *D. melanogaster* [Verkhusha et al., 1999]. Direct labeling of actin, however, may interfere with its dynamic [Yamada et al., 2005] and consequently with the normal development of the organism. As an alternative to direct labeling of acting, Lifeact fused to a fluorescent protein has

emerged as widely used alternative. Lifeact is a 17-amino-acids peptide that links the filamentous actin (F-actin) in eukaryotic cells and tissues without interfere with actin dynamics [Riedl et al., 2008]. The peptide Lifeact in frame with the fluorescent protein mCherry was recombinantely expressed in *E. coli* and injected in *M. abdita* embryos at blastoderm stage. After injection, the embryos were mounted for the MuVi-SPIM as described in Appendix 1. Using this method I was able to ubiquitously label the cell boundaries in fly embryos during the entire embryonic development.

Analysis of extraembryonic development in *M. abdita* required to observe the dorsal side of the embryo – where the serosa and amnion anlage are specified – and the ventral side of the embryo – where the serosa eventually fuses – all at the same time. To achieve this, the 3D reconstructed embryo (called fusion in Fig. 2.10.1) had to be transformed into a 2D image using a cylindrical projection that simultaneously displayed the dorsal as well as the ventral side of the embryo. To this end, I collaborated with Everado Gonzalez, who developed a dedicated image-processing algorithm for this task. In brief, the algorithm was programmed to process a recorded 3D volume such that (1) it recognized the shape of the embryo, (2) it removed the volume around the embryo, (3) eroded the outermost layer of image information from the embryo, and (4) subtracted the eroded image from the full embryo to end up with a thin layer that was just a few micrometers in thickness and contained all relevant image information of cells at the surface of the embryo minus the yolk and other cells that were deeper in the embryo. This process reduced the data to a quasi two-dimensional image that was projected onto a flat surface and thus generated a 2D map of the embryo surface, which contained ventral as well as dorsal views in one image simultaneously (Fig. 2.10.5). In the rest of the thesis I will refer to this process as “unrolling” and at the 2D movie as “unrolled movie”.

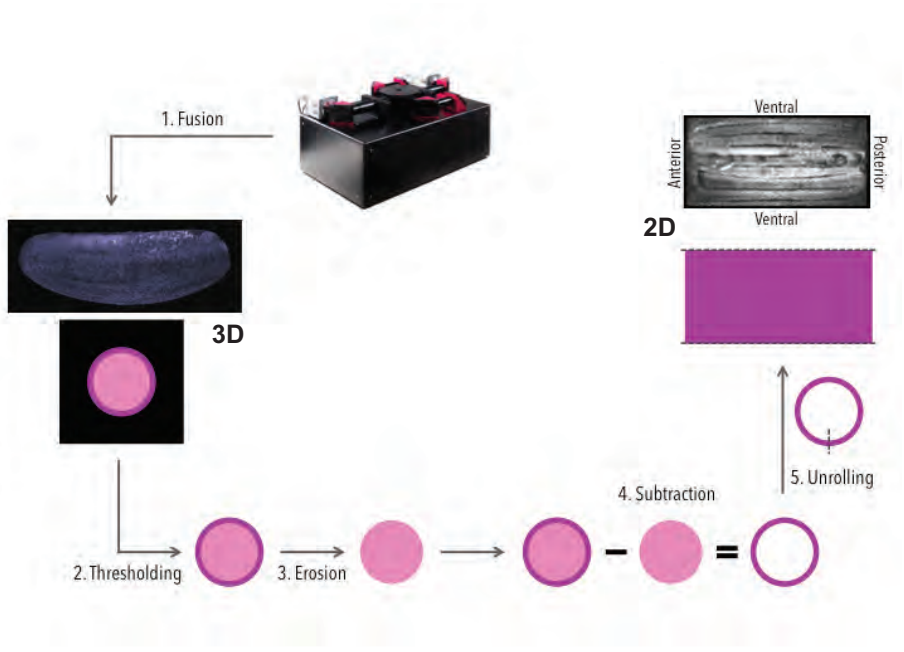

Figure 2.10: Processing of the data from the microscope to the analysis. The four views obtained with the MuVi-SPIM were fused together to form a complete 3D embryo (1). To be able to transform this 3D information into 2D, the volume around the embryo was removed by the thresholding (2). The surface of the embryo was eroded until only the volume inside it was left (3). The eroded embryo was subtracted from the thresholded embryo therefore only the surface was left (4). The cylindrical surface was cut on the ventral side and unrolled (5) giving rise to an entire embryo in 2D, where dorsal and ventral sides were visible at the same time. Black is the volume around the embryo; purple is the surface of the embryo; pink is the yolk; grey dashed line indicates the position of the cut. The 3D and 2D embryos are oriented with the anterior side to the left.

2.3.2 The dataset

Two time-lapse recordings have been taken to analyze wild-type development. The main results were qualitatively comparable and could be represented by the detailed analysis of a single data set. This recording comprised *M. abdita* embryonic development from end of cellularization to beginning of dorsal closure at 22°C and the cell outline was fluorescently labeled by injection of recombinant Lifeact-mCherry protein. One volume of the embryo was taken every 2min and each volume was recorded in four views. A 25x objective was used and stacks were taken every micrometer. Registration and fusion of the individual views resulted in a single isotropic 3D volume. The movie of the wild-type embryo has been unrolled. The wild-type analysis comprises devel-

opment of the serosa and the amnion at the organismal level, and then focus on two newly observed types of tissue/cell behavior during serosa/amnion dissociation, i.e. bulging and pulsation.

2.3.3 Serosa development

The extraembryonic tissues of *M. abdita* were studied *in vivo* taking in account as landmark the end of cellularization, different percentage of germband extension, germband retraction and beginning of dorsal closure at tissue and cellular level. At the end of cellularization, the cells of the presumptive extraembryonic tissue were visually indistinguishable from adjacent cells in the dorsal epidermis at the beginning of my time-lapse recordings (Fig. 2.11A-A"), which is consistent with previous analyses in fixed tissue [Wotton et al., 2014]. The cells of the extraembryonic tissue started to change their morphology when the tip of the germband reached the dorsal side of the embryo (Fig. 2.11B-B"). Subsequently, during the continued elongation of the germband, the amniotic fold was formed (Fig. 2.11C,C') while the serosal cells were still mainly columnar in shape even though the serosa started to be stretched. During the prolonged stretching, the serosa cells became larger and thinner, thus acquiring a squamous shape (Fig. 2.11D). Prior to serosa detachment, actin accumulated at the boundary of the serosa, presumably at the contact with the amnion, forming an actin cable (Fig. 2.11E). When the germband reached around 60% of the embryo length (Fig. 2.11F), the anterior side of the serosa appeared to separate from the amnion as evidenced by the anterior actin cable that was moving towards the head while the rest stayed in place (movie 1). Twenty minutes after anterior detachment, the serosa detached at the posterior (Fig. 2.11G), and subsequently at the lateral sides (36 minutes after anterior detachment; Fig. 2.11H). When the serosa detached at the posterior side of the embryo, the tissue expanded in a continuous movement without apparent interruption and fused in a zippering-like manner on the ventral side 184 minutes after anterior detachment (Fig. 2.11I,J). Serosa fusion was initiated at the anterior and posterior pole and occurred in one swift and uniform movement of the opposite actin cables, suggesting that the fusion proceeded without the formation of filopodia, contrary to the dorsal closure of *D. melanogaster* [Nowotarski et al., 2014] (Nowotarski et al., 2014).

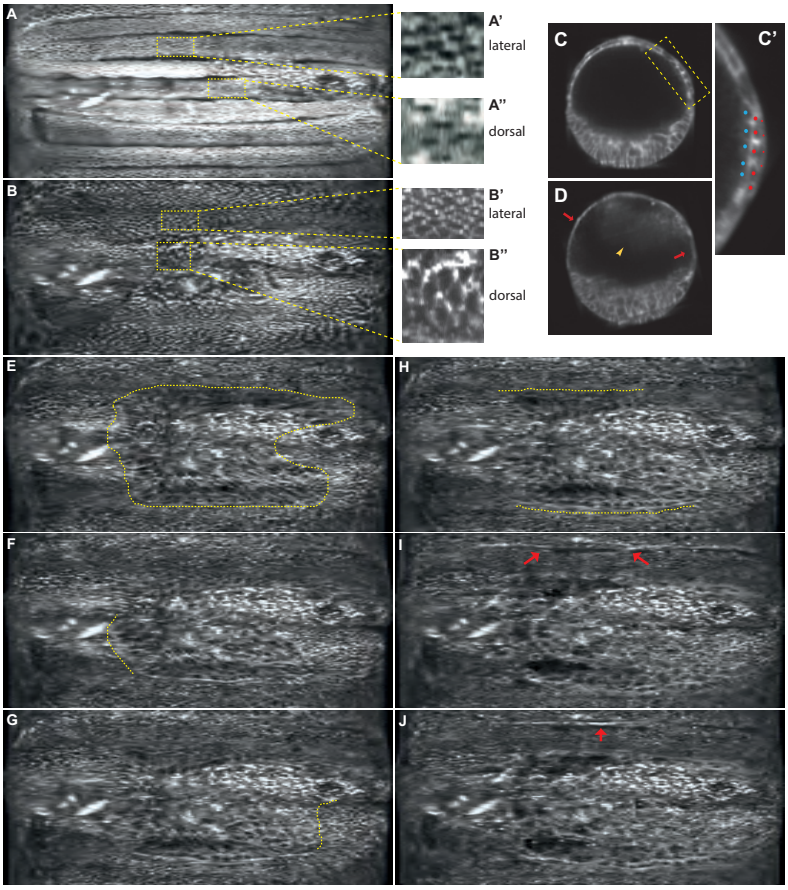

Figure 2.11: Expansion of the serosa in a wild-type embryo. The unrolled movie of wild-type *M. abdita* illustrates the embryo from the specification until the fusion of the serosa. (A) The embryo is at the end of cellularization and the dorsal cells, which are specified to become the extraemrbyonic tissue, are indistinguishable from the adjacent cells (A',A"). (B) The tip of the germband is on the dorsal side of the embryo and the cells of the extraemrbyonic tissue changed shape becoming larger than the lateral cells (B',B"). (C,C') The amniotic fold is formed during germbend extension and probably formed by the amnion (light blue) and the serosa (red). The dots mark cells but the type of tissue they belong to is ambiguous. (D) The serosa (pointed by the red arrows) was stretched and thin while the germband increase its elongation (yellow arrowhead). (E) The actin cable starts to be formed at the boundary of the serosa (internal side of the dashed yellow line). (F) The serosa detaches anteriorly, then (G) posteriorly and finally (H) laterally. (I,J) The serosa fuses ventrally in a zippering-like mode. The red arrows point at the position where the serosa is fusing. The yellow dashed lines (E-H) indicate the area where the serosa is detaching or the outline of the serosa boundary. (A,B,E-J) Anterior is left; (C,D) dorsal is up.

When the serosa detached from the amnion, could spread uniformly as a circle or primarily along the AP-axis as an ellipse. The change of shape of the serosa during its expansion can be described by the mathematical parameters eccentricity, which describes how an ellipse is close to a perfect circle. The eccentricity of a perfect circle is equal to 0 while the eccentricity of a line is equal to 1. An ellipse has an eccentricity between 0 and 1, depending from its elongation. When the serosa is still in contact with the amnion, its shape is closer to a circle (eccentricity = 0,88). After the anterior detachment, and even more after the posterior one, the serosa is elongated and becomes more similar to an ellipse (eccentricity = 0,94), until also the lateral sides are detached. This means that the serosa is first expanding along the AP-axis. Accordingly, the serosa eccentricity is from closer to 0 to closer to 1 and after the complete detachment it will decrease until its fusion (eccentricity = 0,92) even though overall, due to the shape of the embryo, the serosa has a shape closer to an ellipse than a circle (Fig. 2.12).

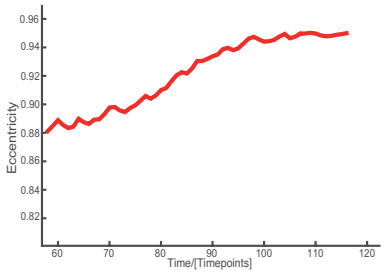

Figure 2.12: Expansion of the serosa in *M. abdita* wild type described by eccentricity. The graph represents the shape that the serosa acquires during its expansion in a wild type embryo. The parameter eccentricity increases over time meaning that the serosa shape changes toward an ellipse. The curve reaches a plateau, meaning that the eccentricity is stable therefore the serosa stopped to change shape. This happens when the serosa is completely expanded and fuses.

2.3.4 Serosa and amnion separate along numerous bulges of the amniotic fold

During germband extension in M. abdita embryos, the ectoderm extends underneath the extraembryonic tissue. The extending germband remains attached to the dorsally expanding extraembryonic tissue, pulls the posterior-most part of it along and thus generates the so-called amnioserosal fold ([Rafiqi et al., 2008] and see above). Analyses in fixed tissue have described how the outer cell layer of this fold becomes the serosa that detaches and encloses the embryo, while the inner cell layer of the fold gives rise to the amnion [Rafiqi et al., 2008]. Using time-lapse recordings, this process could be analyzed with a dramatically increased temporal resolution that provided insights into tissue-level and cell-level dynamics of serosa/amnion disjunction along the anterior/posterior axis as well as at the lateral flanks of the embryo. To better understand whether serosa separation was dependent on serosa expansion, or whether serosa/amnion disjunction was more likely to be independent and possibly even preceded tissue expansion, I specifically analyzed the formation and behavior of the amnioserosal fold while it outlined the dorsal serosa (Fig. 2.13A). To observe tissue behavior at the amnioserosal fold, the actin cable was used as reference. During serosa/amnion disjunction, a second actin cable appeared to be forming ahead to the single cable marking the serosa circumference (Fig. 2.13C). While the serosa was unfolding and therefore the area area was expanding (Fig. 2.13C',D"), the second formed cable, which is the most external one, increased the actin accumulation while the other one decreased it (Fig. 2.13C"'). This unfolding of the serosa appeared as a bulging of the tissue, so this process was called "bulging". This bulging appeared in small areas at the time indicating two possibilities: (1) the serosa did not detached at the same time in the entire front or (2) part of the detached serosa was left behind.

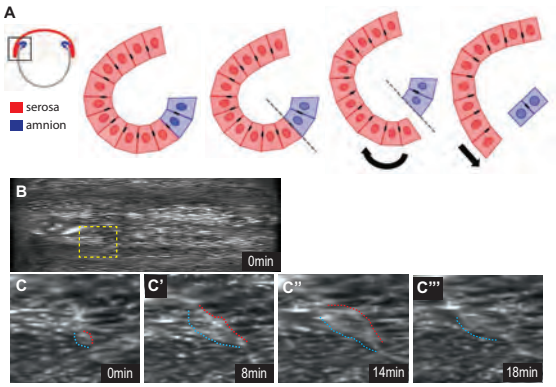

Figure 2.13: Serosa explanation by bulging. (A) The cartoon represents a cross section of *M. abdita* embryo showing the amniotic fold with the amnion (blue) and the serosa (red). Once the serosa splits from the amnion, it unfolds and expands crawling over the embryo. (B) Frame of the unrolled wild-type recorded embryo where the area of bulging is included in yellow dashed square. (C'-C"') Close up of the selected area in B at different time points. In (C-C"') the red dashed line indicates the actin cable of the bulging area that was the original front of the serosa. The blue dashed line indicates the actin cable on the side of the serosa that was unfolding and previously was in contact with the amnion. (B-C"') Anterior is left.

2.3.5 Serosa/amnion separation is associated with tissue-wide pulsations

Coincidently with bulges at the amnion/serosa interface, I observed the onset of pulsatile contractions in serosal cells just prior to the split between amnion and serosa. Similar oscillations of contracting extraembryonic tissues cells have been previously reported during later stages of amnioserosa and serosa development [Panfilio and Roth, 2010]; [Panfilio et al., 2013], but not, however, during its differentiation. A semi-quantitative analysis of the pulsations in individual cells showed how those oscillations effectively dictated the oscillation in the area of the entire tissue (Fig. 14). The constriction of individual cells differed in between them, so they contributed differently at the change of the serosa's area (Fig. 2.14A). The total area of the serosa depended on the area of each cell (Fig. 2.14B). When many of them contracted the area of the tissue decreased, instead when most of them released, the area of the tissue increased. The fluctuation of the serosa as total tissue was higher in the first part of the process but its expansion started to increase toward the end when the individual cell contractions were less intense.

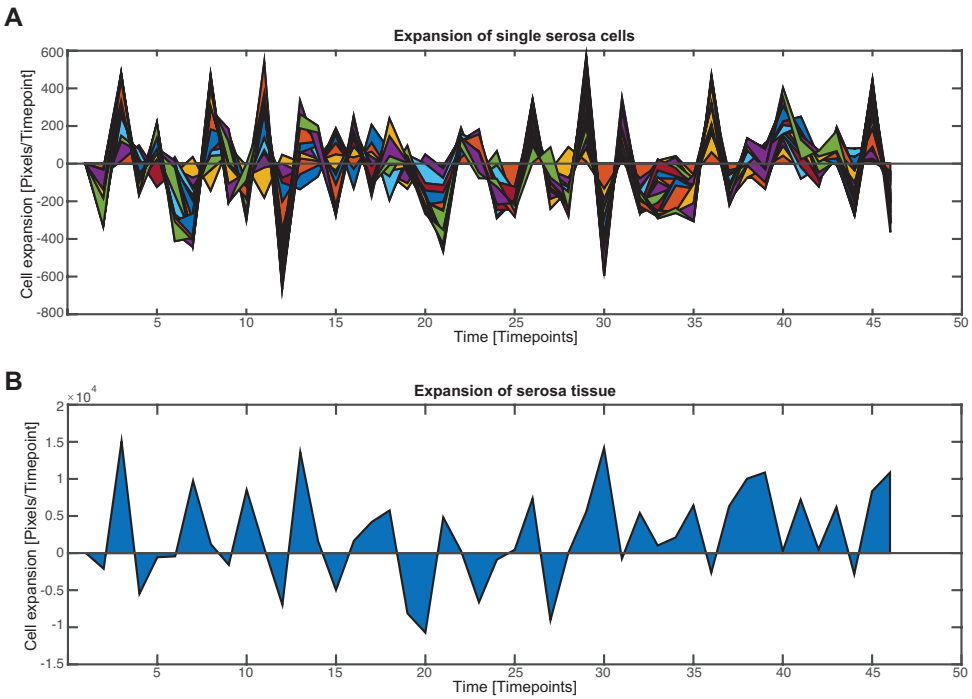

Figure 2.14: Correlation between single serosa cells pulsations and area of the serosa as total tissue. (A) Each color in the graph represents one cell that contributes differently at the area of the serosa. The sum of their area defines the area of the serosa. In this graph only eight cells are taken in account. (B) The graph represents the total area of the serosa. The difference between the positive and the negative peaks indicate the change of the area of the serosa. The second part of the graph shows a reduced difference between the peaks, meaning that the area of the serosa is pulsating less and has the tendency to increase. The area was measured in pixel/time point.

To identify the source of constriction in the expanding serosa, I analyzed a transversal section of the MuVi SPIM time-lapse recording. In these recording, it was possible observe a basal accumulation of actin and constriction of the pulsating serosal cells (Fig. 2.15). Most of the cells that were pulsating were located between the head of the embryo and the anterior tip of the germband, sitting above the yolk. These cells where going through consecutive rounds of constriction and release exclusively on their basal side (Fig. 2.15A'-C').

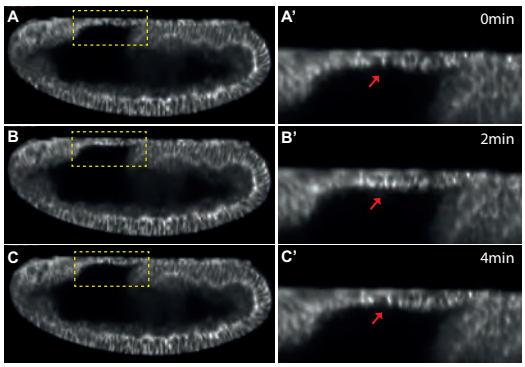

Figure 2.15: Pulsations of the serosal cells in a wild-type embryo. (A-C) Cross-section along the AP-axis; the area in the yellow-dashed square is the position of the serosa pulsating cells shown in the relative close up. (A'-C') Close up of the pulsating cells showing the actin accumulation at the basal side of these cells during their phase of release (A'), constriction (B'), release (C'). The arrows indicate the central pulsating cells of the serosa. Anterior is left.

2.3.6 Amnion development

The analysis of *Mab-egr* staining in late stages of embryonic development suggested that the gene meight serve as marker of the amnion. According to *Mab-egr* expression, the amnion would close rather late, i.e. during germband retraction, and in a process that may involve filopodia reaching out from either side to seal the dorsal midline similar to ectoderm closure in *D. melanogaster* and different from serosa fusion in *M. abdita* (Fig. 2.16G,H). To test whether the amnion was closing late, I was analyzing late time intervals in the time-lapse recordings. Indeed, amnion closure could be observed when the most peripheral layer on the dorsal side of the embryo was removed (Fig. 2.16A) or in a cross-section along the DV-axis in between the head and the germband (Fig. 2.16A'). The time-lapse recordings indicate that before the onset of germband retraction, the yolk sack/dorsal hole was covered by the serosa (Fig. 2.16B). As soon as the serosa separated from the amnion, it became thin and not visible anymore in the dorsal section. At the same time the germband continued to retract and the amnion was reduced to a small area that covered the tip of the germband (Fig. 2.16C). Therefore, the dorsal side of the embryo was not covered by the amnion but exclusively by the serosa. As the germband started to retract, protrusions/filopodia appeared to crawl from the lateral ectoderm towards the dorsal midline of the dorsal opening (Fig. 2.16D). The filopodia of the amnion elongate on the internal side of the serosa, using it as support (Fig.

2.16D',E'). At the same time, actin accumulated at the boundary between the amnion and the epithelium and persisted at least until the amnion started to fuse (Fig. 2.16D'-F'). The amnion's filopodia continued to move dorsally until they met and fused at the dorsal midline (Fig. 2.16E,E'). The amnion fusion did not progress in a continues manner from anterior to posterior but it fused in a few areas at the time, leaving some separated parts in between (Fig. 2.16F). The closure of the amnion brought the two sides of the epithelium closer to each other (Fig. 2.16F,F') and more protrusions were formed toward the yolk sac (Fig. 2.16F). Serosa rupture and dorsal closure of the ectoderm were not part of the time-lapse recordings. The observation of the amnion closure in vivo is complementing the initial observations made by the *Mab-egr* staining in the situ hybridization (Fig. 2.4I-K'). The observations *in vivo* as well as in fixed tissue support the model that the amnion is actively involved in dorsal closure and that *Mab-egr* is an amnion marker.

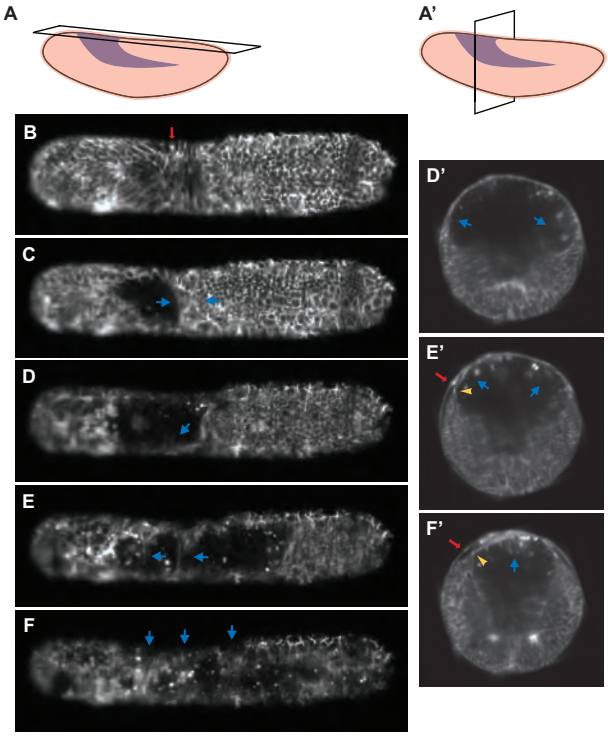

Figure 2.16: In *M. abdita* the amnion is open and closes during germband retraction. (A,A') The cartoons show the position and orientation of the sections taken from the live imaging of the wild-type embryo. (B) While the serosa and the amnion are not yet separated, the dorsal opening is covered by the serosa, which is still thick and therefore not completely removed by the section along the dorsal side of the embryo. (C) The amnion is visible on the tip of the germband but it does not cover the dorsal opening. (D,D') As soon as the germband starts to retract, the amnion begins to show thin protrusions, similar to filopodia, along the lateral sides. (E) The amniotic protrusions coming from the opposite sides are touching and fusing at the dorsal midline while the germband retracts. (E') The filopodia seem to crawl on the serosa, actin is accumulated at the boundary between the amnion and the epithelium, and the amnion, while closing, brings the epidermis dorsally. (F) The amnion is now fusing in three different positions along the AP-axis but the tissue is not completely closed. (F') The opposite sides of the amnion meet at the dorsal midline and the connection between amnion and epithelium is still visible. The amnion seems to form protrusions also toward the yolk sac. (A-F) Anterior is left; (D'-F') dorsal is up. The red arrows point to the serosa; blue arrows point to the amnion; yellow arrowheads point to the actin accumulation between amnion and epidermis.

2.4 Functional analysis of extraembryonic dynamics in *M. abdita*

To understand how changes in either patterning or ECM dynamics could affect amnion and serosa development in *M. abdita*, the dynamics of extraembryonic development were analyzed in time-lapse recordings of *Mab-zen* and *Mab-mmp1* RNAi embryos. *Mab-zen* was selected because the function of zen has been previously studied in extraembryonic development of *M. abdita* and other insects [Panfilio et al., 2006]; [Rafiqi et al., 2008]; [van der Zee et al., 2005], and it had been suggested that loss of zen activity transformed *M. abdita* towards a *D. melanogaster*-like mode of extraembryonic development. *Mab-mmp1* was selected as putative common target of *Mab-doc* and *Mab-egr* regulation and its potential function in extracellular matrix remodeling that could explain the observed serosa pulsations in *M. abdita* wild-type embryos.

2.4.1 *D. melanogaster* wild type and *Mab-zen* RNAi embryos represent two distinct types of dorsal extraembryonic tissues

Expression of the homeobox gene *Mab-zen* in *M. abdita* is critically required for serosa formation, and *Mab-zen* RNAi embryos develop only a single dorsal extraembryonic tissue, the amnion [Rafiqi et al., 2008]. As has been pointed out before, this dorsal amnion bears resemblance to the amnioserosa in *D. melanogaster* in topology, function, and gene expression [HallgrÍmsson et al., 2012]; [Schmidt-Ott and Kwan, 2016]. To test whether the dorsal tissues in *M. abdita zen* RNAi and *D. melanogaster* wild-type embryos could be homologous, I compared development and tissue dynamics side-by-side in MuVi-SPIM time-lapse recordings. The cell membranes of *D. melanogaster* in the live imaging were marked with Gap43-mCherry, and the time-lapse recordings were kindly provided by Dimitri Kromm and Dr. Matteo Rauzi.

At the end of cellularization, dorsal cells of *Mab-zen* RNAi embryos were indistinguishable from the other cells by shape (Fig. 2.17A,A") as *in D. melanogaster* (Fig. 2.17B,B") and *M. abdita* wild-type embryos (Fig. 2.11A,A"). When the germband reached the dorsal side of the embryo, the dorsal cells were

stretched and the extraembryonic tissue became recognizable from the rest of the embryo in all three cases (Fig. 2.17C-D"; Fig. 2.11B,B"). Contrary to *M. abdita* wild type, the extraembryonic tissue of *Mab-zen* RNAi embryos did not proper detach from the embryo and instead stayed in contact with the epithelium like the amnioserosa (compare Fig. 11F-H with Fig. 2.17E-H). The amnioserosa-like of *Mab-zen* RNAi embryo and the amnioserosa of *D. melanogaster* expanded with a different shape (Fig. 2.17E,F) and they cover a different percentage of the surface of the embryo (20% in *Mab-zen* RNAi and 9% in *D. melanogaster*). During germband retraction, the shape of the extraemrbyonic tissue of the two species became similar (Fig. 2.17G,H). *Mab-zen* RNAi embryo had the dorsal opening continuously covered by its amniosersa-like tissue and appeared similar to *D. melanogaster* wild-type embryos, in which the amnioserosa covered the dorsal opening until dorsal closure occurred (Fig. 2.17I,J). No bulging or pulsations were present in the extraembryonic tissues of either *Mab-zen* RNAi or *D. melanogaster* wild-type embryos (compare Fig. 2.17 with Fig. 2.13 and Fig. 2.15).

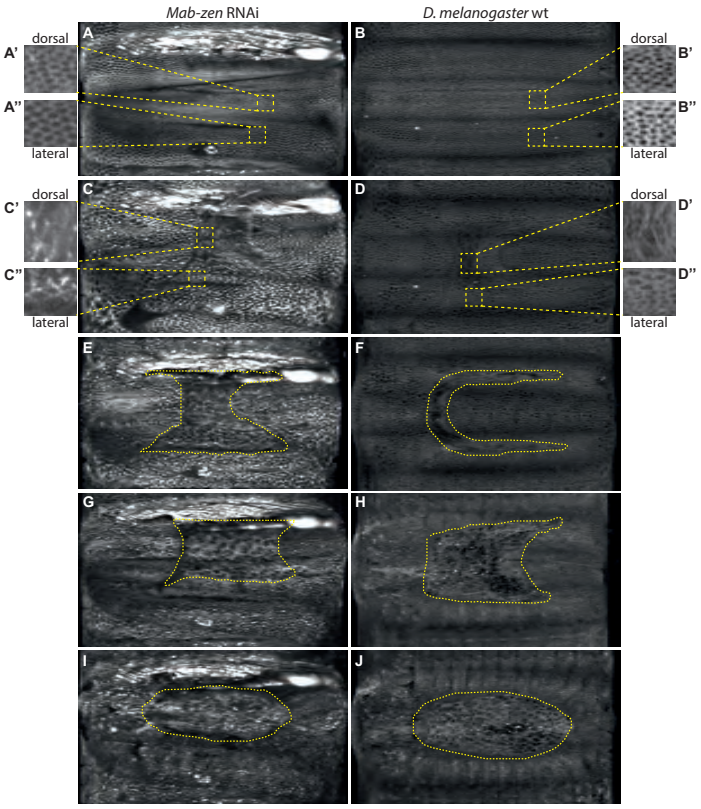

Figure 2.17: Comparison of the extraembryonic tissue between *Mab-zen* RNAi embryos and *D. melanogaster*. Extraembryonic tissue development of *Mab-zen* RNAi embryos was compared with the amnioserosa of *D. melanogaster* by unrolling of the time-lapse recording. (A,B) The dorsal cells of the M. abdita mutant embryo had the same shape of the others as well as *D. melanogaster* embryo. Cells of different areas are compared for *Mab-zen* RNAi (A',A") and *D. melanogaster* (B',B"). (C-C",D-D") In both species, the dorsal cells of the embryos were elongated, while the other cells where columnar. (E,F) At the maximum germband elongation, the extraembryonic tissue of Mab-zen RNAi embryo was more expanded than the amnioserosa. (G,H) During germband retraction and at its completion (I,J), the extraembryonic tissue of *Mab-zen* RNAi and *D. melanogaster* embryos appeared similar. (A,C,E,G,I) *Mab-zen* RNAi embryos. (B,D,F,H,J) *D. melanogaster* wild-type embryos. (A-D) Yellow boxes delimit the zoomed in areas. (E-J) Yellow dashed lines outline the boundary of the extraembryonic tissue.

Once the dorsal closure began, the cells of the extraembryonic tissue of *Mab-zen* RNAi contracted and oscillated to bring closer the leading edge of the epidermis. This mechanism of dorsal closure appeared to be different from the one of *D. melanogaster*, mainly for the activity of the cells. In fact the extraembryonic cells of the *Mab-zen* mutant *M. abdita* were evenly active and contracting in a non-coordinated manner but reflecting their constriction to the next tissue with more strength than the amnioserosal cells. In *D. melanogaster*,

amnioserosal cells showed coordinated contractions and, as described in previous works (Solon et al., 2009; Wada et al., 2007), have a different behavior depending from their position within the tissue. Precisely, the central cells are constricting while the cells in contact with the leading edge stop in a contracting phase so to reduce the size of the dorsal opening. Although *Mab-zen* RNAi embryos and *D. melanogaster* wild type embryos have only one extraembryonic tissue, these showed different activity and distribution of oscillating cells.

2.4.2 Serosa disjunction is affected and delayed in *Mab-mmp1* RNAi embryos

My analyses of *Mab-mmp1* function in fixed tissue strongly indicated a role of extracellular matrix remodeling in serosa disjunction and expansion. To understand how decreased levels of *Mab-mmp1* activity affected extraembryonic development, *Mab-mmp1* embryos were analyzed in time-lapse recordings. Consistent with observations in fixed tissue (see section 2.4), the time-lapse recordings indicated a significantly delayed in the serosa detachment. After anterior detachment of the serosa was observed (Fig. 2.18A), the posterior detachment took place after 45 minutes (Fig. 2.18B; wild type: 20 minutes), and lateral detachment after other 10,5 minutes (Fig. 2.18C; wild type: 16 minutes), for a total of 55,5 minutes in *Mab-mmp1* RNAi embryo versus 36 minutes observed in the wild type. Apart from the delay, the process appeared to be superficially similar to wild-type serosa development: the actin cable was formed at the boundary of the serosa as in the wild type, the order of tissue detachment (anterior, posterior, lateral), and serosa expansion by crawling and fusion on the ventral side were as observed for wild type (Fig. 2.18D-E and Fig. 2.11). However, the observed delay in serosa expansion did influence the serosa shape during its expansion. Particularly, the delay in the detachment of the lateral sides of the serosa caused first its elongation along the main axis and only later expanded laterally. Therefore initially the eccentricity in the *Mab-mmp1* RNAi embryo increased from 0.80 to 0.94 in a shorter amount of time compare to the wild type (Fig. 2.18F). With the actual data set it was not possible to determine whether the serosa *Mab-mmp1* RNAi embryos fused at the same developmental stage as the wild type or if it took longer since the process of detachment was delayed. Next, I analyzed the attachment

of the serosa to the underlying epidermis, the amnion, and the yolk sac in transversal sections of embryos with fully extended germband and prior to the beginning of amnion/serosa disjunction. In these transversal sections, it was possible to observe the serosa detachment at the anterior and posterior poles. The behavior of this tissue and its cell shape differed in wild type and mutants. In wild-type embryos the serosa detached from the amnion, started to crawl over the embryo and the serosal cells became immediately very thin (Fig. 2.18G,G'). In *Mab-mmp1* RNAi embryos, by contrast, the posterior side of the serosa appeared to be unable to split from the amnion. The tissue was unable to move posteriorly on the germband, accumulating at the posterior extremity without encountering any obvious obstacle. Presumably, due to the continuous attachment of serosa and amnion, the posterior serosa cells acquired a square shape until they became able to migrate (Fig. 2.18H,H').

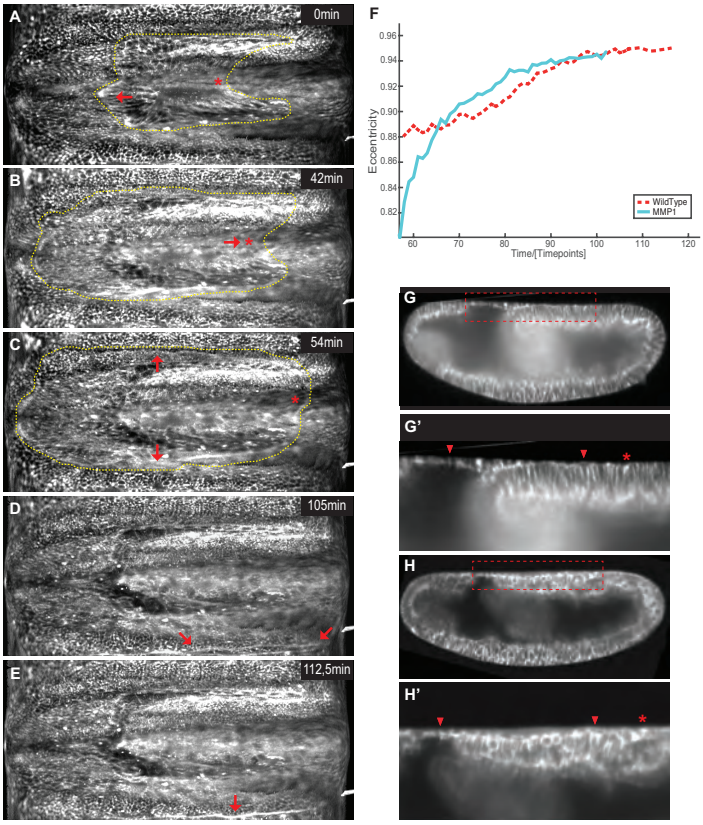

Figure 2.18: *In vivo* description of the serosa expansion in *Mab-mmp1* RNAi embryo. The unrolled movie of *Mab-mmp1* RNAi embryo, showed the serosa expansion and its detachment first anteriorly (A), then posteriorly (B) and in the end on the lateral sides (C). Eventually the serosa fused on the ventral side of the embryo in a zippering mode as described for the wild type (D,E). (F) The graph describes changes of the serosa's shape during its expansion: fast increment of the eccentricity, meaning fast elongation along the AP-axis; later, the eccentricity did not increase significantly, meaning lateral expansion. (G) Middle cut of *M. abdita* wild type embryo along the AP-axis. The close up (G') showed the central and posterior areas of the serosa indicating the different serosa's thickness along the AP-axis (arrowheads) and at its posterior end (asterisk). (H) *Mab-mmp1* RNAi embryo in a middle cut along the AP-axis. (H') Close up of the embryo shown in (H). The arrowheads indicate the serosa's thickness that did not change along the AP-axis. The asterisk indicates the posterior end of the serosa that, since was not able to detach, was accumulating at its posterior extremity. Anterior is left. (A-C) The arrows indicate the detaching front of the serosa. (A-C, G',H') The asterisk indicates the posterior extremity of the serosa. The yellow dashed line outline the boundary of the serosa. (D,E) The arrows point where the serosa is fusing.

To identify a putative cause for the delay in tissue expansion, I first explored the possibility that the serosa disjunction was affected at the interface of serosa and amnion, i.e. the tip of the amnioserosal fold. However, despite the serosa bulging resulted to be faster compared to the wild type, its dynamics was very similar (Fig. 2.19C-D"'). This suggests that this final phase of serosa detachment in *Mab-mmp1* RNAi embryos was performed by the same molecular mechanism as in the wild type (Fig. 2.19A-B"'). Therefore, the global expansion of the serosa in *Mab-mmp1* RNAi embryos was comparable to the serosa expansion of wild type but the entire process was progressing with a different speed.

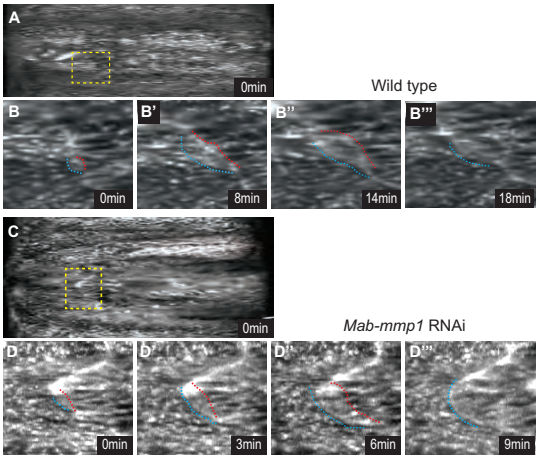

Figure 2.19: Bulging of the serosa in *Mab-mmp1* RNAi embryo. (A,C) Unrolled time-lapse recording of wild type (A) and *Mab-mmp1* RNAi (C) embryos. The yellow dashed squares indicate the area analyzed in the relative close up at consecutive time points. (B-B"') Bulging of the wild type embryo. (D-D"') Bulging of the *Mab-mmp1* RNAi embryo. (B-B"', D-D"') The red dashed line indicates the first formed actin cable. The blue dashed line indicates the actin cable formed at the tip of the unfolding serosa, which was in contact with the amnion. Anterior is left.

In addition to differences in serosa detachment and crawling, analyses of cell behavior in transversal sections of *Mab-mmp1* RNAi embryos, revealed differences in how serosal cells pulsated and accumulated actin at their basal side. Moreover these serosal cells were positioned on the germband, probably in contact with the amnion, instead on the yolk sac as in the wild type. This difference was due to a major elongation of the germband prior to cell contractions in *Mab-mmp1* RNAi. Specifically, during pulsations the germband of the injected embryo was between 65% and 69% of elongation while in the wild-type embryo was between 53% and 57% (compare Fig. 2.20 with Fig. 2.15). With the actual data it was not possible to clarify whether the different position of the pulsating cells was due to a delay in the starting of the process or to a faster germband elongation. Since the germband's length was already advanced when the pulsations began, the different substrate of the pulsating cells could have affected their behavior. In fact, serosa cells in *Mab-mmp1* RNAi and wild-type embryos appeared to contract with a different dynamics, such that in contrast to the continuous cycle of contraction and release in wild-type cells, only basal contraction could be observed in *Mab-mmp1* RNAi embryos (Fig. 2.20).

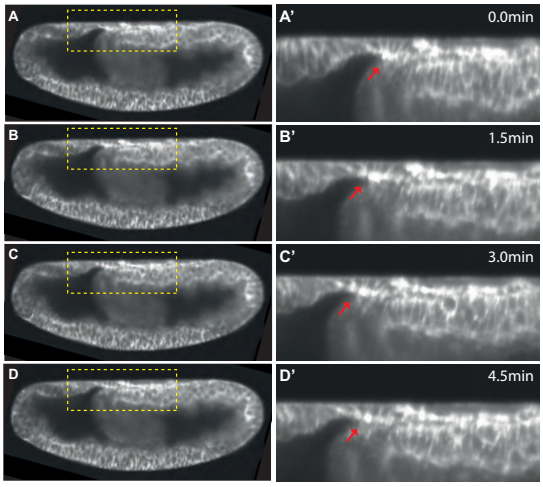

Figure 2.20: Pulsations of the serosa of *Mab-mmp1* RNAi embryo. (A-D) Middle cut along the AP-axis of *Mab-mmp1* RNAi embryo at four consecutive time points. Relative close up (A'-D') showed the contraction of the serosal cells at their basal side that missed the phase of release. (A'-D') Arrows indicate the basal side of the pulsating cells. Anterior is left.

To specifically analyze the differences in basal contraction and release of serosal cells in the wild type and *Mab-mmp1* RNAi embryo, contraction and release was quantified in groups of three cells. Within each group of cells, contraction was measured by determining the angle between the lateral cell membranes of the outermost cells. Accordingly, positive values represented basal constriction, negative values represented apical constriction, and higher values stronger constriction than lower values (Fig. 2.21). Angles were measured in transversal sections around the dorsal midline for a total of four angles per embryo.

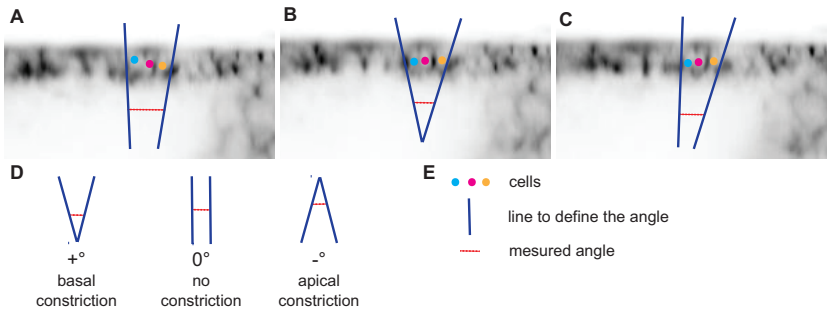

Figure 2.21: Method used to analyze the pulsations of the serosal cells. (A-C) Example of three consecutive time points in the middle-cut along the AP-axis of the wild-type embryo. This analysis was made with a wild type movie in which the time between each stack was 2min while for the *Mab-mmp1* RNAi was of 1,5min. This difference can influence the angle of the maximum constriction of the cells, especially for the wild type where the interval is longer. This, however, does not affect the comparison of the general behavior of the pulsating cells between wild type and mutant embryo. In this example the lines are drawn along the cell membrane to define the group of three cells. The angle formed by these lines was measured. Anterior is left, dorsal is up. (D) Basal constriction: positive angle; release phase: angle equal to zero; apical constriction: negative angle. (E) Light blue, dark pink and yellow dots are used to identify the cells; blue lines are used to delimit the group of three cells; red dashed line marks the measured angle.

Overall the serosal cells of the wild-type embryos formed smaller angles than in the *Mab-mmp1* RNAi embryos (Fig. 2.22A), suggesting that wild-type serosa cells constricted to a lesser degree than when *Mab-mmp1* was knocked down (Fig. 2.22B). The higher degree of basal constriction observed in *Mab-mmp1* RNAi embryos could be the result of stronger contraction in each serosal cell, e.g. resulting from higher amounts of basal actin. Rather than being the result of a singular pulse of constriction, the higher degree of basal constriction observed in *Mab-mmp1* RNAi embryos could be the result of cumulative constrictions in the absence of the wild-type release phase. This interpretation is consistent with the recorded basal constrictions in the live imaging, which demonstrated how cells of the *Mab-mmp1* RNAi were not able to release the contractions as completely as wild-type embryos and remained partially constricted (Fig. 20).

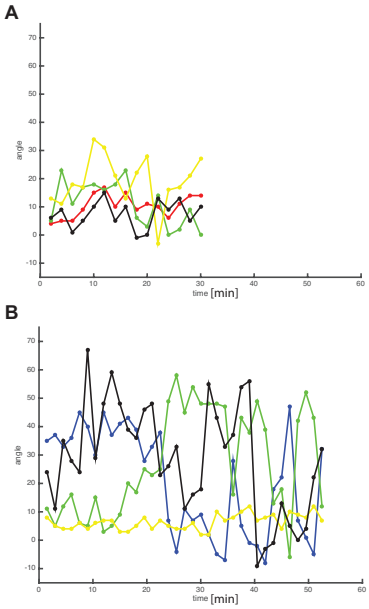

Figure 2.22: Comparison of wild type and *Mab-mmp1* RNAi pulsations in the serosa. The graphs represent the angles of the pulsating cells over time in the wild type (A) and in *Mab-mmp1* RNAi embryo (B). Each color represents a different measured angle. The time is in minutes. The meaning of the positive and negative angles is explained in Fig. 2.20.

Pulsations in wilt-type embryos were uniform throughout the entire process, which lasted 30min. On the contrary, when *Mab-mmp1* was knocked down, this process resulted subdivided into two phases: the first one in which the cells were basically constricted and not able to have a complete release, and a second one where the cells were able to release the contraction and pass from a basal to an apical constriction. In the absence of *Mab-mmp1*, the process lasted almost the double amount of time than in the wild type (52,5min). The analysis of multiple cell triples demonstrated, however, that different cell triples entered the period of contraction/stalled release at different time points and not uniformly throughout the epithelium. This suggests that the pulsations are not coordinated between the serosa cells in wild type as well as in *Mab-mmp1* RNAi embryos.

2.5 Expression of *Mab-mmp1* and *Mab-mmp2* in *M. abdita* embryos is consistent with putative role in extracellular matrix remodeling

The functional studies described above in fixed tissue and *in vivo* suggested that MMP1 and MMP2 dependent ECM remodeling contributed to serosa detachment in *M. abdita*. In particular the observation that knock down of *Mab-mmp1* was affecting serosa development was strongly indicating differences in embryonic expression compared to *D. melanogaster*, where *mmp1* expression begins in embryos 15h post deposition. Expression of*mmp2* starts after 8h of embryonic development, and neither gene provides an essential function to *D. melanogaster* development (Page-McCaw et al., 2003). During cellularization, *Mab-mmp1* mRNA was detected throughout the embryo with an increased signal at the basal side of cells (Fig. 2.23A). Also in embryos at the onset of germband extension, the signal was ubiquitous and basal (Fig. 2.23B), suggesting that *Mab-mmp1* was expressed in the presumptive serosa, which was in contact with the yolk sac (Fig. 2.23B'). During germband extension, *Mab-mmp1* expression was detected in areas of the embryo that were forming folds (Fig. 2.23C). At the same time, the signal was lost in the serosa but still

present in the tissue underlying it (Fig. 2.23C'). When the germband was completely extended and the serosa was ready to split from the amnion, *Mab-mmp1* mRNA was detected in the cells located below the serosa, probably amniotic cells (Fig. 2.23D-D'). Between 7,5 and 8h post deposition, when the serosa was completely extended and fused on the ventral side of the embryo, the signal could be detected in the yolk, where transcripts appeared to form small aggregates of mRNA (Fig. 2.23E). Around 9h post deposition, the expression was detected exclusively in the serosa (Fig. 2.23F) and later, during the dorsal closure, at the leading edge of the ectoderm (Fig. 2.23G). These results were reproduced in independent in situ hybridizations and with two RNA antisense probes of different length. As a control in situ hybridization was performed using the sense strand of the shorter probe. In whole mount in situ hybridizations, embryos aged 8h post deposition and younger showed a weak background as detected with the sense. In the same in situ hybridization, the corresponding antisense probe showed the same weak background, suggesting possible problems with the fixation of the embryos. In the embryos that were 9h post deposition, the serosa was stained with the sense and antisense probe (Fig. 2.23F,H). In embryos with a retracted germband *Mab-mmp1* mRNA was detected at the leading edge of the ectoderm around the dorsal opening and a background in the yolk (Fig. 2.23G). Using the sense probe the embryo did not show any signal (Fig. 2.23I).

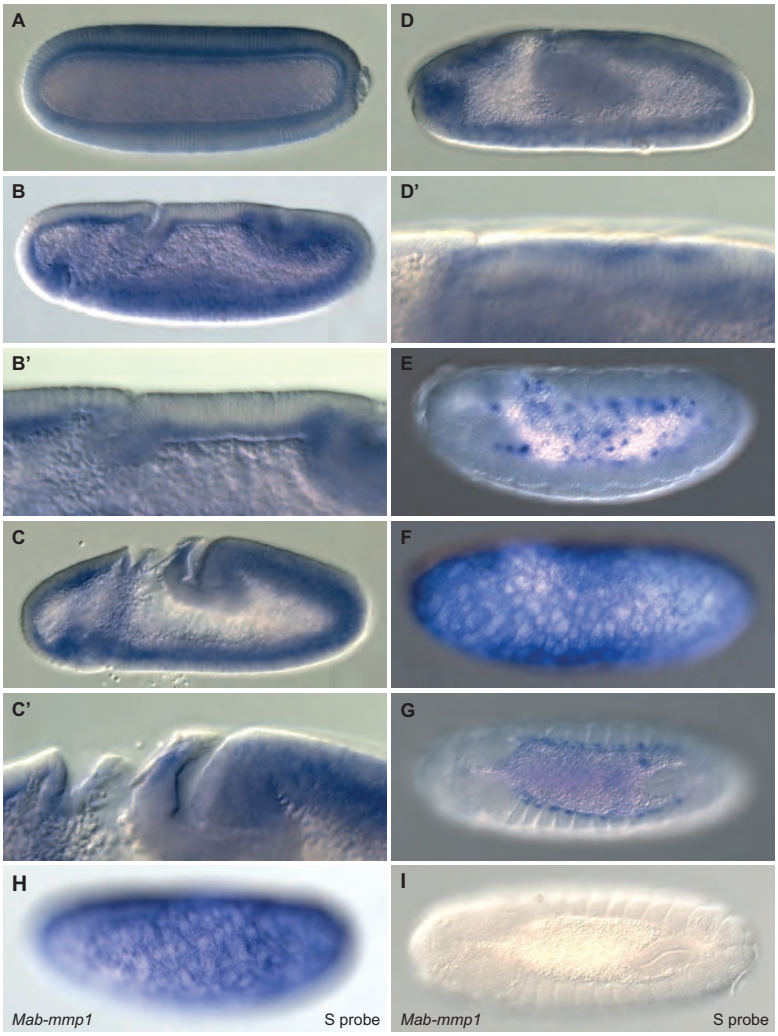

Figure 2.23: *Mab-mmp1* expression pattern in wild-type embryos. In situ hybridization using *Mab-mmp1* short antisense probe (A-G) or *Mab-mmp1* sense probe (H,I). The embryos are shown during cellularization (A), at the onset of germband extension (B), at the end of the fast phase of germband extension (C), at the end of germband extension prior serosa detachment (D) and after serosa fusion (E), at 9h post deposition (F,H) and after germband retraction (G,I). (A-F, H) Embryos are shown in a lateral view. (G,I) Embryos are shown in a dorsal view. Sense probe: S probe. Anterior is left.

Expression of *Mab-mmp2* was analyzed by in situ hybridization using two antisense probes of a different length. During blastoderm development, the long probe resulted weak background in the embryo but not in the yolk (data not shown), while the short probe resulted in unspecific staining between cellularization front and yolk sac (Fig. 2.24A,A'). Starting with the onset of germband extension, the short probe resulted in a presumably more specific signal at the basal side of the cells (Fig. 2.24B-B',E-F'). This staining varied in repeated rounds of in situ hybridization and therefore was controlled with a sense probe of the short sequence. Using the sense probe, embryos either did not show any staining, a weak background as the long antisense probe, or unspecific signal during cellularization (Fig. 2.24C-C'). With the onset of germband extension, a specific staining could be detected at the basal side of the cells very similar to the staining observed for the short antisense probe (Fig. 2.24D-D',G-H').

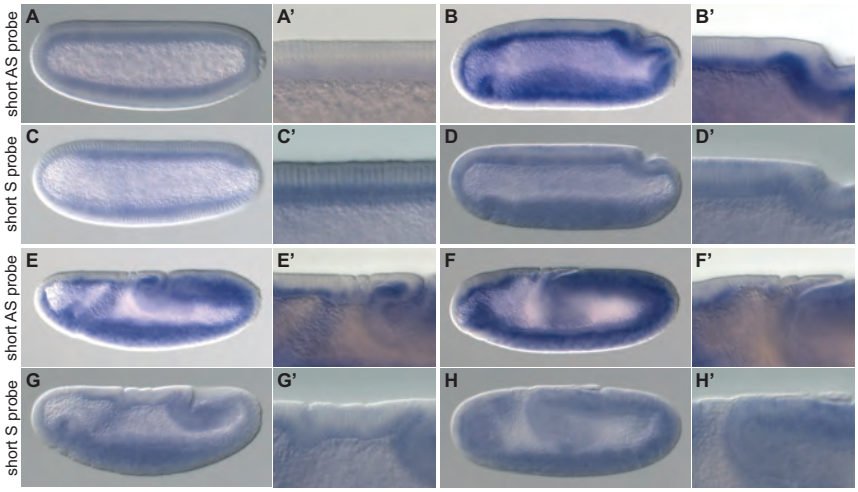

Figure 2.24: *Mab-mmp2* expression pattern at early stages of wild-type embryos. In situ hybridization for *Mab-mmp2* short antisense probe (A-B',E-F') or *Mab-mmp2* short sense probe (C-D',G-H'). These two probes gave a very similar staining from cellularization to germband extension. Antisense: AS; sense: S. Embryos are in a lateral view. Anterior is left.

The long antisense probe was detected in the serosa at 9h post deposition (Fig. 2.25A) and at the end of germband retraction appeared in a few areas of the head and weakly at the posterior side of the dorsal opening and along the leading edge (Fig. 2.25D). Also the short antisense probe was staining the serosa from 9h post deposition (Fig. 2.25B) but none parts of the embryo during the dorsal closure (Fig. 2.25E). As the other probes, the sense probe stained the serosa in embryos 9h post deposition (Fig. 2.25C) but not the embryo during germband retraction and dorsal closure.

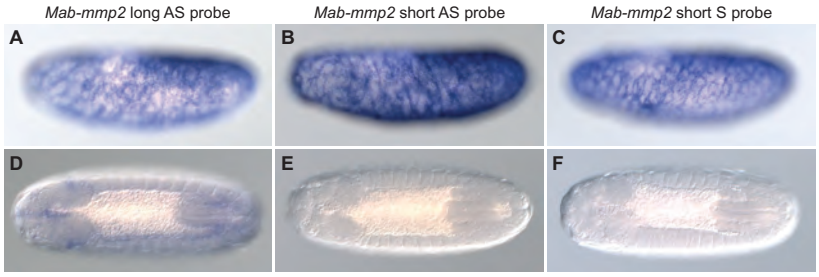

Figure 2.25: Expression of *Mab-mmp2* at late stages of wild-type embryos. This in situ hybridization compare the expression of *Mab-mmp2* obtained with the long antisense probe (A,D), the short antisense probe (B,E) and the short sense probe (C,F) from 9h to 11h-old embryos. (A-C) Lateral view. (D-F) Dorsal view. Anterior is left. Antisense: AS; sense: S.

The result obtained at late stages with *Mab-mmp1* and *Mab-mmp2* probes may suggest that the serosa after 9h of development may become sticky for some probes but not for others and that this characteristic is lost during germband retraction.

3
Discussion

In this thesis I analyzed the morphology of the extraemrbyonic tissue in *M. abdita* using *in toto* live imaging. This allowed the characterization of the serosa and amnion movements during development. Specifically, I was able to identify and describe new features of the serosa, bulging and pulsations, and the topology and morphology of the amnion. The observation that the amnion is an open tissue that is closing only during germband retraction and that therefore the dorsal opening is covered exclusively by the serosa let me reconsider the function of these tissues in *M. abdita*. Moreover, I studied the role of *Mab-zen*, *Mab-docA* and *Mab-docB*, *Mab-egr* and *Mab-mmp1* in the extraembryonic development to understand which are the mechanisms involved in the serosa detachment and expansion. The combination of functional studies with *in vivo* imaging added important knowledge on the complex development of the serosa and amnion and opened new hypothesis on their evolution toward the amnioserosa.

3.1 The double difficulties of studying evolution of the extraembryonic tissue

During this study, I encountered several technical issues. First I had to set up the non-model system *M. abdita* in the lab and learn how to handle it. Even though some techniques had been previously established in this species [Rafiqi et al., 2011], many other tools had to be developed and a wild-type descrip-

tion of late embryonic stages was missing until recently [Wotton et al., 2014]. Furthermore, the genome of *M. abdita* is not yet completely assembled causing some limitation in the genetic approach. The second problem that I encountered, was the morphology of the extraembryonic tissue of *M. abdita*. The serosa becomes very thin therefore is not easy to detect, especially during live imaging. Moreover, once the serosa detaches from the amnion, it is fragile and easy to break during fixation and the removal of the vitelline membrane around the embryo. Part of these technical issues caused uncertainty in the interpretation of some results. For example, the expression patterns of *Mab-mmp1* and mainly *Mab-mmp2* in *M. abdita* were not always reproducible. A more careful analysis of their sequence in silico is necessary to synthetize new RNA probes that can be used in the in situ hybridization. Moreover, the presence of staining in the serosa at late stages with the sense and antisense RNA probes of these genes let me wonder whether it is specific signal. The identification of the full length of these genes is necessary to allow the injection of their mRNA fused in frame with the CDS of a fluorescent protein that should show the real expression pattern of these genes and solve the uncertainty of the previous obtained results. Another problem faced during the functional studies at late embryonic stages was that RNAi does not seem to be efficient in the serosa once it was detached from the embryo. The CRISPR/Cas9 knock out could solve this problem at least for some genes. The knock out of *Mab-mmp1* in somatic cells gave the same result of its knock down. This could be due to a functional redundancy with another gene (maybe *Mab-mmp2*) or even due that the few left wild-type cells were sufficient to produce enough proteins to modify the ECM, which needed only more time to obtain the proper consistence. If this is the case, a stable transgenic line for *Mab-mmp1* (and *Mab-mmp2*) knock out should be established. Since the MMPs are essential at larva stage, the mutant flies have to be kept in heterozygosity. Due to the absence of balancer chromosomes, this implies the genotyping of each adult fly using genomic DNA extracted from one leg at each generation. Common techniques, such as antibody stainings, are also not yet established in *M. abdita*. This is complicated by the low cross-specificity of the primary antibodies that many proteins have. Improvement of this tool would be very helpful to detect activity and localization of cellular components during several cellular and morphogenetic processes. I demonstrated that in principle it is possible to generate transgenic

lines in *M. abdita* [Caroti et al., 2015] and that the CRISPR/Cas9, at least for the knock out, works also in this species. Therefore, random insertion or homologous recombination techniques could be used to establish reporter lines, which improve and facilitate *in vivo* studies. The last difficulty arises from the analysis and processing of *in toto* imaging with the MuVi-SPIM. After image acquisition, special algorithms have to be applied to register and fuse the different views before the actual image analysis can start. Further development of a fast and functional pipeline to process the generated data is essential to increase the number of embryos to analyze.

3.2 The amnion closure and the new functions of the serosa

Several new dynamic processes were made visible for the first time during the time-lapse recording of the wild-type embryo. Specifically, I could observe that the amniotic fold was forming during germband extension and that the amnion and the serosa are in contact through their basal side. After detachment, the serosa crawled over the embryo while the amnion stayed in contact with part of the germband. Only during germband retraction did the amnion unfold and flip back, starting to close dorsally, forming filopodia that resembled the dorsal closure of *D. melanogaster*. The new discovery of the initial open amnion and then its late closure, supports the idea that the serosa does not only protect the embryo physically and from pathogens but may also play a key role in the embryonic morphogenesis of *M. abdita* and possibly of other flies with a dorsal amnion and a serosa. The *in vivo* analysis in this work suggests that the serosa may have a role as support for the amnion during its closure, since the filopodia seem to use it to reach the dorsal midline to fuse. This, points to the serosa being essential during embryonic development and dorsal closure. Interestingly, the expression pattern of *Mab-egr* is in line with the observed amnion dynamics. In fact the dorsal hole is not always completely covered by the expression domain of *Mab-egr* but from the one of the serosa markers. This would mean that in *M. abdita* the serosa is the tissue covering the dorsal opening. These observations leaded me to reconsider and revise the old model of the extraembryonic tissue development proposed by Rafiqi and colleges in the

2008. This current accepted model, proposes the presence of an amnion that closes immediately after the serosa detachment, covering the embryonic dorsal opening from its formation until its closure. At the light of the important function that the serosa seems to have during the embryonic development, the evolution of the extraembryonic tissue from the ancient modus of development i.e. two tissues to one tissue, also has to be reconsidered. In previous works the amnioserosa was considered as a dorsal amnion for their similar topology and function in germband retraction and dorsal closure even thought they differ in genetic specification [HallgrÍmsson et al., 2012, Rafiqi et al., 2008]. From the time-lapse recording presented in this work, the topology and the function of amnioserosa and dorsal amnion also differ. First, the amnion is not covering the dorsal opening but it is a serosa's function; secondly, an open amnion has less strength than a close tissue to pull the germband and allow its retraction. With this new knowledge, I propose that during evolution the serosa could have not just disappeared but may first have lost its capability to detach from the amnion and enclose the embryo. This hypothesis is supported by observations of sub-compartmentalization of the amnioserosa dynamics during dorsal closure. Specifically, the amnioserosa cells in contact with the epidermis have a different shape and express a different cell-specific marker [Wada et al., 2007]. Moreover, these cells do not oscillate as the other amnioserosa cells showing a minor contribution to the reduction of the dorsal opening [Solon et al., 2009]. Another possibility is that the amnion started to close immediately after the serosa detachment and it remained in contact with the embryo during the development, acquiring part of the serosa function that in this different context lost importance and it was not essential anymore. Probably only after a topologic change it could have been possible to fuse the characteristics of the amnion and the serosa in a unique tissue that developed into the amnioserosa. In fact, this tissue in *D. melanogaster* expresses serosa and amnion markers as *zen* and *egr*, respectively. Changes in the regulation of genes that control the extraembryonic development, but not its specification, can be the first cause of the change in the morphology of the extraembryonic tissue in flies. Once the morphology was modified, other genes increased their regulation flexibility allowing mutations that in the end were fixed in the genome.

3.3 Differences in *zen* expression may correspond to different functions

D. melanogaster expresses *zen* from blastoderm stage until mid-germband extension. In contrast, both *M. abdita* and *Episyrphus balteatus* (Syrphidae) have a dorsal amnion and a serosa with a prolonged *zen* expression ([Rafiqi et al., 2008] and Steffen Lemke own data). The different morphology of the extraembryonic tissue seems to correlate with a different expression of *zen*. Therefore late *zen* expression may be linked to a specific function of the serosa that went lost during evolution or that was taken over by the amnion and in the end to the amnioserosa. At the moment this theory cannot be tested by the analysis and comparison of the regulatory sequences of *zen* between the two species, since the assembly of the genome sequence in *M. abdita* is not complete. It is possible to speculate that the early and late expression of *zen* is based on two different enhancers and that the last common ancestor of *M. abdita*, *E. balteatus* and *D. melanogaster* had early and late activation of zen. Two possible evolutionary scenarios could explain the different expression of *zen* in *D. melanogaster* and *M. abdita*. The first hypothesis is that *M. abdita* and *E. balteatus* could have maintained both activation while *D. melanogaster* could have lost the late one. The second one is the presence of a repression site that *D. melanogaster* acquired after his divergence from the common ancestor, inhibiting *zen* expression after mid-germband extension.

3.4 Changes in *zen* pathway during evolution

Other studies about *dpp* and *zen* signaling pathway have reported evolutionary changes in the regulation of *zen* and its downstream genes such as *dorsocross* and *eiger*. For example in 2014 Gavin-Smyth and Ferguson [Gavin-Smyth and Ferguson, 2014] showed that *zen* expression is not the same in all the Drosophilidae. Indeed *Drosophila yakuba* and *Drosophila santomea* do not have the broad early *zen* expression at blastoderm stage that *D. melanogaster* has, resulting in a *egr* low early expression. *dorsocross* genes are similarly expressed in *D. melanogaster* and *M. abdita* in the extraembroynic tissue and in other parts of the embryo during development ([Rafiqi et al., 2010, Reim et al., 2003]and

this work) but they show some differences in their genetic interaction with *zen* and/or *dpp*. I observed that when *Mab-docA*, *Mab-docB* or *Mab-egr* are knocked down, *zen* expression is prolonged. In fact the serosa was still expressing *Mab-zen* at 7h post deposition suggesting a negative feedback-loop of these genes on *zen*. *Mab-docA* and *Mab-docB* or *Mab-egr* seems to be responsible of *Mab-zen* inhibition at 6,5h post deposition. This feedback-loop is not present in *D. melanogaster* but it has been shown that in *T. castaneum* *Tc-doc* regulate *Tc-dpp* expression [Horn and Panfilio, 2016]. Moreover, the *dorsocross* genes in *D. melanogaster* are necessary for the amnioserosa maintenance while *Tc-doc* has no role in the serosa or amnion maintenance but it regulates morphogenetic movements of the extraembryonic tissue [Horn and Panfilio, 2016]. *Mab-docA-B* RNAi embryos did not show any defect in serosa maintenance but a delay in the serosa expansion. These results suggest that also in *M. abdita dorsocross* genes are involved in the regulation of extraembryonic morphogenesis but not maintenance. Therefore, *dorsocross* genes may have acquired their role in the maintenance of the extraembryonic tissue during evolution. This role could be linked with the transition from amnion and serosa to the amnioserosa. My results show a difference between *M. abdita* and *D. melanogaster* in *egr* expression. *Mab-egr* is expressed first dorsally in the presumptive extraembryonic tissue. Later on it is restricted to the amnion and its expression persists until germband retraction and amnion closure. In *D. melanogaster egr* is also expressed in the presumptive extraembryonic tissue but it is present in the amnionserosa only until the end of germband extension. My hypothesis is that this divergence could be partially related to the difference in the extraembryonic tissue morphology since the amnioserosa is a close tissue while the amnion is open and needs to close. In previous works, the amnioserosa is considered a dorsal amnion [Hamaguchi et al., 2012, Rafiqi et al., 2008] but *egr* expression does not support this hypothesis, instead it contributes to support the possibility that the amnioserosa maintained several serosa features. These changes in *zen* regulation, *doc* function and *egr* expression show the flexibility of this pathway at different levels of the genetic cascade and point to several positions where the first mutation, which allowed the switch in the extraembryonic tissue morphology, could have hit.

3.5 Cytoskeleton reorganization and remodeling of the extracellular matrix are involved in the extraembryonic tissue morphogenesis of *M. abdita*

In this study, I showed that *Mab-egr* is expressed at early stages in a broad dorsal domain including the amnion and the serosa, and that *Mab-egr* seems to specify the amnion of *M. abdita*. Formation of filopodia in the amnion and their role in the amnion closure was visible in the time-lapse recording analyzed here. *egr* is a component of the JNK signaling pathway. In *D. melanogaster* the JNK signaling is involved in the dorsal closure ([Jacinto et al., 2002]; Martin and Wood, 2002) being necessary for the formation of filopodia and lamellipodia. Its mutations cause defects in the organization of F-actin in the epidermal-leading edge cells (Kaltschmidt et al., 2002). These observations suggest the involvement of the JNK pathway in the amnion closure of *M. abdita*, which is a phenomenon similar to the dorsal closure of *D. melanogaster*. *Mab-egr* and the JNK signaling could be involved in the reorganization of the cytoskeleton of the amnion cells to allow the amnion and, consequently, the dorsal closure. Therefore, genes like POSH (a target gene of *egr*), *canoe* (an afadin) and d*iaphanous* (the Diaphanous-related formin) may be involved in the amnion closure. In fact the proteins of these genes are known to be involved in the regulation of the actin filaments, lamellipodia formation, cytoskeleton dynamics and adherence junctions maintenance in some morphologically active cells ([Homem and Peifer, 2008]; [Sawyer et al., 2009]; [Zhang et al., 2010]). The cytoskeleton is in communication with the ECM via integrin and it is known that the remodeling of the ECM is necessary for tissue and cell migration. Knocking down *Mab-mmp1*, I interfered with the ECM remodeling and the serosa showed a delay in its expansion. From the *in vivo* analysis of *Mab-mmp1* RNAi embryos, it was possible to observe that the contractions at the basal side of the serosa cells prior to detachment appeared to have a different dynamic, suggesting that the connection with the ECM was stronger. In *M. abdita* the serosa contracting cells are located on the yolk sac and in *D. melanogaster* βPS integrin is located on the basal side of the amniosersa

and of the yolk sac. βPS integrin is necessary to hold the two tissues together and their adhesion is required for the amnioserosa contraction [Narasimha and Brown, 2004]. As the amnioserosa of *D. melanogaster*, the serosa of *M. abdita* may need to adhere at the yolk sac to be able to contract. Rule out whether the interaction of the serosa with the yolk sac has a function in this process and in morphological movements during the embryogenesis of *M. abdita*, could shed light on the role of the yolk sac, which has been under estimated for a long time. Another possible link between the remodeling and weakening of the connection of the serosa cells with the ECM is Ninjurin A, a protein that co-localizes and physically interacts with MMP1 in *D. melanogaster* [Zhang et al., 2006]. Ninjurins are conserved two-pass transmembrane proteins that were discovered to be upregulated in rats during nerves injury [Araki and Milbrandt, 1996]; [Araki and Milbrandt, 2000]. *D. melanogaster* has three Ninjurins: Ninjurin A (NijA), Ninjurin B (NijB) and Ninjurin C (NijC). Zhang et al. (2006) shown that the NijA ectodmain is cleaved by MMP1 and it regulates the adhesion of the surrounding cells in a cell-nonautonomous fashion, promoting loss of adherence. Blasting the amnioacidic sequence of *D. melanogaster* NijA against *M. abdita* transcriptome, I verified that NijA has 62% degree of homology between the two species. Therefore, I hypothesized that their extracellular released domain could have the same function that it has in *D. melanogaster* and possibly be the signal for the serosa detachment. The delay in the serosa detachment observed in *Mab-mmp1* RNAi may be due to a missed remodeling of the ECM, or to a missed cleavage of NijA that prevented the loss of detachment of the serosa cells. The delay and not complete prevention of the serosa split from the amnion may be explained by the presence of a small amount of MMPs that may be sufficient to carry out their function. This has been shown also in clones of MMP mutants [Kiger et al., 2007] [Kuo et al., 2005]. For these reasons, further investigations on the role of NijA in *M. abdita*, could increase our knowledge on the mechanisms involved in the serosa detachment and expansion. I hypothesized and verified that also in the migration of the serosa in *M. abdita* the ECM has an important role. For these reasons a possible explanation for the delayed serosa expansion in *Mab-mmp1* RNAi embryos, is that MMP1 is required to remodel the ECM weakening the attachment of the serosa cells to the underlying matrix. In the absence of this remodeling, the extraembryonic tissue needs to generate more tension or takes longer time to

be able to overcome the strong connection with the ECM and so as to be able to crawl over the embryo and eventually enclose it. At late stages, the possible high expression of *Mab-mmp1* and *Mab-mmp2* in the serosa would suggest a role in the detachment of this extraembryonic tissue in preparation of its rupture, retraction and internalization into the embryo during dorsal closure. These results showed that in *M. abdita* the MMPs have a function during embryogenesis. In clear contrast with this consideration, in *D. melanogaster* the two MMPs do not have a function during embryonic stage but they are only required during larval and pupa stages where they are important for normal tracheal growth, to release the old cuticle at molting and head eversion during pupation [Page-McCaw et al., 2003]. The delay in the serosa detachment was observed also in *Mab-egr* RNAi and *Mab-docA-docB* RNAi embryos and resembled the delay encountered knocking down *Mab-mmp1*. This suggests that *Mab-egr*, *Mab-docA* and *Mab-docB* may regulate the remodeling of the ECM. Moreover, when *Mab-egr* was co-knocked down with *Mab-docA* and *Mab-docB* the percentage of embryos showing the phenotype increased to the level of *Mab-mmp1* RNAi. This raises the possibility that *Mab-docA*, *Mab-docB* and *Mab-egr* are involved in the regulation of a common target gene, probably *Mab-mmp1*. Further investigations are necessary to validate this hypothesis.

3.6 Tensions may have a role in serosa and amnion separation

The split between the amnion and the serosa seems to happen at the amniotic fold. This morphological structure may have an important role even though many of its characteristics are not known yet. As observed *in vivo*, there is the formation of an actin cable at the boundary of these two tissues, which is not present in *Mab-zen* RNAi embryos that have a unique extraembryonic tissue. This amnioserosa-like tissue is connected to the epithelium as the amnion in the wild-type *M. abdita* and the amnioserosa in *D. melanogaster*, without the formation of the actin cable at their boundary. Probably this actin cable is not necessary to separate tissues with a different fate, but rather may be involved in the crawling of the tissue. This hypothesis is supported by the presence of the actin cable between amnion and serosa in *Mab-mmp1* RNAi embryos

that have two separating tissues as the wild type. It should be considered that the extraembryonic tissue is stretched and under tension, therefore the split between the amnion and the serosa may be due, at least in some extent, to the forces acting on or within the serosa. This observation opens the question whether the separation of the serosa from the amnion is genetically regulated. Because the serosa is stretched and exposed to forces, actin accumulation at its boundary may be necessary for the migration of the tissue. It is known that tension in an actin cable along a tissue generates or contributes to generate forces that maintain a uniform advance of an epithelium [Bloor and Kiehart, 2002] [Hutson et al., 2003] [Jacinto et al., 2002] [Kiehart et al., 2000] [Rodriguez Diaz et al., 2008] [Wood et al., 2002]. It may be possible that the actin cable formed in *M. abdita* contributes to the advancement of the serosa as a unique front, without leaving behind any detached part. As a result of these considerations, I hypothesize that forces are generated by a genetic control in a regulated manner in time and strength to cause the split between the two tissues. In *O. fasciatus* and *T. castaneum*, it has been hypothesized that forces are essential for the serosa rupture prior dorsal closure and that possible coordinators of this process are *Of-zen* and *Tc-zen2* respectively (Panfilio, 2009; Panfilio et al., 2010). However, there is a main difference between *O. fasciatus*, *T. castaneum* and *M. abdita* that should be considered: in the first two species *zen* is not exclusively expressed in the serosa but also in the amnion, instead in *M. abdita* it is expressed exclusively in the serosa. As it has been pointed out from Schmidt-Ott and Kwang (2016), this hypothesis does not consider the role of *zen* in the amnion. Therefore, there is the possibility that the serosa is not the only responsible tissue for the serosa detachment but that also the amnion has an active role in this process. To better analyze the role and importance of forces in the extraembryonic tissue dynamic, future experiments of laser ablation may be useful.

4

Materials & Methods

4.1 Materials

4.1.1 Fly strain

Megaselia abdita Schmitz (Sander strain) descends from the strain maintained in the Schmidt-Ott laboratory (The University of Chicago, Chicago, USA) and was obtained from Johannes Jäger (CRG, Barcelona, Spain). The culture was maintained, as previously described (Rafiqi et al., 2011; Caroti et al., 2015) at 25°C in a 16/8h day/night cycle.

4.1.2 Injection material

- 27-halocarbon oil (Sigma H8773)
- 700-halocarbon oil (Sigma H8898)
- Oil mixture: 3 parts 27-halocarbon oil + 1 part 700-halocarbon oil
- Borosilicate glass capillaries (World Precision Instrument, 1,0mm outer and 0,58mm inner diameter)
- Light oil for imaging with water index reflection
- Needles were backfilled using Eppendorf Microloader tips (0,5-20µl)
- FEP tube

50x TAE	
Tris Base	242g
Glacial Acetic Acid	57,1ml
EDTA pH 8	100ml
H_2O up to 1l	
6x Gel loading dye	
Tris HCl pH 7,6	10mM
EDTA	60mM
Glycerol	60%
Orange G	0,03%
Store at -20℃	
Hoyers medium	
Gum Arabic	30g
H_2O	50ml
Chloral hydrate	200g
Glycerol	20g
10x PBS	
NaCl	80g
KCl	2g
Na_2HPO_4	14,4g
KH_2PO_4	2,4g
H_2O	800ml
Adjust pH to 7,4 with HCl	
Add H_2O to 1l	
Autoclave	
PBT	
PBS 1X	
Tween-20 0.1%	

4.1.3 General solutions

Luria-Bertani (LB) medium	
Bacto-Tryptone	10g
Bacto-yeast extract	5g
NaCl	10g
H_2O	900ml
Adjust the pH to 7 with 10M NaOH	
H_2O up to 1l	
Autoclave and store at room temperature	

LB plates

Add 15g Bacto-Agar to 1l of LB medium and autoclave. Let the medium cool down to about 50°C and add the antibiotic (Ampicillin 100µg/ml; kanamycin 50µg/ml). Pour the medium into sterile plates, allow it to solidify and store the plates at 4°C.

4.1.4 Chemicals

Name	Company	Catalogue number
Agar	Roth	5210.2
Agarose universal	peq GOLD	35-1020
Ampicillin	Sigma	A9518
BCIP	Roche	11383221001
Chloral hydrate	Sigma	15307
Chloroform/Isoamylalcohol	Fluka/Sigma	25666
DAPI	Molecular Probes Life Technologies	D1306
DNA ladder mix ready to use	Thermo Scientific	SM1173
dNTP	Sigma	D7295
DIG RNA Labeling Mix	Roche	11277073910
EDTA	Applichem	A3553

Name	Company	Catalogue number
EtBr	Roth	2218.2
Ethanol	Sigma	52603
Formaldehyde 37%	Sigma-Aldrich	252549
Formamide	Sigma-Aldrich	47670
Glacial Acetic acid	Merk	607002006
Glycerol	Sigma	54997
Glycogen	Thermo Scientific	R0561
Goat serum	Sigma	G6768
Gum Arabic	Sigma	51198
Heparin	Sigma	H5515
Isopropanol	Sigma	69694
Kanamycin sulphate	Sigma	60615
KCl	Applichem	A3582
KCH_3COO	Grüssing	12001
KH_2PO_4	Applichem	3620
LiCl	Merck	B481279512
Methanol	Sigma	32213-2.5L
NaCl	Sigma	31434
$\mathrm{Na_2}EDTA \cdot 2\,\mathrm{H_2O}$	Fluka/Sigma	34549
Na_2HPO_4	Grüssing	12133
NaOAc	Grüssing	1131
NaOH	Fluka/Sigma-Aldrich	35256-1L
NBT	Roche	11383213001
n-Heptane	Roth	8654.3
NTPs	Thermo Scientific	R0481
Phenol/Chloroform/Isoamylalcohol	Roth	A156.1
SDS pellet	Roth	CN30.2
tRNA	Sigma	R8508

Name	Company	Catalogue number
Triton X100	Merck	1086031000
Trizol	Life technologies	15596062
Tween-20	Sigma	P1379
Tris Base	Roth	4855.2
Tris HCl	Roth	9090.3
X-Gal	Roth	2315.2
Xylene	VWR Prolabo Chemicals	28975.325

4.1.5 Kits

Name	Company	Catalogue number
MAXIscript T7 kit	Ambion	AM1314
mMessage mMachine T7 Ultra Kit	Ambion Life Technologies	AM1345
Plasmid midi kit	QIAGEN	12143
QIAquick gel extraction kit	QIAGEN	28706
QIAprep Spin Miniprep kit	QIAGEN	27106
Oligotex mRNA Midi kit	QIAGEN	70042
RNA easy MiniKit	QIAGEN	74104
SMART RACE cDNA Amplification Kit	Clonetech	634923

4.1.6 Enyzmes

Name	Company	Catalogue number
*BamH*I	Thermo Scientific	ER0051
*Bsa*I FD	New England BioLabs	R3535S
*Dra*I FD	Thermo Scientific	FD0224

Name	Company	Catalogue number
*EcoR*I FD	Thermo Scientific	FD0274
*Hind*III HF	New England BioLabs	R3104
iProof DNA Polymerase	BioRad	172-5331
*Mss*I FD	Thermo Scientific	FD1344
*Not*I	Thermo Scientific	ER0591
Protector RNase inhibitor	Roche	11801800
Proteinase K	Invitrogen	25530-015
*Pst*I	Thermo Scientific	ER0611
RNA SP6 polymerase	Roche	10810274001
RNA T7 polymerase	Roche	10886520
RNaseA	Thermo Scientific	EN0531
*Spe*I/*Bcu*I FD	Thermo Scientific	FD1253
T4Ligase 5U/µl	Thermo Scientific	EL0011
Taq DNA Polymerase F-100L	Finnzymes Biozym	out of production

4.1.7 Antibody

Name	Company	Catalogue number
Anti-DIGOSSIGENIN-AP fab fragment	Roche	11093274910
Anti-Engrailed/Invected antibody	Hybridoma Bank	4D9
Secondary biotinylated horse anti-mouse antibody	Vector Laboratories	BA-2000

4.1.8 Instruments

- Electroporator MicroPulser (Bio Rad)
- Eppendorf FemtoJet express microinjector

- MuVi SPIM EMBL
- Needles puller Flaming/Brown micropipette puller (Sutter Instruments P-97)
- Zeiss Axio Imager M1

4.2 Methods

4.2.1 Genomic DNA extraction from adult flies

The genomic DNA was extracted from 10 adult flies that were homogenized in 500µl lysis buffer with a micropestle. Following, 15µl ProteinaseK (10µg/µl) were added and incubated 1h at 56°C. The DNA was cleaned by phenol/chloroform extraction and the RNA was degraded with 5µl RNaseA (10µg/µl) and an incubation of 10 min at 37°C. In order to purify the genomic DNA, phenol/chloroform extraction was performed and it was precipitated with 50µl NaOAc (3M pH6) and 1ml EtOH. The pellet was dissolved in 30µl Tris/HCl 10mM pH 8,5 and stored at -20°C.

Lysis buffer
Tris/HCl pH7.5 20mM
NaCl 200mM
EDTA 20mM
SDS 2%

4.2.2 Total RNA extraction

To isolate total RNA, fly embryos were homogenized in 1ml of Trizol and incubated for 5min at room temperature to permit complete dissociation of the nucleoprotein complex. The RNA was first separated with chloroform (200µl) then precipitated with isopropanol (500µl) and incubated 10min at room temperature, and the pellet was dissolved in 100µl RNase free water. The quality was detected on a 1% agarose gel and the concentration with UV photospectroscopy. The total RNA was store at -80°C.

4.2.3 Isolation of polyA mRNA

The poly-A mRNA was isolated from the total RNA extracted from the fly embryos, using the Oligotex mRNA Midi kit (QIAGEN) and following the midi protocol in the user manual.

4.2.4 cDNA synthesis

The amount of polyA mRNA necessary to synthesize the cDNA is (between 10pg and 500ng), so for M. abdita cDNA 226ng were used and the following reagents were mixed in the specified amount:

Primer $(dT)_{20}$ SL0001 (50µM)	1µl
dNTP (10mM)	1µl
poly-A mRNA	2µl
H_2O up to 13µl	

The reaction was incubated at 65°C for 5min then in ice for at least 1min. The poly-A mRNA was retro-transcribed adding and incubating for 1h at 50°C:

5x First strand buffer	4µl
DTT (0,5M)	1µl
RNase inhibitor (40U/µl)	1µl
SuperScript III RT (200U/µl)	1µl

The reaction was heat inactivated and the RNA complementary to the cDNA was removed adding 40µl of nuclease-free water.

4.2.5 Polymerase chain reaction

The polymerase chain reaction (PCR) was used to amplify specific region from genomic DNA or cDNA. The amplification was achieved using a forward and revers primers (0,2µM), a thermo-stable DNA polymerase, dNTP (0,2mM) and about 50ng of template. The reactions were performed with two different poly-

merases: Taq DNA Polymerase F-100L (Finnzymes) and iProof Hight-Fidelity DNA polymerase (BioRad). Depending which one was used the protocol was different in the reaction mix and in the program used in the thermo-cycler since they have a different temperature of activation and speed of processing. In both cases the reactions were performed in a total volume of 30µl.

Reaction mix Taq DNA Polymerase F-100L	
10x Optimized Taq buffer	3,0µl
dNTP (10mM)	0,6µl
primer forward (10µM)	1,0µl
primer revers (10µM)	1,0µl
gDNA/cDNA (50ng/µl)	1,0µl
Taq DNA Polymerase F-100L	0,2µl
ddH_2O	23,2µl

Program		
1. Initial denaturation	94℃	2min
2. Denaturation	94℃	20sec
3. Annealing	depending from Tm primers	30sec
4. Elongation	72℃	depending from size fragment
Repeat 36 times from step 2 to step 4		
5. Final extension	72℃	5min
6. Hold	12℃	forever

Reaction mix iProof Hight-Fidelity DNA polymerase	
5x iProof GC buffer	6,0µl
dNTP (10mM)	1,0µl
primer forward (10µM)	1,0µl
primer revers (10µM)	1,0µl
gDNA/cDNA (50ng/µl)	1,0µl
iProof DNA Polymerase	0,5µl
ddH_2O	19,5µl

Program		
1. Initial denaturation	94℃	5min
2. Denaturation	94℃	20sec
3. Annealing	depending from Tm primers	30sec
4. Elongation	72℃	depending from size fragment
Repeat 36 times from step 2 to step 4		
5. Final extension	72℃	7min
6. Hold	12℃	forever

The entire reaction was loaded in an agarose gel and the PCR product was analyzed by electrophoresis. The DNA band of the right size was cut and purified by kit. The iProof DNA polymerase did not add the tail of poly-A therefore, if the amplicon was afterward inserted in pCRII-TOPO vector, the PCR product was A-tailed by Taq DNA Polymerase F-100L with the following protocol and an incubation of 20min at 72°C:

Reaction mix	
Purified PCR product	8,0µl
10x Optimized Taq buffer	1,0µl
dATP (100mM)	1,0µl
Taq DNA Polymerase F-100L	0,5µl

To increase the length of an identified fragment, the 5' and 3'-RACE are used. This technique was used to prolong the Mab-mmp1 sequence. A PCR (primer pair SL153-SL154/SL711) and a nested PCR (primer pair SL155/SL712) were performed using the 5'-RACE cDNA as template and the iProof DNA polymerase. With this reaction the 5'UTR of mmp1 was identified and a longer RNA probe for the in situ hybridization synthetized. The primers SL153, SL154 and SL155 were from the SMART RACE cDNA Amplification Kit and

SL153, SL154 were used in a mix 1:1 ratio as forward primers.

4.2.6 Agarose gel electrophoresis

Agarose gel electrophoresis was used to assess quality, concentration and size of the DNA or RNA fragments. The agarose gel was prepared in 1x TAE with a percentage of agarose depending from the size of the fragment that was analyzed. EtBr was added to the melted agarose in a concentration of about 1:20000. The DNA or RNA were mixed with a 6x loading dye and loaded into the gel. Positive and negative electrodes were applied to the gel chamber filled with 1x TAE. The negative charged DNA and RNA migrated toward the positive pole and bind the EtBr, so that it can be visualized using an UV lamp. In order to distinguish the size of the fragment of interest, a DNA ladder mix was loaded next to the samples. The DNA ladder had bands of specific size and concentration that were used to compare with the samples.

4.2.7 Gel extraction

The DNA band was cut from the agarose gel and weighted with a balance. The elution of the DNA was then performed with the QIAquick gel extraction kit following the user manual.

4.2.8 Ligation

The sequence of the genes of interest was eluted from the agarose gel, as above described, and ligated into the pCRII-TOPO TA vector with the TA system. The reaction was incubated at least 30min at room temperature.

Reaction mix	
Insert	4,0µl
Salt solution (1:4)	1,0µl
pCRII-TOPO vector	0,5µl
ddH_2O	0,5µl

4.2.9 Electrocompetent cells preparation

TOP10 electrocompetent cells were prepared setting up a pre-culture with one clone (2x 100ml LB medium) incubating over night in a shaker at 37°C. The pre-heated 3x 1l LB medium were inoculated, each liter with 10ml 1:100 pre-culture and incubated at 37°C shaking until the OD_{600nm} was equal to 0,6-0,8. From now on the steps are performed at 4°C and on ice. The cells were transferred in ice for 15min and then centrifugated 20min at 4000rpm. The pellets were dissolved in 20ml ice-cold water and then filled up to 200ml. The centrifugation step was repeated but the final volume was 100ml, so that two tubes could be pooled together. A third step of centrifugation was performed. The pellets were dissolved in 15ml ice-cold 10% glycerol, transferred in 50ml tubes and the volume was filled up to 50ml with ice-cold 10% glycerol. After a centrifugation of 40min at 4000rpm, the pellet was dissolved in about one volume of the pellet with 10% glycerol. Aliquots of 50µl were made in pre-cooled 1,5ml tubes, shock frozen in liquid nitrogen and stored at -80°C.

4.2.10 Cell transformation

Electrocompetent cells were transformed by electroporation. 40µl of cells were defrosted in ice and 1µl of ligation was added, for a final concentration of 10pg/ml-7,5µg/ml. After have a gently mix, cells and ligation were transferred into a pre-ice cooled cuvette that was then dried and inserted between the electrodes of the electroporator. Immediately 250µl LB were added and everything was transferred into a 1,5ml tube where the bacteria were recovering and growing shaking at 300rpm for 45min at 37°C. Afterward the cells were plated on LB-agar plates with ampicillin (100µg/ml) or kanamycin (50µg/ml) depending from the resistance gene the incorporated vector was carrying. On these plates 60µl X-Gal (20mg/ml) had been previously plated to allow the selection of positive (white) and negative (blue) colonies. This blue/white screening is based on the enzymatic activity of the β-galactosidase that transforms the colorless X-Gal in 5-bromo-4-chloro-3-hydroxyindole, which is blue. The insert interrupts the gene lacZ that codify the enzyme, indicating a successful insertion of the sequence into the vector.

4.2.11 Plasmid preparation

About ten colonies per gene were picked and grown in 5ml LB medium for at least 6h or over night. DNA plasmid was prepared by centrifugation of 4ml bacteria culture for 2min at 4000rpm. The pellet was resuspended in 200µl cold P1 buffer. Then the cells were lysated with 200µl P2 buffer that was neutralized with 200µl P3 buffer. The sample was centrifugated at 14000rpm and the supernatant transferred to a new tube. In order to precipitate the DNA 500µl isopropanol were added and left incubate for 10min. Following it was spin down for 15min at 14000rpm and the pellet was washed with 70% EtOH and dissolved in 30µl ddH2O. The clones were analyzed by test digest with EcoRI to verify whether the correct sequence was inserted into the vector. One of the clone showing fragments of the proper size, was sent to sequence by Eurofins. The positive clone was then purified with the QIAprep Spin Miniprep kit. Briefly, the Binding buffer of the kit was added to the DNA plasmid up to 750µl and transfer to the column. At this point the purification proceeded following the user manual. Large scale DNA plasmid was extracted using the Plasmid midi QIAGEN kit following the user manual.

P1 buffer:

- Tris base 6,06g
- $Na_2EDTA \cdot 2\,H_2O$ 3,72g

Dissolve the powders in 800ml ddH_2O and adjust to pH 8 with HCl. Then add ddH_2O up to 1l and autoclave the buffer. Once cooled down, add 100mg RNase A per liter and store at 4°C.

P2 buffer:

- NaOH 8g
- 10% SDS 100ml

Dissolve NaOH in 900ml ddH_2O, add 100ml 10% SDS and filter the buffer. Store it at room temperature.

P3 buffer:

- KCH_3COO 3M pH 5.5

  Autoclave the buffer and store at 4°C.

4.2.12 dsRNA synthesis

The template to synthesize the dsRNA was done by PCR, using a linearized plasmid. The used primers (SL0049 and SL0059) contain the T7 promoter sequence and a priming sequence residing on the multiple cloning site of pCRII-TOPO, accordingly to Kennerdell and Carthew, 1998.

Reaction mix	
10x Buffer	10µl
Linearized plasmid	1µl
dNTP (10mM)	2µl
SL0049 (10µM)	3µl
SL0050 (10µM)	3µl
Taq DNA Polymerase	2µl
mQH_2O up to 100µl	

The PCR product was purified by Phenol/Chloroform extraction and precipitated with 1µl of glycogen (10mg/ml), 1/10 volume NaOAc (3M, pH6) and 3 volumes of EtOH 100%. After centrifugation the pellet was dissolved in 10µl of mQ H2O. The quality and concentration of the template was evaluated on a 1% agarose gel in a dilution series. For the RNA synthesis a reaction is set

Program		
1. Initial denaturation	94℃	2min
2. Denaturation	94℃	20sec
3. Annealing	60℃	30sec
4. Elongation	72℃	1min
Repeat 45 times from step 2 to step 4		
5. Final extension	72℃	5min
6. Hold	12℃	forever

up using 1-2µg of template and incubated 4-6h at 37°C.

Reaction mix	
10x Buffer	10,0µl
NTPs (2,5mM each)	40,0µl
RNase inhibitor	2,0µl
T7 RNA Polymerase	2,5µl
DNA template	1-2µg
RNase freeH_2O up to 100µl	

The DNA template is degraded adding 1,5µl of RNase free DNase and incubating the reaction at 37°C for 15min. Then 200µl RNase free H2O and 1/10 volume NaOAc (3M, pH 6) were added, followed by the phenol/chloroform purification. The dsRNA was precipitate with 2,5 volumes of EtOH and storing the sample over night at -20°C. The pellet was dissolved in 20µl of RNase free H2O and, to avoid the clogging of the needle during injection, it was centrifugated for 20min and only 18µl were transferred in a fresh tube and tested for quality and concentration on a 1% agarose gel in dilution series. To obtain the molarity of the dsRNA, the sample was measured by UV photospectroscopy and the molecular mass was obtained with the oligonucleotide calculator http://www.basic.northwestern.edu/biotools/oligocalc.html. The dsRNA was stored at -20°C.

4.2.13 Cas9 mRNA synthesis

In this work has been used the mammalian codon optimized Cas9 (addgene 43861). 5-10µg of plasmid were linearized with 5µl MssI FD for 1h at 37°C. After heat inactivation of the enzyme, the template was cleaned from protein traces adding 2µl ProteinaseK (10mg/ml) and 5µl 10% SDS, and incubating the reaction for 30min at 50°C. Following, the volume was filled up to 200µl with nuclease free water and the phenol/chloroform extraction was performed. The sample was precipitated with 1/10 volume of NaOAc and 3 volumes EtOH, incubating at least 2h at -20°C. The pellet was then dissolved in 10µl nuclease free water and linearization and concentration were checked on agarose gel. Cas9 mRNA was synthetized using mMessage mMachine T7 Ultra Kit with the following reaction:

Linear template DNA	1µg	
2x NTP/ARCA	10µl	
10x T7 Reaction Buffer	2µl	(add after H2O and NTPs)
T7 Emzyme Mix	2µl	
Nuclese freeH_2O up to 20µl		

ownprimer After an incubation of 2h at 37°C, 1µl Turbo DNase was added for 15min at 37°C. The poly-A-tailing was performed with the following reaction:

RNA 20µl	
H_2O	36µl
5x E-PAP Buffer	20µl
MnCl2 (25mM)	10µl
ATP solution	10µl
As minus-enzyme-control remove 2,5µl of reaction	
E-PAP	4µl

The reaction was incubated 45min at 37°C and then moved in ice. The mRNA was recovered using RNA easy MiniKit following the user manual. Its

quality was assessed by gel electrophoresis and the concentration with UV photospectroscopy. mRNA aliquots were prepared and stored at -80°C.

4.2.14 sgRNA synthesis

The expression vector DR274 (LP381), was linearized over night by BsaI in the following reaction mix:

Plasmid DNA	5µg
BsaI FD	2µl
10x FD Buffer	2µl
H_2O up to 20µl	

The linearization of the plasmid was analyzed by gel electrophoresis and the digested product of 2147bp cut and purified, eluted in 30µl of 10mM Tris-HCl(pH 8,5) and vector diluted to 40ng/µl (0,025pmol). At the same time, the oligos for the specific target site were annealed, mixing 10µl of each primer and 20µl annealing buffer (10mM Tris, 30mM NaCl) with the following program in the thermocycler:

96°C 5min

Ramp down to 70°C (0,1°C 7sec)

Hold 10min

Ramp down to 65°C (0,1°C 7sec)

Hold 10min

Ramp down to 60°C (0,1°C 7sec)

Hold 10min

Ramp down to 10°C (0,1°C 7sec)

At the end of the program, the annealed oligos were diluted to a final concentration of 0,075pmol/µl. They were ligated into the linearized vector for at least 2h or over night at a temperature of 17-22°C with the following reaction mix:

Linearized DR274	1µl
Annealed primers	1µl
PEG	1µl
T4 Ligase (5U)	1µl
Ligase Buffer	1µl
H_2O up to 10µl	

40µl of TOP10 electrocompetent cells were transformed with 1µl of this ligation and plated on LB plates containing Kanamycin. Mini prep, test digest with BsaI and sequencing were performed. The positive clone was used to in vitro transcribe the sgRNA. As first, 10µg of plasmid were digested with DraI FD/HF over night and, after gel electrophoresis, the fragment of 3Kb was purified. Then the in vitro transcription was performed using the MAXIscript T7 kit.

Reaction mix		
Dna template	1µg	(300ng are sufficient)
10x Transcription buffer	2µl	
ATP (10mM)	1µl	
CTP (10mM)	1µl	
GTP (10mM)	1µl	
UTP (10mM)	1µl	
Enzyme Mix	2µl	
H_2O up to 20µl		

The reaction was incubated over night at 37°C then 1µl Turbo DNase was added and incubated other 15min. To purify the RNA, 30µl H_2O, 5µl 5M NaOAc and three volumes EtOH were added and incubated at -20°C for at least 30min. Following a centrifugation of 15min at 4°C was performed and the pellet was dissolved in 30µl RNase free water. The RNA quality was check by electrophoresis, aliquots were made and stored at -80°C

4.2.15 RNA labeled probes synthesis

The template was prepared by vector linearization on the opposite side of the promoter that had to be used. 10µg of plasmid were linearized for 4h in a total volume of 50µl and purified with phenol/chloroform. The sample was then precipitated adding 1µl glycogen (10mg/ml), 1/10 volume NaOAc (3M, pH6) and 3 volumes EtOH. The pellet was dissolved in 10µl RNase free H2O and the quality and concentration of the digested vector was tested on 1% agarose gel in a dilution series. The probe synthesis was performed in a 10µl reaction using 1µg of template and incubated at 37°C for 2h.

Reaction mix	
DNA template	1µg
10x Buffer	1µl
DIG-NTP	1µl
RNase inhibitor	1µl
RNA polymerase	1µl
RNase free H_2O up to	10µl

The probe was tested for quality and concentration on 1% agarose gel in a dilution series. To the sample were added 90µl RNase free H2O and then it was precipitated with 10µl RNase free LiCl (4M), 10µl tRNA (10mg/ml), 300µl EtOH and store at -20°C for 30min or over night. The probe was dissolved in HYB in order to have a concentration of at least 6ng/µl, in a maximum volume

of 150µl. The RNA probe was stored at -20°C.

4.2.16 Dechorionation of M. abdita embryos

M. abdita embryos were dechorionated in 50% commercial bleach (chlorix) for 2min. They were then transferred into a net and abundantly washed with tap water.

4.2.17 Heat fixation

Heat fixation of *M. abdita* embryos was performed as outlined in Rafiqi et al. (2011a). Briefly, the dechorionated embryos were transferred in a 50ml tube with a brush and the just boiled fixing solution I was poured into this tube. After 20sec, room temperature ddH_2O was added up to 50ml. Once the embryos sank, about 30ml of solution were removed and the embryos were transferred in a 1,5ml tube, washed with 1ml ddH_2O and devitellinized shaking the embryos for 30sec in n-heptane and MetOH in a ratio 1:1. The devitellinized embryos sank while the rest was at the interphase. The solution was completely removed and the embryos washed three times in MetOH. The fixing solution II was added and left incubate 25min at room temperature rocking. Then the embryos were washed three times in MetOH and stored at -20°C. The injected embryos were cleaned from the oil prior fixation. The slide was immerged in n-heptane and, after brief air dry, the embryos were transfer in a 50ml tube by pouring tap water along the slide. After fixation II, the fixative was removed first below the interphase and then the top layer in order to keep also the non-devitellinized embryos that will be later manual devitellinized.

Fixing solution I	
28% (w/v) NaCl	500µl
5% (v/v) Triton X100	200µl
ddH_2O up to 20ml	
To avoid Triton precipitation, water has first to be added to the salt.	

Fixing solution II

37% formaldehyde stock solution is diluted to 5% in 1x PBS:MetOH (3:1)

4.2.18 Manual devitellinization

The vitelline membrane was manually removed (as outlined in Rafiqi et al., 2011a) from the embryos that have been previously injected, washed in n-heptane to remove the oil and heat fixed. In these embryos, the vitelline envelope was broken during the fixation but not completely removed. Therefore they were transferred in MetOH on a 1% agar plate and with the help two tungsten needles the membrane was removed. These needles were previously sharpened using an electrolytic apparatus and 10% NaOH as strong electrolyte.

4.2.19 Whole mount in situ hybridization

Unless stated otherwise, all the steps were performed at room temperature. The colorimetric whole mount in situ hybridization was based on Crombach et al. (2012) with some modifications. The fixed embryos were washed in EtOH and cleared with Xylene in a gradual passage. First a wash in Xylene/EtOH 1:1, 1h in Xylene/EtOH 3:1 rocking and then back to EtOH passing by a wash in Xylene/EtOH 1:1. After 3 washes in EtOH and 3 in MetOH, the embryos were re-hydrated with a wash in PBT/MetOH 1:1. Following, three more washes in PBT and 5min rocking were performed. The embryos were treated with proteinase K (0,08U/ml) diluted in PBT, rocking for 2min and then 1h in ice to reduce the enzymatic activity. Two washes in ice with ice-cold PBT were performed, followed by 5% formaldehyde fixation for 25min rocking. The embryos were rinsed three times and then washed two times rocking for 5min each in PBT. From the 1,5ml tube the embryos were transferred in a 0,5ml tube and rocked for 10min in PBT/HYB (1:1), washed 2min in HYB rocking and pre-hybridized for 1h in HYB at 56°C in a water bath. The probe was prepared in 10µl HYB (0,5-2,0ng/µl), heated for 5min at 80°C to resolve secondary RNA structures and immediately put in waterish ice. The probe was added to the embryos and the hybridization was performed over night. The

embryos were post-hybridized for 15min in pre-wormed HYB and then washed twice for 30min in HYB at 56°C. After a wash of 15min in HYB/PBT (1:1), other four washes of 15min rocking in PBT were performed. The blocking step was performed rocking the embryos for 30min in PBT with 5% goat serum. The incubation with the anti-DIG antibody (1:2000) was 1h long rocking. The embryos were then rinsed twice in PBT followed by four washes of 15min rocking. Two washes of 5min in AP buffer were performed and the embryos were transferred in a glass cube where NBT/BCIP in AP buffer was added (NBT 0,7mg/ml; BCIP 0,35mg/ml) to stain in the dark. The reaction was stopped with three washes in PBT and the embryos were transferred back to a 1,5ml tube where they were rinsed with PBT/EtOH (1:1) and washed rocking 10min for three times in EtOH to remove the background. After a rinse of PBT/EtOH (1:1), three washes rocking of 5min each in PBT followed. 50% glycerol (diluted in PBS) was added to the embryos that, once settled, were transferred in a new tube with 75% glycerol. When the DAPI staining was performed in combination with the whole mount in situ hybridization, the DAPI was added before the embryos were transferred in glycerol.

AP Buffer		
	Stock	Final conc.
NaCl	5M	100mM
MgCl	2M	50mM
Tris pH 9.5	1M	100mM
Tween-20	10%	0.1%
ddH_2O up to the final volume		

4.2.20 DAPI staining

M. abdita embryos were washed in MetOH then in MetOH/PBT (1:1) and finally in PBT. Following, they were rocked 4min in DAPI (final concentration 0,2µg/ml) diluted in PBT. The embryos were consequently rinsed five times

Hybridization buffer
50% Formamide
5X SSC
Torula yeast RNA 5mg/ml
Heparin 50µg/ml
Tween-20 0.1%
RNase free H_2O up to the total volume
pH 5-6

and washed twice for 2min in PBT. Glycerol/PBS (1:1) was added and once the embryos settled, were transferred in a tube with 75% glycerol.

4.2.21 Antibody staining

The antibody staining was performed for Engrailed based on published protocol (Lemke et al., 2009) with modifications. The fixed embryos were rinsed twice in MetOH, once in MetOH/PBT (1:1) and three times in PBT. ProteinaseK (0,08U/ml in PBT) treatment was done for 2min rocking and three washes in PBT followed. The embryos were then fixed in 3,7% formaldehyde (diluted in PBT) rocking for 1h. Afterward, they were rinsed three times in PBT and washed four times for 15min rocking in PBT. The blocking step was done with 10% goat serum in PBT for 1h. The primary antibody against Engrailed was added (1/10 of the total volume, goat serum 1%) and incubated over night at 4°C. The embryos were rinsed three times with PBT and four washes of 15min followed. A second blocking step was performed for 30min as stated above. At this point the secondary biotinylated horse anti-mouse antibody was added (1/500 of the total volume, goat serum 1%) and incubated for 2h at room temperature rocking. The embryos were then rinsed three times washed four times for 15min with PBT. Following, two washes of 5min in AP buffer were performed and the embryos were stained in the dark rocking over night at 4°C with NBT/BCIP (NBT 0,08µg/µl; BCIP 0,04µg/µl final concentration). The day after the staining is stopped with three washes in PBT and the background cleared washing once the embryos in PBT/EtOH (1:1) and three times rocking for 10min in EtOH. After a passage in PBT/EtOH (1:1), three washes of 5min rocking in PBT followed. Glycerol/PBS 1:1 was added and once the embryos

sunk were transferred in a tube with 75% glycerol in PBS.

4.2.22 Cuticle preparation

M. abdita embryos were injected and left develop until first instar larvae. The slide with the embryos was immerged in n-heptane to remove the oil where the larvae were gently detached from the slide and transferred into a 1,5ml tube. The cuticles were prepared based on a previously published protocol (Hu and Castelli-Gair, 1999). Briefly, n-heptane and MetOH were added in a ratio 1:1 and, to remove the vitelline membrane, the larvae were shake for 1min. Several times this treatment is not sufficient for *M. abdita*, so the larvae have to be manually devitellinized. Four washes in MetOH and four in water with 0,1% Tween-20 followed. The larvae were then mounted in Hoyer's medium on a slide and left for two or three days at 60-70°C.

4.2.23 Needles preparation

Borosilicate glass capillary were pulled with a horizontal micropipette puller. The following one step program was used: P: 500; Heat: 500; Pull: 115; Vel: 15; Time: 250. Afterward, needles have been opened by beveling or forcepes.

4.2.24 Injection of *M. abdita* embryos

The embryos were collected after 40min deposition, dechorionated, lined up on a slide along a capillary, dried and covered with a mixture 1+3 of 27-halocarbon oil and 700-halocarbon oil as previously outlined (Rafiqi et al., 2011b, Rafiqi et al., 2011c). The embryos were injected in the center and usually on their ventral side.

4.3 Primers and plasmids

All primers used in this thesis were synthetized by Eurofins or Sigma and are here listed:

Name	Sequence (5’ to 3’ orientation)
SL153 (UPM long)	5’-CTAATACGACTCACTATAGGGCAAGCAGTGGTATCAACGCAGAGT
SL154 (UPM short)	5’-CTAATACGACTCACTATAGGGC
SL155 (NUP)	5’-AAGCAGTGGTATCAACGCAGAGT
SL172	5’-ACCTCAGTTCATGATGCCACCTCA
SL173	5’-TGACGATGACGACCCAGACACATT
SL174	5’-TGACAGTCCAGCATCTGGTTCACA
SL175	5’-TGGTTAGGTGACAATGGTGGTGGT
SL261	5’-CAGTTCTACCTGTCTCAATTTGGA
SL262	5’-ACCTGGTAATCCTACCCATCCTTC
SL259	5’-AAAGTTATCTTTTCCCTTCCAGGC
SL260	5’-ATCGATCTCATTGGACAATTGACA
SL311	5’-ATGATTACCATGAATGAATTAGTGGATTTA
SL312	5’-CTAACATTGCGCAACACCC
SL314	5’-CTATCTTTCTAGTATTGATGATATCGAGAA
SL318	5’-CCCGAGAAAAAGAGTGGCA
SL323	5’-ACAAACTTTGCGGTTGAATTTTT
SL324	5’-ACTATGAGACAAATACTTAACGGAGA
SL346	5’-GGAATACCACATTCACCTCATAGT
SL349	5’-TTCCGTTCATTCTCATCTCCAA
SL569	5’-TAggGACAATCAATAGTCCACG
SL570	5’-AAACCGTGGACTATTGATTGTC
SL571	5’-TAggAAAGAGATACGCTCTGCA
SL572	5’-AAACTGCAGAGCGTATCTCTTT
SL573	5’-TAggTGAAAACTCGGTTGCCGA
SL574	5’-AAACTCGGCAACCGAGTTTTCA
SL583	5’-TTGATGGTCCTGGTATGGTG
SL584	5’-AGTTTTCCTCTGAAGTGGGC
SL650	5’-TAGGCGCATTCTACCCTGGTGA

Name	Sequence (5' to 3' orientation)
SL651	5'-AAACTCACCAGGGTAGAATGCG
SL652	5'-TAGGACGAATGGCCCAACCCCA
SL653	5'-AAACTGGGGTTGGGCCATTCGT
SL654	5'-TAGGACACCGGTAGAGTGGAGT
SL655	5'-AAACACTCCACTCTACCGGTGT
SL711	5'-ACCCCGATAGAATGGAGCCA
SL712	5'-ATGACTGAGGCCGAGAGAGT

All plasmids, with the exception of the ones received from Dr. Schmidt-Ott' s lab (University of Chicago), were sequenced by Eurofins and all the constructs used in this thesis are here listed with the relative RNA probes when synthetized:

Table 4.6: Clones used in this thesis and relative RNA probes when synthetized

Name	Gene	Specification	Size	Vector
LP203	*Mab-zen*	ORF	848bp	pGEM-T Easy
This clone is from Dr. Schmidt-Ott' s lab, University of Chicago				
LP256	*Mab-ddc*	gene fragment		
This clone is from Dr. Schmidt-Ott' s lab, University of Chicago				
LP337	*Mab-mmp1*	gene fragment	1002bp	pCRII TOPO-TA
LP338	*Mab-mmp2* short	gene fragment	414bp	pCRII TOPO-TA
	Mab-docA	gene fragment	636bp	pCRII TOPO-TA
This clone is lost but the sequence was a sub-fragment of LP339				
LP339	*Mab-docA*	full length	bp	pCRII TOPO-TA
LP341	*Mab-egr*	full length	1463bp	pCRII TOPO-TA
	Mab-docB	gene fragment	755bp	pCRII TOPO-TA

Table 4.6: Clones used in this thesis and relative RNA probes when synthetized

Name	Gene	Specification	Size	Vector
This clone is lost but the sequence was a sub-fragment of LP342				
LP342	*Mab-docB*	full length	1408bp	pCRII TOPO-TA
LP349	*Mab-en*	gene fragment	1282bp	pCRII TOPO-TA
LP544	*Mab-mmp2* long	gene fragment	bp	pCRII TOPO-TA
LP545	*Mab-mmp1* long	gene fragment	bp	pCRII TOPO-TA
LP472	*Mab-mmp1*	sgRNA1		
LP473	*Mab-mmp1*	sgRNA2		
LP474	*Mab-mmp1*	sgRNA3		
LP546	*Mab-mmp2*	sgRNA1		
LP547	*Mab-mmp2*	sgRNA2		
LP548	*Mab-mmp2*	sgRNA3		

5

Appendix 1

5.1 Establishing a protocol for *in toto* time-lapse recordings of *M. abdita* wild type and RNAi embryos

In vivo imaging captures dynamics of developmental processes and allows observations of interconnected spatiotemporally separated aspects of development. The development of an organism is a dynamic process that ranges from subcellular rearrangements and cell movements to structural changes at the whole-organism level. The dynamics of this process are key to investigate the underlying mechanisms and are revealed only by *in vivo* imaging [Keller, 2013]. The usage of *in vivo* imaging has led to substantial insights in model systems such as *Drosophila melanogaster* and *Caenorhabditis elegans*. Likewise, live imaging in non-model system has been used to gain critical insights into core developmental processes, e.g. ex-traembryonic tissue formation in insects [Panfilio et al., 2013]. *In vivo* imaging provides key observations into core developmental processes, and helps to formulate specific hypothesis on gene function. Such hypotheses are tested by analyzing mutants (model system) or specimen in which the gene function has been knocked down, e.g. by RNAi. For example, *in vivo* functional studies of mesoderm invagination in *D. melanogaster* [McMahon et al., 2010] and dorsal closure in *Tribolium castaneum* [Panfilio et al., 2013] linked genes with key morphogenetic processes of fly embryogenesis. An increasingly popular microscope technology aiming for fast *in toto* imaging with low photo-toxicity that allows the analysis of morphogenetic processes during embryonic development is light sheet microscopy. In light sheet microscopy a fluorescent sample has to be used. Illumination with light sheet excites only fluorophores from and near the focal plane. Moreover,

SPIM microscope can record one plane at the time allowing fast imaging (about 100 fps) and exposes the specimen to less light thus reducing sample bleaching and phototoxicity and allowing long imaging. Additional features like the possibility to rotate the sample and reconstruct a 3D embryo improved the process even further. All these together enable the analysis of morphogenetic movement during organismal development. In fact light sheet microscopy was used, e.g., in fish and flies in processes as analysis of the nervous system, mesoderm invagination and cell tracking, and allowed to address long-standing questions in their embryonic development [Keller and Stelzer, 2008, Lemon and Keller, 2015, Rauzi et al., 2015]. In contrast to conventional microscopy, light sheet microscopy requires particular mounting techniques for the specimen. Because the sample needs to be freely rotated and accessible to four different lenses, the embryo is typically mounted along its longest axis in a block of agarose [Keller and Stelzer, 2008, Keller et al., 2010]. Alternatively, the specimen resides within a plastic tube made of fluorinate ethylene propylene (FEP) that has refractive index close to the one of water making it well suited for imaging aqueous samples [Kaufmann et al., 2012]. This mounting technique has proved challenging at times for embryos of model systems (Drosophila, fish embryo), and it required substantial efforts to ensure that wild-type development was not affected by the mounting methodology [Kaufmann et al., 2012]. For non-model systems the use of injection-based tools to knock down or constitutively activate gene function represents an additional challenge. Insect embryos, for example, are typically injected under oil. Differences in surface tension of oil and water seal the injection wound and thus allow quick healing and development for conventional *in vivo* imaging, e.g. on a confocal microscope. This, however, is not possible in SPIM microscopy, where the mounted specimen is entirely submerged under water. To make non-model species accessible for functional studies using SPIM imaging, there is the necessity to improve the tools that are currently available for the non-model organisms. Spe-cifically, to allow time-lapse recordings for *M. abdita* extraembryonic development similar to those available in *D. melanogaster* and *T. castaneum*, I developed a mounting method to image fly embryos with the MuVi-SPIM after injection. On the one hand, this method can be used for wild type description if a transgenic line with a particular cell marker is not available by injecting a fluorescent protein as cellular marker; on the other hand, this method may

be used for functional studies by injecting pre-mixed dsRNA or mRNA. Both approaches can be combined. The fly embryos were injected under oil with a refractive index similar to water and one was mounted with the same oil in the FEP tube. This tube was then submerged into water filled imaging chamber. For all the optics involved, the embryo is still in water. How-ever, the injection site is protected and sealed by thin film of oil and separated from any contact with water by FEP tube that otherwise would lead to an abundant leakage of the embryo.

5.1.1 Injection of fly embryos

In order for any injected agent (dsRNA, mRNA, protein) to diffuse throughout the embryo, injections had to be performed at the blastoderm stage. These injections were technically comparable to injections performed for functional studies in fix tissue or live imaging with a confocal microscope (Rafiqi et al., 2011). However, rather than using halocarbon-oil to cover the embryos, I used oil with a refractive index close to the reflection index of water (oil=1,335; water=1,333). Embryos were dechorionated, aligned on a slide and partially dried as for a standard injection and covered with oil. As this oil was more fluid than the standard halocarbon-oil, the angle between the needle and the slide had to be rather steep (about 45°) to avoid that the needle attached to the oil and thus removing it from the embryos while moving during the injection process. The needle clogged more easily when a mix of protein and highly concentrate dsRNA were co-injected. As a countermeasure, the pressure of the injector was set very high (Pc=300; Pi=1000) before the needle was lowered into the oil, and only later decreased as desired. Injections themselves were carried out as described previously (Rafiqi et al., 2011). After injection, the embryos were transferred to a moist chamber until mounting.

5.1.2 Mounting of injected fly embryos

Fly embryos were left to recover from injection. When they reached the proper stage, they were inserted in a FEP tube (wall thickness = 50µm) via capillarity. To mount the FEP tube in the holder of the microscope, the FEP tube was mounted into a sleeve of wire insulation (Fig. 5.1A,B), which in turn was

mounted into a glass capillary (Fig. 5.11C) that fit into the microscope holder. For the actual mounting, the tube (already positioned into the wire) was used to suck the embryo via capillarity. Specifically, the capillary along which the embryos were aligned for the injection was moved on a side using forceps and a bit of oil was allowed to enter into the FEP tube. At this point the tube was positioned close to the embryo, which was gently detached and sucked in. The tube was turned and the oil with the embryo moved toward the bottom of the tube. Shortly before reaching the lower opening, this side of the tube was sealed with superglue. The tube was turned back with the open side up and the embryo slowly mi-grated at the meniscus of the oil and it stabilized there. Agarose 1,5-2% dissolved in water was used to secure the FEP tube once inserted into the glass capillary. A 2ml tube containing a solidified agarose was prepared and the glass capillary was pushed into it until half of the capillary was filled (Fig. 5.1D). The FEP tube with the embryo was inserted in the empty half of the capillary (Fig. 5.1E). Then the agarose was slowly pushed against the FEP tube using a wire so that the glued end was embedded into the gel (Fig. 5.1F).

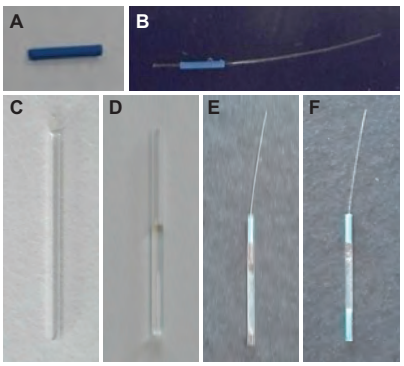

Figure 5.1: Mounting procedure. Here are shown the material and the passages necessary to mount a fly embryo after injection for SPIM imaging. Adaptor (A), FEP tube inserted into the adaptor (B), glass capillary (C), glass capillary half filled with agarose (D), tube into capillary (E) final step: wire being inserted at the bottom of the capillary to push the gel towards the tube (F).

5.1.3 Time lapse recordings and image processing using a MuVi-SPIM

The MuVi-SPIM has two illumination and two detection objective lenses that focus on the sample from four different directions along two perpendicular axes, forming four distinct illumination-detection pairs called imaging branches [Krzic et al., 2012]. The embryo was positioned into the chamber located at the center of the imaging branches and imaged with a 25x objective that allows the recording of the entire fly embryo at a cellular resolution. When a membrane marker is used, stacks of 1µm are suggested and the frames should be taken at least every two minutes in order to detect the fast morphogenetic movement typical of fly development. Each of the imaging branches produces a 3D image and the four images have to be fused into one. To do so, it is necessary to transform the four images to a common coordinate system [Krzic et al., 2012]. The parameters used for this transformation are calculated from the imaging of fluorescent beads imbedded in agarose that serve as artificial landmarks. This transformation is called registration. Once the images are transformed, they are combined in a single image as a weighted average. Our raw data of the time-lapse recordings were fused to reconstruct the embryo in 3D as described above (done by Everardo Gonzalez and Dimitri Kromm).

6

Appendix 2

6.1 Generation of a transgenic line in *M. abdita*

Current research makes use of several genetic tools, such as transgenesis, in different type of studies. In *D. melanogaster* these techniques are available and allowed to understand developmental processes from the genetic and morphological point of view. In non-model organisms there is a constrain in the use of transgenic tools, mainly for technical reasons as for example the absence of a fully sequenced assembled genome, the setting up of crosses and the subsequent screen of the progeny. At the moment there is the possibility to knock down genes by RNA interference (RNAi), injecting dsRNA of the coding sequence of the target gene, and over-express them injecting mRNA. To label genes ubiquitously expressed there is the possibility to put in frame the gene of interest with the coding sequence of a fluorescent protein or, alternatively and inject the mRNA or synthesize the protein and inject it directly into the embryos. This technique is mainly used to label cell membranes and cell nuclei since it allows to track changes of cell shape and their movements during development. While these techniques are valid and useful, they present some technical limitations when compared to the use of transgenes. Nowadays there is a strong effort in generating transgenic animal in new species. Examples are *Tribolium castaneum*, *Anopheles gambiae* and *Musca domestica*. Studies in the development of *T. castaneum* are increasing and it is used in an evolutionary context as out-group of Diptera. Mosquitoes are mainly studied for the transmission of pathologies. Increasing knowledge about their genetics and development has given the possibility to create transgenic sterile mosquitoes to decrease their fitness and reduce the viral transmission [Benedict and Robinson, 2003]; [Harris et al., 2011]. *M. domestica* transgenic flies are preferentially used for developmental and genetic studies, as for example sex determination

cascades, to apply these discoveries in genetic tools for population control of pest insects [Hediger et al., 2004]. Evo-devo studies use satellite species to compare morphological traits and the morphogenetic networks that regulate these aspects. To this end is advantageous to have the possibility to generate and use transgenic lines to better understand gene function and regulation, compare development and morphology between flies, labeling cells, either ubiquitously or/and in specific tissue at specific time as it is done in *D. melanogaster*. For this purpose, during my PhD I performed a first attempt to establish a transgenic line in *M. abdita* [Caroti et al., 2015]. In other species, transgenic lines were obtained using transposon elements such as piggyBac, Hermes, Minos and Mariner [Horn et al., 2002, O'Brochta and Atkinson, 1996]. In this work, the germline transformation was based on the piggyBac transposon system and a construct with the fly specific variant of the highly conserved Histone-2A (His2Av) [van Daal and Elgin, 1992] in frame with mCherry was generated.

6.1.1 Germline transformation of *M. abdita* using the piggyBac transposon element

The generation of a transgenic line in *M. abdita* was performed using the standard 3xP3-eGFP piggyBac vector. In *D. melanogaster* this vector shows expression of the reporter eGFP in the larval nervous system and in the eyes of adult flies (Horn et al., 2000). To generate a transgenic line, the embryos have to be injected before the formation of the pole cells. Therefore, *M. abdita* embryos were collected after 30 min of deposition at 25°C. They were aligned on a slide along a glass capillary and covered with halocarbon oil, and injected with both the vector and the *in vitro*-synthesized *piggyBac* transposase mRNA. The embryos were inject through the chorion at the posterior pole and kept in a moist chamber at 25°C. The larvae started to hatch after around 28h, after which, they were then transferred into a vial containing soaked cotton with nipagin (an anti-fungi) and wet fish food. A week later, the larvae pupated and after three weeks the adult flies eclosed. One thousand and hundred embryos were injected. 103 larvae hatched (9,4%) and 38 adults eclosed (G_0, 38/103=36.9%). In order to identify transgenic flies, the G_0 was in-crossed in pools and the adult F_1 was screened for eGFP expression, visible both in the compound eyes and in the ocelli. From these crosses we obtained two indepen-

dent lines of transgenic flies (germ line transformation rate, 2/38=5,2%). The transgenic lines in *M. abdita* were maintained inbreeding the flies and screening the progeny for the eGFP expression in each generation.

6.1.2 Synthetic locus drives ubiquitous His2Av during *M. abdita* gastrulation

His2Av is commonly used to mark cells and it is ubiquitously expressed throughout the development. To test whether piggyBac based germ line transformation could be used also in *M. abdita* we used the His2Av. To generate His2Av-mCherry fusion protein in *M. abdita*, the orthologue locus of *His2Av M. abdita*, including the putative 5' regulatory region, was identified. Since the 3' untranslated region and regulatory DNA was poorly assembled and thus less well defined, it was decided to complement the reporter construct with the 3' UTR of *M. abdita spaghetti squash* (*sqh*) that codes for the ubiquitous myosin light chain (Fig. 6.1A,B). Moreover, to facilitate the cloning of this and similar constructs, a 3-way-gateway piggyBac destination vector was generated and used to make a synthetic fusion construct that combines the 5' portion of the *M. abdita His2Av* locus (1,4kb) in frame with a mCherry reporter and the putative 3'-regulatory DNA (1,1kb) of *M. abdita sqh* (pBacDEST-His2Av-mCherry, Fig. 6.1A). This construct was injected with the piggyBac transposase mRNA as mentioned above.

Of the 2100 injected embryos 92 larvae hatched (4,3%) and of these, 36 adult flies eclosed (G_0, 36/92=39,1%). The crosses of the G_0 and the screening of their progeny were performed as described in the previous section. Transgenic flies were obtained from two independent crosses (2/36=5,5%) and maintained through continuous inbreeding (Fig. 6.2).

6.1.3 Molecular characterization of the *M. abdita* transgenic line

One of the obtained transgenic *M. abdita* lines was characterized. First, the number of insertions of pBacDest{His2Av-mCherry}was determine by southern blot hybridization using a probe against eGFP. Only a single insertion of the construct was detected (Fig. 6.3A). As next step, to determine more accurately

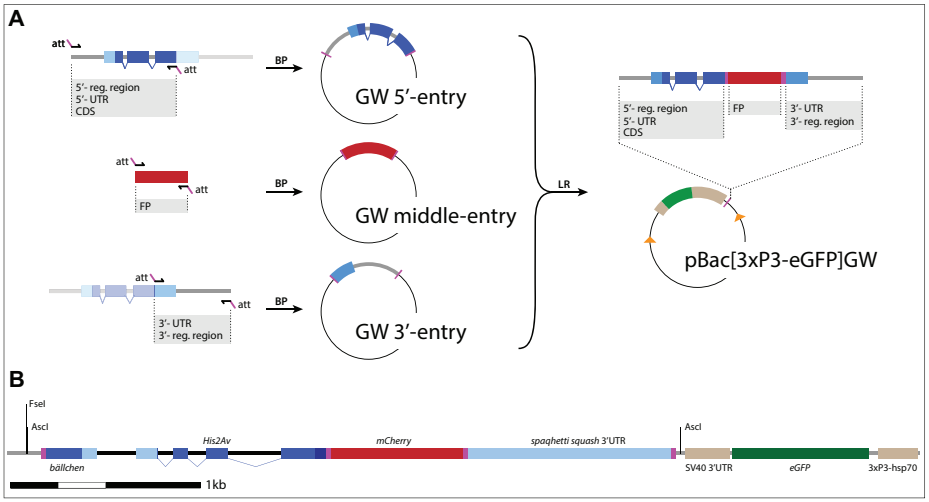

Figure 6.1: Structure of the synthetic locus and its assembly in the pBacDest{3xP3-eGFPafm}. A) Schematic overview of the three entry vectors for the three-gateway system. The fragments were amplified by PCR and inserted into the entry vectors by BP reaction. GW 5'-entry contains the 5'UTR and coding sequence of *Mab-His2Av*; GW middle-entry contains mCherry coding sequence; GW 3'-entry contains the 3'UTR of Mab-sqh. The three entry vectors are assembled into the pBacDest3xP3-eGFPafm by LR reaction. (B) Illustration of the pBacDest{His2Av-mCherry} between the piggyBac flanks containing the complete construct. Adapted from [Caroti et al., 2015].

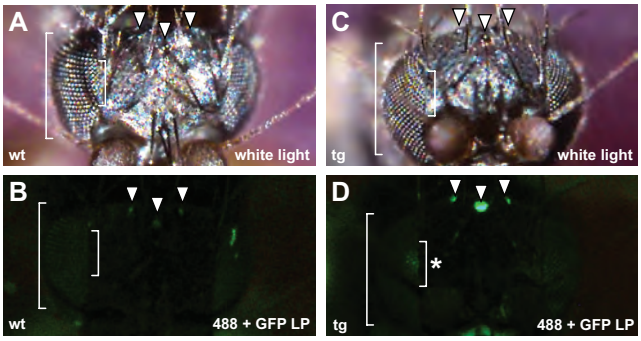

Figure 6.2: 3xP3-eGFP expression in adults *M. abdita* transgenic flies. Heads of wild-type (A,C) and transgenic (B,D) *M. abdita* are shown with white light (A,C) and under fluorescent illumination (B,D). Transgenic flies showed eGFP expression in the ommatidia (D, Brackets, asterix) and ocelli (D, arroheads). Scale bar is 0,2mm. Adapted from [Caroti et al., 2015].

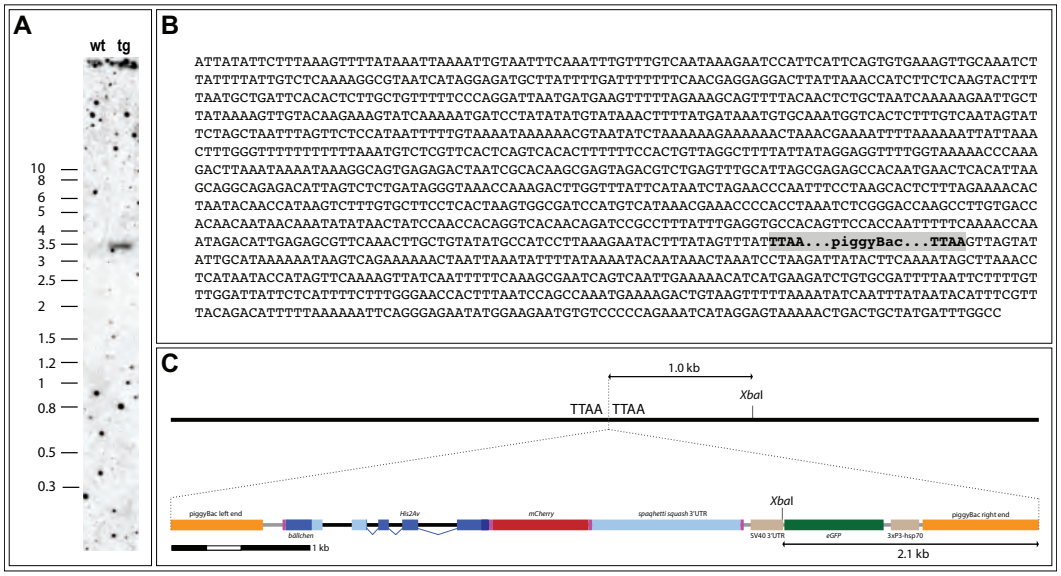

Figure 6.3: Molecular characterization of the transgenic line His2Av/sqh::His2Av-mCherry. (A) The southern blot hybridization revealed one band of 3,4Kb, indicating a unique insertion of the construct in the *M. abdita* transgenic line. A probe against eGFP was used on the genomic DNA digested by XbaI. (B) The sequence adjacent the pBacDest{His1Av-mCherry} insertion is shown in a 5' to 3' orientation with the duplicated TTAA integration site highlighted in bold in the grey box. (C) Schematic overview of the pBacDest{His2Av-mCherry} integration site into the genome of *M. abdita*. Here are marked the TTAA integration site and the two relevant XbaI restriction sites that results in a fragment of about 3,1Kb. Adapted from [Caroti et al., 2015].

the insertion of the pBacDest{His2Av-mCherry} in the genome of *M. abdita*, the sequence adjacent to it was analyzed. To do so, an inverse PCR was performed and the obtained amplicons were sequenced (Fig. 6.3B). Based on a preliminary genome assembly (Steffen Lemke, Thomas Sandmann, and Urs Schmidt-Ott, unpublished), all the obtained sequences (16/16) were mapped to a unique insertion site. This flanking region had a duplicated TTAA integration site, suggesting that the piggyBac insertion into the genome was bona fide (Fig. 6.3C).

6.1.4 *In vivo* analyses of the transgenic line His2Av/sqh::His2Av-mCherry

It has been previously shown in *D. melanogaster* and *T. castaneum* how the dynamics of early embryonic development and gastrulation can be imaged and quantitatively analyzed using ubiquitous fluorescent cell labeling in combina-

tion with *in toto* high-speed imaging [Krzic et al., 2012, Strobl and Stelzer, 2014]. For an initial assessment of the *His2Av-mCherry* expression in *M. abdita*, embryos in the late blastoderm stage and during the onset of gastrulation were imaged using a multi-view light-sheet microscope (MuVi-SPIM) [Krzic et al., 2012]. In late blastoderm stage, all nuclei in the periphery appeared elongated with the pole cells presenting a more spherical shape (Figure 6.4A,A'). Using automated image segmentation, we extracted the nuclear positions at the late blastoderm stage from the His2Av-mCherry reporter line that yielded a mean nuclear density of 29 nuclei per 100µm^2, which is very similar to the 32 nuclei per 100µm^2 that have been reported in fixed embryos stained with DAPI [Wotton et al., 2014]. In total, *M. abdita* embryo at blastoderm stage contained 4534 nuclei in the periphery, of which 23 nuclei were identified as pole cell nuclei based on their position and spherical appearance (Fig. 6.4E). The mesoderm started to internalize at the ventral midline of the embryo (Figure 6.4B,B'), then the onset of germband extension began, the ventral furrow formed and the first cells of the future cephalic furrow were sinking in (Figure 6.4C,C'). Along the dorsal midline, between cephalic furrow and the amnioproctodeal invagination, three dorsal folds could be detected (Figure 6.4D,D'). All these observations are in line with a recent description of embryonic development in M. abdita [Wotton et al., 2014]. At later stages of development, the His2Av-mCherry fusion protein was still expressed but it was not possible to segment the nuclei due to a decreased in the signal to noise ratio. The two transgenic lines His2Av/sqh::His2Av-mCherry were maintained by screening for the eGFP signal as described in previous sections. However, in time, the expression of *His2Av-mCherry* was shown to decrease in early stages of embryonic development while increasing during late stages. This decrease in the early stages was observed after 20 generations in both independent lines. An attempt to restore the expression of *His2Av-mCherry* at early embryonic stages repeated outcrosses against wild-type flies were performed. However, despite this, the expression of *His2Av-mCherry* was not restored.

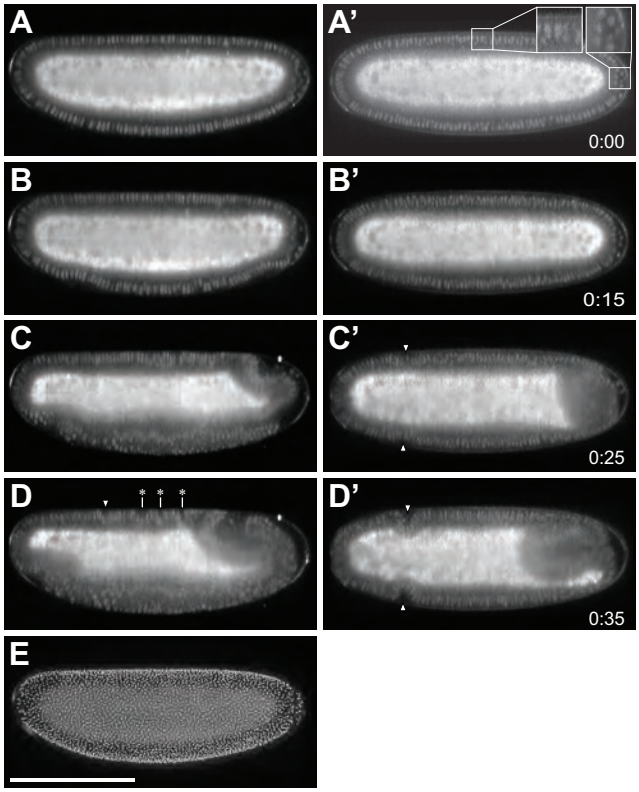

Figure 6.4: *In vivo* description of the *M. abdita* transgenic line describing His2Av-mCherry. (A-D) The embryos are shown in a mid-sagittal section. (A'-D') The embryos are shown in a transverse section. (A,A') At blastoderm stage the nuclei in the periphery of the embryo were elongated while the pole cells showed a spherical shape. (B,B') At the onset of gastrulation indentations on the ventral side of the embryo were visible, indicating the beginning of the ventral furrow formation. (C,C') The germband started to elongate and the pole cells reach the dorsal side of the embryo. At the same time the cephalic furrow was forming. (D,D') The germband extension progressed and three dorsal folds appeared. (E) Nuclear position extracted by automated image segmentation at late blastoderm stage. Each grey sphere indicates one nucleus. Cephalic furrow: white triangles; Dorsal folds: asterix. Embryos are oriented with the anterior side to the left. Scale bar is 200µm. Adapted from [Caroti et al., 2015].

6.2 Discussion

In this work, we established a method to generate transgenic *M. abdita* lines, based on the piggyBac transposase. As evinced from the live imaging, this ubiquitous nuclear labeling is a valid approach for a detailed wild-type description of the *M. abdita* embryonic development and it is a first step to bring this specie available for a wider spectrum of analysis. The loss of the *His2Av-mCherry* early expression represents an issue that has to be considered whenever the

piggyBac approach for germline transformation is used in the future. The random insertion of the construct in the genome can lead to multiple insertions and at their partial lost. This phenomenon has been previously reported for other species such as *Bombyx mori* [Toshiki et al., 2000] and *Ceratitis capitata* [Handler et al., 1998], where weakening of the fluorescent signal was also observed. The results obtained in this study show a similar scenario. Since the lost of the signal at early embryonic stages of *M. abdita* was not due to the homozygosing of the flies, as shown from the outcrosses, it is more reasonable to speculate that initially the flies carried multiple insertions and that secondarily they had been silenced or lost. For future generation of transgenic lines in *M. abdita*, the flies should be screened not only for eGFP but also for the expression of the reporter gene. Moreover, from the F_1 onward repeatedly outcrosses against wild type are necessary. This will allow the separation of potential multiple piggyBac insertions and only later, when they are separated, the inbreeding can start. To avoid multiple insertions CRISPR/Cas9 could be used. This technique allows performing transgenesis in a precise manner and gives the possibility to target an endogenous locus that is not completely sequenced or assembled as it is the case of *His2Av* in *M. abdita*. A possible method to increase the expression level of *His2Av-mCherry* transgene could be the generation and insertion of a piggyBac containing a tandem duplication of the *His2Av-mCherry* fusion locus.

6.3 Material and methods

6.3.1 Fly cultures

M. abdita transgenic flies were kept at 16/8-h day/night cycle and at 25°C with 65% humidity as the wild-type culture. The transgenic lines were grown in a 50ml plugged Drosophila vials (Nerbe, 29x95 mm) with fish food and, to avoid mold formation, 4-hydroxybenzoic acid methyl ester (Diluted stock solution used in vials: 3% v/v in water) was used to wet cotton. Constant inbreeding and screening for eGFP expression in the eyes and ocelli of the adults was performed each generation to maintain the transgenic lines.

- 4-hydroxybenzoic acid methyl ester/Nipagin stock solution: 10% w/v in 70% v/v EtOH

6.3.2 Plasmid construction

A ccdB cassette flanked by attR4 and attR3 was inserted in the plasmid pBac{3xP3-eGFPafm} (Horn and Wimmer, 2000), to allow the assembly of three-fragment cassettes with the Gateway system (made by Maike Wosch). Using primer pair cAscI-TOL2/SL105 the ccdB cassette was amplified by PCR from pDestTol2pA2 (Kwan et al., 2007). This amplified sequence was then digested with AscI and cloned into the AscI site of the pBac3xP3-eGFPafm. This modified vector was called pBacDest{3xP3-eGFPafm}. The three modules were 5'-pENTR-His2Av, middle-pENTR-mCherry and 3'-pENTR-sqh. These vectors were prepared as following. As first the *His2Av* and *sqh* were amplified by PCR from the *M. abdita* genomic DNA with the pairs of primers SL214/SL215 and SL210/SL188 respectively, using the iProof DNA Polymerase (BioRad). An A-taile was added to these fragment with Taq DNA polymerase F-100L (Finnzymes) and cloned into the pCRII-TOPO (Invitrogen) vector. The cloned *His2Av* locus started at the position –585 to position +834 (+1 being the beginning of the ORF). *M. abdita sqh* 3'-UTR contained 1077bp immediately downstream of its CDS and was cloned with the same procedure of *His2Av* fragment. As second step these inserts were modified to recombine with the pENTR vectors via BP reaction. At the 3' end of the cloned *His2Av* of *M. abdita*, was added a fragment encoding the 20 C-terminal amino acids of the *D. melanogaster His2Av* CDS (+531 to +590, +1 being the beginning of the CDS in NM_079795) and in-frame the attB1r sites for BP recombination with the reverse primer SL228 by PCR, using the previous clone as template and the iProof DNA Polymerase. At the 5'-*His2Av* of *M. abdita* the attB4 was added in-frame with the forward primer SL227. By BP recombination, the *His2Av* fragment was inserted into the 5'-pENTR vector, forming the 5'-pENTR-His2Av. The middle-pENTR vector contained mCherry CDS, was amplified by PCR from the plasmid pCaSpeR4-His2Av-mCherry (gift from Lars Hufnagel) using the primer pair SL101/SL102 containing in-frame attB1 and attB2 sites. The mCherry sequence was recombined in the middle-pENTR vector by BP reaction, giving rise to the middle-pENTR-mCherry. The cloned *M. abdita sqh* 3' UTR was used as template for the PCR to add attB2r and attB3 sites with primer pairs SL225/SL226 and by BP reaction was recombined into the 3'-pENTR vector, forming the 3'-pENTR-sqh. The three-entry

vectors 5'-pENTR-His2Av, middle-pENTR-mCherry and 3'-pENTR-sqh were recombined into the pBacDest{3xP3-eGFPafm} by LR reaction, giving rise to the final construct called pBacDest{His2Av-mCherry}. The BP and LR reactions were performed accordingly to the three-Gateway system user manual (Invitrogen). The piggyBac transposase was injected into the embryos as mRNA therefore it was cloned into an expression vector (made by Maike Wosch). The *piggyBac* transposase CDS was amplified from phsp-pBac (Handler and Harrel, 1999) with the primer pair pBac_fw/pBac_rev, digested with NcoI/SalI and cloned into pSP35 (Amaya et al., 1991). This final vector was called pSPiggyHelp.

6.3.3 Synthesis of capped mRNA

The sequence of the piggyBac transposase was the expression vector pSP that, to be used as template, was prepared as midi (QIAGEN kit) and 20µg of it were linearized by EcoRI in a 50µl reaction at 37°C for 4h. After heat inactivation of the enzyme, the template was cleaned adding 5µl SDS 10%, 2µl proteinaseK (10mg/ml, Invitrogen) and incubating for 30min at 50°C. Following phenol/chloroform extraction was performed, 1/10 volume NaOAc (3M, pH6) and 3 volumes EtOH were added and stored at -20°C longer than 2h or over night, in order to precipitate the sample. The pellet was dissolved in 10µl nuclease-free water. The capped mRNA was then synthetized using Ambion' s mMessage mMachine SP6 kit. Transcription was performed following the user manual of the kit.

Reaction mix	
10x reaction buffer	4µl
2x NTP/CAP	20µl
Linearized DNA template	2µg
Enzyme mix	4µl
RNase free H_2O up to 40µl	

The reaction was incubated 4h at 37°C and the DNA was degraded adding

2µl Turbo DNase for 20min. Following, one volume NH4OAc was added and phenol/chloroform extraction performed. The mRNA was precipitated with one volume of isopropanol and incubated at -20°C over night. The pellet was dissolved in 10µl RNase free water. The mRNA quality was assessed on 1% agarose gel and the concentration by UV photospectroscopy. The capped mRNA was stored at -80°C in aliquots of 0,5µl each.

6.3.4 Germ line transformation

The embryos of *M. abdita* were collected, aligned, let dry and covered with halocarbon oil as already explained in the Material and methods section of the thesis and as previously outlined (Rafiqi et al., 2011a; Rafiqi et al., 2011b). The embryos were injected in the posterior pole with a pre-mixed pBacDest{His2Av-mCherry} plasmid and *in vitro*-synthetized *piggyBac* transposase mRNA at a DNA/mRNA concentration of 100:300ng/µl. The needles were made out of pulled borosilicate glass capillaries (World Precision Instrument, 1.0 mm outer and 0,58mm inner diameter), using a Flaming/Brown micropipette puller (Sutter Instruments P-97). By beveling, these needles were opened and backfilled using Eppendorf Microloader tips (0.5-20µl). The injections were performed using an Eppendorf FemtoJet express microinjector. The adult flies were screened with a fluorescent binocular (Olympus MVX 10, light source: X-cite Series 120Q).

6.3.5 Southern blot hybridization

Standard procedures were followed to perform DNA digestion, transfer and probe hybridization (Sambrook and Russell, 2001). The genomic DNA was extracted by SDS lysis and DNasefree RNase treatment (Andreas and Thummel, 1994) from a pool of transgenic or wild-type flies. The genomic DNA was then digested with XbaI over night and separated on a 1% TAE agarose gel. This gel was incubated in denaturation buffer for 20 min and then used to transfer over night the DNA from the gel to a positively charged nylon transfer membrane (GE Healthcare). Once the DNA was transferred, the neutralization buffer was used to wash the membrane, rinsed with 2x SSPE buffer and in the end the DNA was UV cross-linked to the membrane. Using PCR dig Probe Syn-

thesis Kit (Roche), a digoxigenin labeled probe against eGFP was synthesized according to the user manual. The probe was hybridized to the DNA then the incubation with alkaline phosphatase linked Fab fragments against digoxigenin (Roche, 1:20000) followed. For chemiluminescence-based immunodetection of alkaline phosphatase on a ChemoChem Imager (Intas), CDP star (Bright Star Bio Detect, Ambion) was used.

Denaturation buffer	
NaOH	0,5N
NaCl	1,5M
Neutralization buffer	
Tris Base	0,5M
NaCl	1,5M
pH	7,2-7,4
2x SSPE buffer	
NaCl	300mM
Na_2HPO_4-$1H_2O$	20mM
Na_2EDTA	2mM
pH	7,4

6.3.6 Inverse PCR

A pool of adult transgenic flies was used to isolate genomic DNA as described in the previous section. The extracted DNA was digested by HaeIII according to the published protocol (Bellen et al., 2004) and self-circularized using the T4 DNA ligase. By PCR, the circularized fragment containing genomic DNA next to the left arm of the piggyBac were amplified using primer pair SL512/SL513 (Bellen et al., 2004) and then with a nested PCR with the primer pair SL535/SL532. For the fragment containing genomic DNA adjacent to the right arm of the piggyBac, the primer pair SL514/SL515 (Bellen et al., 2004) and SL533/SL534 for the nested PCR, were used. To determine the genomic locus at the 5' and 3' of the integrated piggyBac construct, the amplicons ob-

tained from the nested PCRs were subsequently cloned into pCRII-TOPO and eight clones per side were sequenced.

6.3.7 Outcrossing

Outcrosses of transgenic against wild-type flies were performed for three generations. These crosses were set up in pools of around ten wild-type males with ten transgenic virgin females or ten wild-type virgin females with ten transgenic males. The embryos of the third generation were screened *in vivo* for the expression of *His2Av-mCherry* at several embryonic stages.

6.3.8 Microscopy and image analysis

The development of transgenic *M. abdita* was analyzes with a MuVi-SPIM. The embryos were collected after 40 min of deposition, dechorionated and rinsed with water, and mounted for imaging as described in Krzic et al., 2012. Dr. Paula Gonzalez calculated the nuclei number after have segmented with iLastik (1.0) the image stacks. Matlab (R2013a) was used to determine the position of each nucleus. The nuclear density was calculated by manually counting the nuclei in a defined area.

6.3.9 Primers

Name	Sequence (5' to 3' orientation)
cAscl-TOL2_fw	5'-AGTTGGCGCGCCGTGTCTGAAACACAGGCCAGAT
SL105	5'-ATGGCGCGCCGTAAAACGACGGCCAGTGAATT
SL227	5'-GGGGACAACTTTGTATAGAAAAGTTGCTGCAGGATTGTTTGCCTTGGTAG
SL228	5'-GGGGACTGCTTTTTTGTACAAACTTGCGTAGGCCTGCGACAGAATGACGTT GCCCTTCCGCTGCGGATCCTGCACCGTTTCCTCCTTCTTTCCGATCAAAGA TTTGTGGATATG
SL214	5'-GCAGGATTGTTTGCCTTGGTAG
SL215	5'-TCAAGGCCGAAAAGCACAAAAAC

Name	Sequence (5' to 3' orientation)
SL101	5'-GGGGACAAGTTTGTACAAAAAAGCAGGCTTAATGGTGAGCAAGGGCGAGG
SL102	5'-GGGGACCACTTTGTACAAGAAAGCTGGGTATTAGGCGCCGGTGGAGTGGC
SL225	5'-GGGGACAGCTTTCTTGTACAAAGTGGCTATGGAAAGAAACTGTCGA
SL226	5'-GGGGACAACTTTGTATAATAAAGTTGCAACCTCTTTCGTCTCTTC
SL210	5'-GATGTACAGAGAAGCCCCGATTAAG
SL188	5'-CTAACAACCTCTTTCGTCTCTTCCAATCGC
SL512 [1]	5'-CTTGACCTTGCCACAGAGGACTATTAGAGG
SL513 [1]	5'-CAGTGACACTTACCGCATTGACAAGCACGC
SL535	5'-TTGTTGGTCAACTTCAAAGTCCAC
SL532	5'-CATGCGTCAATTTTACGCAGACTA
SL514 [1]	5'-CCTCGATATACAGACCGATAAAACACATGC
SL515 [1]	5'-AGTCAGTCAGAAACAACTTTGGCACATATC
SL533	5'-CATGATTATCTTTAACGTACGTCACAA
SL534	5'-TCAAAGTAGGAGCTTCTAAACGCT
pBac_fw	5'-CCAAACCATGGGATGTTCTTTAGACGATG
pBac_rev	5'-ATGAGTCGACTCAGAAACAACTTTGGCA

[1] (PLF; [Bellen, 2004])

References

[Anderson, 1966] Anderson, D. T. (1966). The comparative embryology of the Diptera. *Annual Review of Entomology*.

[Anderson, 1972] Anderson, D. T. (1972). *The development of holometabolous insects. In* Developmental systems: insects,. London, New York: Academic Press.

[Araki and Milbrandt, 1996] Araki, T. and Milbrandt, J. (1996). Ninjurin, a novel adhesion molecule, is induced by nerve injury and promotes axonal growth. *Neuron*, 17(2):353–361.

[Araki and Milbrandt, 2000] Araki, T. and Milbrandt, J. (2000). Ninjurin2, a novel homophilic adhesion molecule, is expressed in mature sensory and enteric neurons and promotes neurite outgrowth. *The Journal of neuroscience : the official journal of the Society for Neuroscience*, 20(1):187–195.

[Bellen, 2004] Bellen, H. J. (2004). The BDGP Gene Disruption Project: Single Transposon Insertions Associated With 40 *Genetics*, 167(2):761–781.

[Benedict and Robinson, 2003] Benedict, M. Q. and Robinson, A. S. (2003). The first releases of transgenic mosquitoes: an argument for the sterile insect technique. *Trends in parasitology*, 19(8):349–355.

[Benton et al., 2013] Benton, M. A., Akam, M., and Pavlopoulos, A. (2013). Cell and tissue dynamics during Tribolium embryogenesis revealed by versatile fluorescence labeling approaches. *Development (Cambridge, England)*, 140(15):3210–3220.

[Benton et al., 2016] Benton, M. A., Pechmann, M., Frey, N., Stappert, D., Conrads, K. H., Chen, Y.-T., Stamataki, E., Pavlopoulos, A., and Roth, S. (2016). Toll Genes Have an Ancestral Role in Axis Elongation. *Current biology : CB*, 26(12):1609–1615.

[Bloor and Kiehart, 2002] Bloor, J. W. and Kiehart, D. P. (2002). Drosophila RhoA regulates the cytoskeleton and cell-cell adhesion in the developing epidermis. *Development (Cambridge, England)*, 129(13):3173–3183.

[Brew et al., 2000] Brew, K., Dinakarpandian, D., and Nagase, H. (2000). Tissue inhibitors of metalloproteinases: evolution, structure and function. *Biochimica et biophysica acta*, 1477(1-2):267–283.

[Brown et al., 1994] Brown, S. J., Patel, N. H., and Denell, R. E. (1994). Embryonic expression of the single Tribolium engrailed homolog. *Developmental genetics*, 15(1):7–18.

[Campos-Ortega and Hartenstein, 1997] Campos-Ortega, J. and Hartenstein, V. (1997). *The embryonic development of* Drosophila melanogaster. Berlin, Heidelberg, New York: Springer Verlag.

[Caroti et al., 2015] Caroti, F., Urbansky, S., Wosch, M., and Lemke, S. (2015). Germ line transformation and in vivo labeling of nuclei in Diptera: report on Megaselia abdita (Phoridae) and Chironomus riparius (Chironomidae). *Development genes and evolution*, 225(3):179–186.

[Danai, 2012] Danai, F. (2012). Comparing gastrulation within the genus Drosophila.Master thesisHanded in by: Danai FeidaHeidelberg, December 2012. pages 1–65.

[Doyle et al., 1986] Doyle, H. J., Harding, K., Hoey, T., and Levine, M. (1986). Transcripts encoded by a homoeo box gene are restricted to dorsal tissues of Drosophila embryos. *Nature*, 323(6083):76–79.

[Edwards et al., 1997] Edwards, K. A., Demsky, M., Montague, R. A., Weymouth, N., and Kiehart, D. P. (1997). GFP-moesin illuminates actin cytoskeleton dynamics in living tissue and demonstrates cell shape changes during morphogenesis in Drosophila. *Developmental biology*, 191(1):103–117.

[Foe and Alberts, 1983] Foe, V. E. and Alberts, B. M. (1983). Studies of nuclear and cytoplasmic behaviour during the five mitotic cycles that precede gastrulation in Drosophila embryogenesis. *Journal of cell science*.

[Gavin-Smyth and Ferguson, 2014] Gavin-Smyth, J. and Ferguson, E. L. (2014). zenand the art of phenotypic maintenance: Canalization of embryonic dorsal-ventral patterning in Drosophila. *Fly*, 8(3):170–175.

[Gavin-Smyth et al., 2013] Gavin-Smyth, J., Wang, Y.-C., Butler, I., and Ferguson, E. L. (2013). A Genetic Network Conferring Canalization to a Bistable Patterning System in Drosophila. *Current biology : CB*, 23(22):2296–2302.

[Goltsev et al., 2007] Goltsev, Y., Fuse, N., Frasch, M., Zinzen, R. P., Lanzaro, G., and Levine, M. (2007). Evolution of the dorsal-ventral patterning network in the mosquito, Anopheles gambiae. *Development (Cambridge, England)*, 134(13):2415–2424.

[HallgrÍmsson et al., 2012] HallgrÍmsson, B., Jamniczky, H. A., Young, N. M., Rolian, C., Schmidt-Ott, U., and Marcucio, R. S. (2012). The Generation of Variation and the Developmental Basis for Evolutionary Novelty. *Journal of Experimental Zoology Part B: Molecular and Developmental Evolution*, 318(6):501–517.

[Hamaguchi et al., 2012] Hamaguchi, T., Takashima, S., Okamoto, A., Imaoka, M., Okumura, T., and Murakami, R. (2012). Dorsoventral patterning of the Drosophila hindgut is determined by interaction of genes under the control of two independent gene regulatory systems, the dorsal and terminal systems. *Mechanisms of development*, 129(9-12):236–243.

[Handler et al., 1998] Handler, A. M., McCombs, S. D., Fraser, M. J., and Saul, S. H. (1998). The lepidopteran transposon vector, piggyBac, mediates germ-line transformation in the Mediterranean fruit fly. *Proceedings of the National Academy of Sciences of the United States of America*, 95(13):7520–7525.

[Hara et al., 2016] Hara, Y., Shagirov, M., and Toyama, Y. (2016). Cell Boundary Elongation by Non-autonomous Contractility in Cell Oscillation. *Current biology : CB*, 26(17):2388–2396.

[Harris et al., 2011] Harris, A. F., Nimmo, D., McKemey, A. R., Kelly, N., Scaife, S., Donnelly, C. A., Beech, C., Petrie, W. D., and Alphey, L. (2011). Field performance of engineered male mosquitoes. *Nature biotechnology*, 29(11):1034–1037.

[Hediger et al., 2004] Hediger, M., Burghardt, G., Siegenthaler, C., Buser, N., Hilfiker-Kleiner, D., Dübendorfer, A., and Bopp, D. (2004). Sex determination in Drosophila melanogaster and Musca domestica converges at the level of the terminal regulator doublesex. *Development genes and evolution*, 214(1):29–42.

[Hilbrant et al., 2016] Hilbrant, M., Horn, T., Koelzer, S., and Panfilio, K. A. (2016). The beetle amnion and serosa functionally interact as apposed epithelia. *eLife*, 5.

[Homem and Peifer, 2008] Homem, C. C. F. and Peifer, M. (2008). Diaphanous regulates myosin and adherens junctions to control cell contractility and protrusive behavior during morphogenesis. *Development (Cambridge, England)*, 135(6):1005–1018.

[Horn et al., 2002] Horn, C., Schmid, B. G. M., Pogoda, F. S., and Wimmer, E. A. (2002). Fluorescent transformation markers for insect transgenesis. *Insect biochemistry and molecular biology*, 32(10):1221–1235.

[Horn et al., 2015] Horn, T., Hilbrant, M., and Panfilio, K. A. (2015). Evolution of epithelial morphogenesis: phenotypic integration across multiple levels of biological organization. *Frontiers in Genetics*, 6:107.

[Horn and Panfilio, 2016] Horn, T. and Panfilio, K. A. (2016). Novel functions for Dorsocross in epithelial morphogenesis in the beetle Tribolium castaneum. *Development (Cambridge, England)*, 143(16):3002–3011.

[Hutson et al., 2003] Hutson, M. S., Tokutake, Y., Chang, M.-S., Bloor, J. W., Venakides, S., Kiehart, D. P., and Edwards, G. S. (2003). Forces for morphogenesis investigated with laser microsurgery and quantitative modeling. *Science (New York, N.Y.)*, 300(5616):145–149.

[Jacinto et al., 2002] Jacinto, A., Wood, W., Woolner, S., Hiley, C., Turner, L., Wilson, C., Martinez-Arias, A., and Martin, P. (2002). Dynamic analysis of actin cable function during Drosophila dorsal closure. *Current biology : CB*, 12(14):1245–1250.

[Jankovics and Brunner, 2006] Jankovics, F. and Brunner, D. (2006). Transiently Reorganized Microtubules Are Essential for Zippering during Dorsal Closure in Drosophila melanogaster. *Developmental cell*, 11(3):375–385.

[Kaufmann et al., 2012] Kaufmann, A., Mickoleit, M., Weber, M., and Huisken, J. (2012). Multilayer mounting enables long-term imaging of zebrafish development in a light sheet microscope. *Development (Cambridge, England)*, 139(17):3242–3247.

[Keller, 2013] Keller, P. J. (2013). Imaging morphogenesis: technological advances and biological insights. *Science (New York, N.Y.)*, 340(6137):1234168.

[Keller et al., 2010] Keller, P. J., Schmidt, A. D., Santella, A., Khairy, K., Bao, Z., Wittbrodt, J., and Stelzer, E. H. K. (2010). Fast, high-contrast imaging of animal development with scanned light sheet–based structured-illumination microscopy. *Nature methods*, 7(8):637–642.

[Keller and Stelzer, 2008] Keller, P. J. and Stelzer, E. (2008). Quantitative in vivo imaging of entire embryos with Digital Scanned Laser Light Sheet Fluorescence Microscopy. *Current opinion in neurobiology*.

[Kiehart et al., 2000] Kiehart, D. P., Galbraith, C. G., Edwards, K. A., Rickoll, W. L., and Montague, R. A. (2000). Multiple forces contribute to cell sheet morphogenesis for dorsal closure in Drosophila. *The Journal of cell biology*, 149(2):471–490.

[Kiger et al., 2007] Kiger, J. A., Natzle, J. E., Kimbrell, D. A., Paddy, M. R., Kleinhesselink, K., and Green, M. M. (2007). Tissue remodeling during maturation of the Drosophila wing. *Developmental biology*, 301(1):178–191.

[Krzic et al., 2012] Krzic, U., Gunther, S., Saunders, T. E., Streichan, S. J., and Hufnagel, L. (2012). Multiview light-sheet microscope for rapid in toto imaging. *Nature methods*, 9(7):730–733.

[Kuo et al., 2005] Kuo, C. T., Jan, L. Y., and Jan, Y. N. (2005). Dendrite-specific remodeling of Drosophila sensory neurons requires matrix metalloproteases, ubiquitin-proteasome, and ecdysone signaling. *Proceedings of the National Academy of Sciences of the United States of America*, 102(42):15230–15235.

[Lemke and Schmidt-Ott, 2009] Lemke, S. and Schmidt-Ott, U. (2009). Evidence for a composite anterior determinant in the hover fly Episyrphus balteatus (Syrphidae), a cyclorrhaphan fly with an anterodorsal serosa anlage. *Development (Cambridge, England)*, 136(1):117–127.

[Lemon and Keller, 2015] Lemon, W. C. and Keller, P. J. (2015). Live imaging of nervous system development and function using light-sheet microscopy. *Molecular Reproduction and Development*, 82(7-8):605–618.

[Leontovich et al., 2000] Leontovich, A. A., Zhang, J., Shimokawa, K., Nagase, H., and Sarras, M. P. (2000). A novel hydra matrix metalloproteinase (HMMP) functions in extracellular matrix degradation, morphogenesis and the maintenance of differentiated cells in the foot process. *Development (Cambridge, England)*, 127(4):907–920.

[Leptin and Grunewald, 1990] Leptin, M. and Grunewald, B. (1990). Cell shape changes during gastrulation in Drosophila. *Development (Cambridge, England)*, 110(1):73–84.

[Llano et al., 2002] Llano, E., Adam, G., Pendás, A. M., Quesada, V., Sánchez, L. M., Santamariá, I., Noselli, S., and López-Otín, C. (2002). Structural and enzymatic characterization of Drosophila Dm2-MMP, a membrane-bound matrix metalloproteinase with tissue-specific expression. *The Journal of biological chemistry*, 277(26):23321–23329.

[Llano et al., 2000] Llano, E., Pendás, A. M., Aza-Blanc, P., Kornberg, T. B., and López-Otín, C. (2000). Dm1-MMP, a matrix metalloproteinase from Drosophila with a potential role in extracellular matrix remodeling during neural development. *The Journal of biological chemistry*, 275(46):35978–35985.

[Lohi et al., 2001] Lohi, J., Wilson, C. L., Roby, J. D., and Parks, W. C. (2001). Epilysin, a novel human matrix metalloproteinase (MMP-28) expressed in testis and keratinocytes and in response to injury. *The Journal of biological chemistry*, 276(13):10134–10144.

[Maidment et al., 1999] Maidment, J. M., Moore, D., Murphy, G. P., Murphy, G., and Clark, I. M. (1999). Matrix metalloproteinase homologues from Arabidopsis thaliana. Expression and activity. *The Journal of biological chemistry*, 274(49):34706–34710.

[Marchenko et al., 2001] Marchenko, G. N., Ratnikov, B. I., Rozanov, D. V., Godzik, A., Deryugina, E. I., and Strongin, A. Y. (2001). Characterization of matrix metalloproteinase-26, a novel metalloproteinase widely expressed in cancer cells of epithelial origin. *The Biochemical journal*, 356(Pt 3):705–718.

[Marqués et al., 1997] Marqués, G., Musacchio, M., Shimell, M. J., Wünnenberg-Stapleton, K., Cho, K. W., and O'Connor, M. B. (1997). Production of a DPP activity gradient in the early Drosophila embryo through the opposing actions of the SOG and TLD proteins. *Cell*, 91(3):417–426.

[Martin and Wood, 2002] Martin, P. and Wood, W. (2002). Epithelial fusions in the embryo. *Current Opinion in Cell Biology*, 14(5):569–574.

[McMahon et al., 2010] McMahon, A., Reeves, G. T., Supatto, W., and Stathopoulos, A. (2010). Mesoderm migration in Drosophila is a multi-step process requiring FGF signaling and integrin activity. *Development (Cambridge, England)*, 137(13):2167–2175.

[Moreno et al., 2002] Moreno, E., Yan, M., and Basler, K. (2002). Evolution of TNF signaling mechanisms: JNK-dependent apoptosis triggered by Eiger, the Drosophila homolog of the TNF superfamily. *Current biology : CB*, 12(14):1263–1268.

[Morisalo and Anderson, 1995] Morisalo, D. and Anderson, K. V. (1995). Signaling pathways that establish the dorsal-ventral pattern of the Drosophila embryo. *Annual review of genetics*.

[Narasimha and Brown, 2004] Narasimha, M. and Brown, N. H. (2004). Novel functions for integrins in epithelial morphogenesis. *Current biology : CB*, 14(5):381–385.

[Nowotarski et al., 2014] Nowotarski, S. H., McKeon, N., Moser, R. J., and Peifer, M. (2014). The actin regulators Enabled and Diaphanous direct distinct protrusive behaviors in different tissues during Drosophila development. *Molecular Biology of the Cell*, 25(20):3147–3165.

[O'Brochta and Atkinson, 1996] O'Brochta, D. A. and Atkinson, P. W. (1996). Transposable elements and gene transformation in non-drosophilid insects. *Insect biochemistry and molecular biology*, 26(8-9):739–753.

[Padgett et al., 1987] Padgett, R. W., St Johnston, R. D., and Gelbart, W. M. (1987). A transcript from a Drosophila pattern gene predicts a protein homologous to the transforming growth factor-beta family. *Nature*, 325(6099):81–84.

[Page-McCaw et al., 2007] Page-McCaw, A., Ewald, A. J., and Werb, Z. (2007). Matrix metalloproteinases and the regulation of tissue remodelling. *Nature Reviews Molecular Cell Biology*, 8(3):221–233.

[Page-McCaw et al., 2003] Page-McCaw, A., Serano, J., Santé, J. M., and Rubin, G. M. (2003). Drosophila matrix metalloproteinases are required for tissue remodeling, but not embryonic development. *Developmental cell*.

[Pallavi et al., 2012] Pallavi, S. K., Ho, D. M., Hicks, C., Miele, L., and Artavanis-Tsakonas, S. (2012). Notch and Mef2 synergize to promote proliferation and metastasis through JNK signal activation in Drosophila. *The EMBO journal*, 31(13):2895–2907.

[Panfilio, 2008] Panfilio, K. A. (2008). Extraembryonic development in insects and the acrobatics of blastokinesis. *Developmental biology*, 313(2):471–491.

[Panfilio, 2009] Panfilio, K. A. (2009). Late extraembryonic morphogenesis and its zen(RNAi)-induced failure in the milkweed bug Oncopeltus fasciatus. *Developmental biology*, 333(2):297–311.

[Panfilio et al., 2006] Panfilio, K. A., Liu, P. Z., Akam, M., and Kaufman, T. C. (2006). Oncopeltus fasciatus zen is essential for serosal tissue function in katatrepsis. *Developmental biology*, 292(1):226–243.

[Panfilio et al., 2013] Panfilio, K. A., Oberhofer, G., and Roth, S. (2013). High plasticity in epithelial morphogenesis during insect dorsal closure. *Biology open*, 2(11):1108–1118.

[Panfilio and Roth, 2010] Panfilio, K. A. and Roth, S. (2010). Epithelial reorganization events during late extraembryonic development in a hemimetabolous insect. *Developmental biology*, 340(1):100–115.

[Rafiqi et al., 2008] Rafiqi, A. M., Lemke, S., Ferguson, S., Stauber, M., and Schmidt-Ott, U. (2008). Evolutionary origin of the amnioserosa in cyclorrhaphan flies correlates with spatial and temporal expression changes of zen. *Proceedings of the National Academy of Sciences of the United States of America*, 105(1):234–239.

[Rafiqi et al., 2010] Rafiqi, A. M., Lemke, S., and Schmidt-Ott, U. (2010). Postgastrular zen expression is required to develop distinct amniotic and serosal epithelia in the scuttle fly Megaselia. *Developmental biology*, 341(1):282–290.

[Rafiqi et al., 2011] Rafiqi, A. M., Lemke, S., and Schmidt-Ott, U. (2011). The Scuttle Fly Megaselia abdita (Phoridae): A Link between Drosophila and Mosquito Development. *Cold Spring Harbor Protocols*, 2011(4):pdb.emo143–pdb.emo143.

[Rafiqi et al., 2012] Rafiqi, A. M., Park, C.-H., Kwan, C. W., Lemke, S., and Schmidt-Ott, U. (2012). BMP-dependent serosa and amnion specification in the scuttle fly Megaselia abdita. *Development (Cambridge, England)*, 139(18):3373–3382.

[Rauzi et al., 2015] Rauzi, M., Krzic, U., Saunders, T. E., Krajnc, M., Ziherl, P., Hufnagel, L., and Leptin, M. (2015). Embryo-scale tissue mechanics during Drosophila gastrulation movements. *Nature Communications*, 6:8677.

[Reed et al., 2004] Reed, B. H., Wilk, R., Schöck, F., and Lipshitz, H. D. (2004). Integrin-dependent apposition of Drosophila extraembryonic membranes promotes morphogenesis and prevents anoikis. *Current biology : CB*, 14(5):372–380.

[Reim and Frasch, 2005] Reim, I. and Frasch, M. (2005). The Dorsocross T-box genes are key components of the regulatory network controlling early cardiogenesis in Drosophila. *Development (Cambridge, England)*, 132(22):4911–4925.

[Reim et al., 2003] Reim, I., Lee, H.-H., and Frasch, M. (2003). The T-box-encoding Dorsocross genes function in amnioserosa development and the patterning of the dorsolateral germ band downstream of Dpp. *Development (Cambridge, England)*, 130(14):3187–3204.

[Riedl et al., 2008] Riedl, J., Crevenna, A. H., Kessenbrock, K., Yu, J. H., Neukirchen, D., Bista, M., Bradke, F., Jenne, D., Holak, T. A., Werb, Z., Sixt, M., and Wedlich-Soldner, R. (2008). Lifeact: a versatile marker to visualize F-actin. *Nature methods*, 5(7):605–607.

[Rodriguez Diaz et al., 2008] Rodriguez Diaz, A., Toyama, Y., Abravanel, D. L., Wiemann, J. M., Wells, A. R., Tulu, U. S., Edwards, G. S., and Kiehart, D. P. (2008). Actomyosin purse strings: Renewable resources that make morphogenesis robust and resilient. *HFSP Journal*, 2(4):220–237.

[Rushlow et al., 2001] Rushlow, C., Colosimo, P. F., Lin, M. C., Xu, M., and Kirov, N. (2001). Transcriptional regulation of the Drosophila gene zen by competing Smad and Brinker inputs. *Genes & development*, 15(3):340–351.

[Rushlow and Levine, 1990] Rushlow, C. and Levine, M. (1990). Role of the zerknüllt gene in dorsal-ventral pattern formation in Drosophila. *Advances in genetics*, 27:277–307.

[Sawyer et al., 2009] Sawyer, J. K., Harris, N. J., Slep, K. C., Gaul, U., and Peifer, M. (2009). The Drosophila afadin homologue Canoe regulates linkage of the actin cytoskeleton to adherens junctions during apical constriction. *The Journal of cell biology*, 186(1):57–73.

[Schmidt-Ott et al., 1994] Schmidt-Ott, U., González-Gaitán, M., Jäckle, H., and Technau, G. M. (1994). Number, identity, and sequence of the Drosophila head segments as revealed by neural elements and their deletion patterns in mutants. *Proceedings of the National Academy of Sciences of the United States of America*, 91(18):8363–8367.

[Schmidt-Ott and Kwan, 2016] Schmidt-Ott, U. and Kwan, C. W. (2016). Morphogenetic functions of extraembryonic membranes in insects. *Current Opinion in Insect Science*, 13:86–92.

[Schmidt-Ott et al., 2010] Schmidt-Ott, U., Rafiqi, A. M., and Lemke, S. (2010). *Hox3/Zen* and the Evolution of Extraembryonic Epithelia in Insects . *Advances in experimental medicine and biology*, 689:133–144.

[Schöck and Perrimon, 2002] Schöck, F. and Perrimon, N. (2002). Cellular processes associated with germ band retraction in Drosophila. *Developmental biology*, 248(1):29–39.

[Schöck and Perrimon, 2003] Schöck, F. and Perrimon, N. (2003). Retraction of the Drosophila germ band requires cell-matrix interaction. *Genes & development*, 17(5):597–602.

[Solon et al., 2009] Solon, J., Kaya-Copur, A., Colombelli, J., and Brunner, D. (2009). Pulsed Forces Timed by a Ratchet-like Mechanism Drive Directed Tissue Movement during Dorsal Closure. *Cell*, 137(7):1331–1342.

[Srivastava et al., 2007] Srivastava, A., Pastor-Pareja, J. C., Igaki, T., Pagliarini, R., and Xu, T. (2007). Basement membrane remodeling is essential for Drosophila disc eversion and tumor invasion. *Proceedings of the National Academy of Sciences of the United States of America*, 104(8):2721–2726.

[St Johnston and Gelbart, 1987] St Johnston, R. D. and Gelbart, W. M. (1987). Decapentaplegic transcripts are localized along the dorsal-ventral axis of the Drosophila embryo. *The EMBO journal*, 6(9):2785–2791.

[Strobl and Stelzer, 2014] Strobl, F. and Stelzer, E. H. K. (2014). Non-invasive long-term fluorescence live imaging of Tribolium castaneum embryos. *Development (Cambridge, England)*, 141(11):2331–2338.

[Sui et al., 2012] Sui, L., Pflugfelder, G. O., and Shen, J. (2012). The Dorsocross T-box transcription factors promote tissue morphogenesis in the Drosophila wing imaginal disc. *Development (Cambridge, England)*, 139(15):2773–2782.

[T Lepage, 1990] T Lepage, C. G. (1990). Early expression of a collagenase-like hatching enzyme gene in the sea urchin embryo. *The EMBO journal*, 9(9):3003.

[Toshiki et al., 2000] Toshiki, T., Pierre, C., Chantal, T., Corinne, R., Toshio, K., Eappen, A., Mari, K., Natuo, K., Jean-Luc, T., Bernard, M., Gérard, C., Paul, S., Malcolm, F., and Jean-Claude, P. (2000). Germline transformation of the silkworm Bombyx mori L. using a piggyBac transposon-derived vector. *Nature biotechnology*, 18(1):81–84.

[Turner and Mahowald, 1977] Turner, F. R. and Mahowald, A. P. (1977). Scanning electron microscopy of Drosophila melanogaster embryogenesis. II. Gastrulation and segmentation. *Developmental biology*, 57(2):403–416.

[Turner and Mahowald, 1979] Turner, F. R. and Mahowald, A. P. (1979). Scanning electron microscopy of Drosophila melanogaster embryogenesis. III. Formation of the head and caudal segments. *Developmental biology*, 68(1):96–109.

[Urbansky et al., 2016] Urbansky, S., González Avalos, P., Wosch, M., and Lemke, S. (2016). Folded gastrulation and T48 drive the evolution of coordinated mesoderm internalization in flies. *eLife*, 5.

[Uría and López-Otín, 2000] Uría, J. A. and López-Otín, C. (2000). Matrilysin-2, a new matrix metalloproteinase expressed in human tumors and showing the minimal domain organization required for secretion, latency, and activity. *Cancer research*, 60(17):4745–4751.

[van Daal and Elgin, 1992] van Daal, A. and Elgin, S. C. (1992). A histone variant, H2AvD, is essential in Drosophila melanogaster. *Molecular Biology of the Cell*, 3(6):593–602.

[van der Zee et al., 2005] van der Zee, M., Berns, N., and Roth, S. (2005). Distinct Functions of the Tribolium zerknu¨llt Genes in Serosa Specification and Dorsal Closure. *Current Biology*, 15(7):624–636.

[Verkhusha et al., 1999] Verkhusha, V. V., Tsukita, S., and Oda, H. (1999). Actin dynamics in lamellipodia of migrating border cells in the Drosophila ovary revealed by a GFP-actin fusion protein. *FEBS letters*, 445(2-3):395–401.

[Vicoso and Bachtrog, 2015] Vicoso, B. and Bachtrog, D. (2015). Numerous transitions of sex chromosomes in Diptera. *PLoS Biology*, 13(4):e1002078.

[Wada et al., 2007] Wada, A., Kato, K., Uwo, M. F., Yonemura, S., and Hayashi, S. (2007). Specialized extraembryonic cells connect embryonic and extraembryonic epidermis in response to Dpp during dorsal closure in Drosophila. *Developmental biology*, 301(2):340–349.

[Wada et al., 1998] Wada, K., Sato, H., Kinoh, H., Kajita, M., Yamamoto, H., and Seiki, M. (1998). Cloning of three Caenorhabditis elegans genes potentially encoding novel matrix metalloproteinases. *Gene*, 211(1):57–62.

[Wiegmann et al., 2011] Wiegmann, B. M., Trautwein, M. D., Winkler, I. S., Barr, N. B., Kim, J.-W., Lambkin, C., Bertone, M. A., Cassel, B. K., Bayless, K. M., Heimberg, A. M., Wheeler, B. M., Peterson, K. J., Pape, T., Sinclair, B. J., Skevington, J. H., Blagoderov, V., Caravas, J., Kutty, S. N., Schmidt-Ott, U., Kampmeier, G. E., Thompson, F. C., Grimaldi, D. A., Beckenbach, A. T., Courtney, G. W., Friedrich, M., Meier, R., and Yeates, D. K. (2011). Episodic radiations in the fly tree of life. *Proceedings of the National Academy of Sciences of the United States of America*, 108(14):5690–5695.

[Wolpert, 1992] Wolpert, L. (1992). Gastrulation and the evolution of development. *Development (Cambridge, England)*, 116(Supplement):7–13.

[Wood et al., 2002] Wood, W., Jacinto, A., Grose, R., Woolner, S., Gale, J., Wilson, C., and Martin, P. (2002). Wound healing recapitulates morphogenesis in Drosophila embryos. *Nature Cell Biology*, 4(11):907–912.

[Wotton et al., 2014] Wotton, K. R., Jiménez-Guri, E., García Matheu, B., and Jaeger, J. (2014). A staging scheme for the development of the scuttle fly Megaselia abdita. *PLoS ONE*, 9(1):e84421.

[Wyatt et al., 2009] Wyatt, R. A., Keow, J. Y., Harris, N. D., Haché, C. A., and Li, D. H. (2009). The zebrafish embryo: a powerful model system for investigating matrix remodeling. ....

[Yamada et al., 2005] Yamada, S., Pokutta, S., Drees, F., Weis, W. I., and Nelson, W. J. (2005). Deconstructing the cadherin-catenin-actin complex. *Cell*, 123(5):889–901.

[Zhang et al., 2010] Zhang, M., Zhang, Y., and Xu, Z. (2010). POSH is involved in Eiger-Basket (TNF-JNK) signaling and embryogenesis in Drosophila. *Journal of Genetics and Genomics*, 37(9):605–619.

[Zhang et al., 2006] Zhang, S., Dailey, G. M., Kwan, E., Glasheen, B. M., Sroga, G. E., and Page-McCaw, A. (2006). An MMP liberates the Ninjurin A ectodomain to signal a loss of cell adhesion. *Genes & development*, 20(14):1899–1910.